Recent achievements in GW astronomy
Status of KAGRA and future prospects

National Astronomical Observatory of Japan
Gravitational Wave Science Project
Yoichi Aso

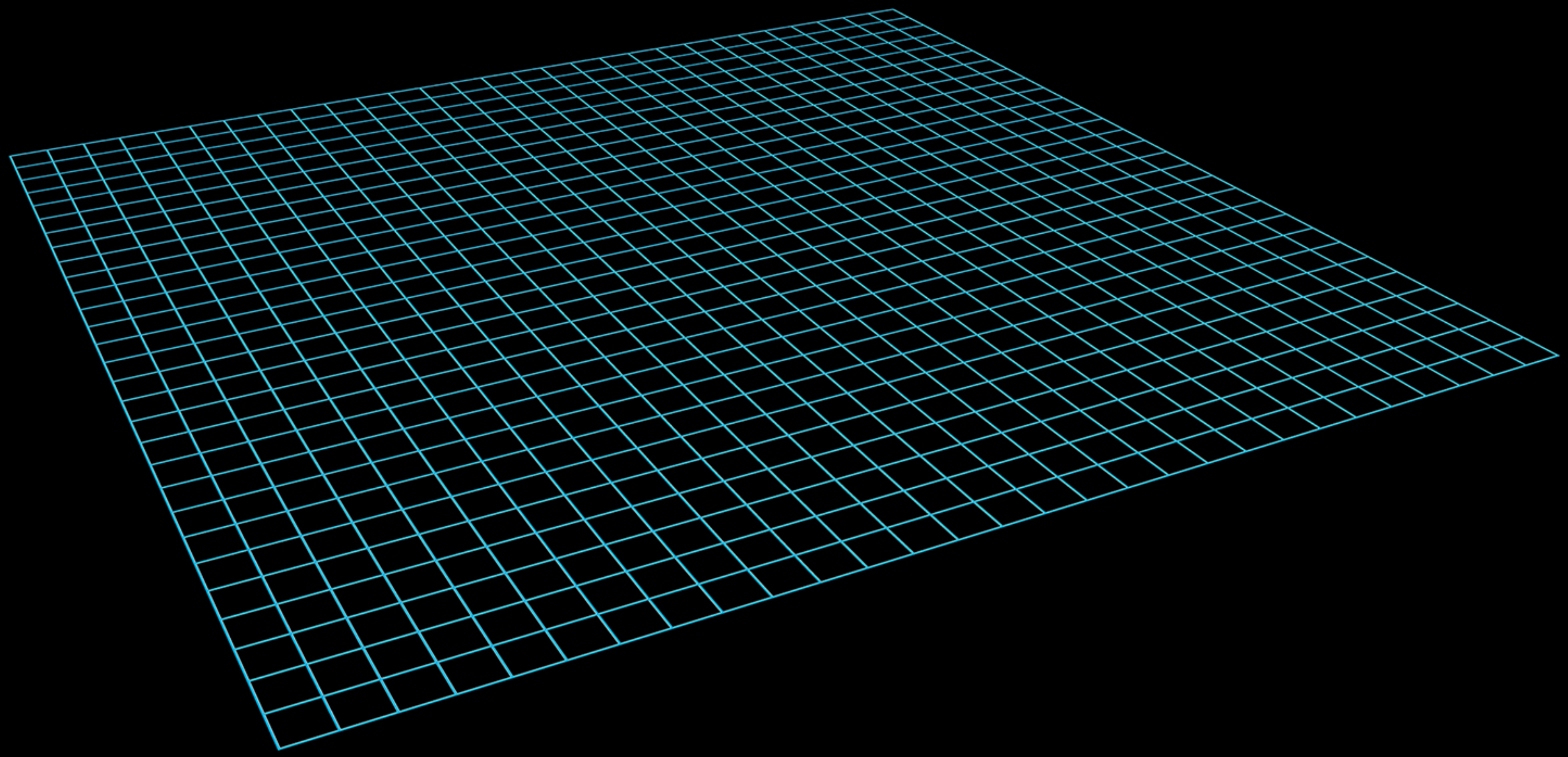

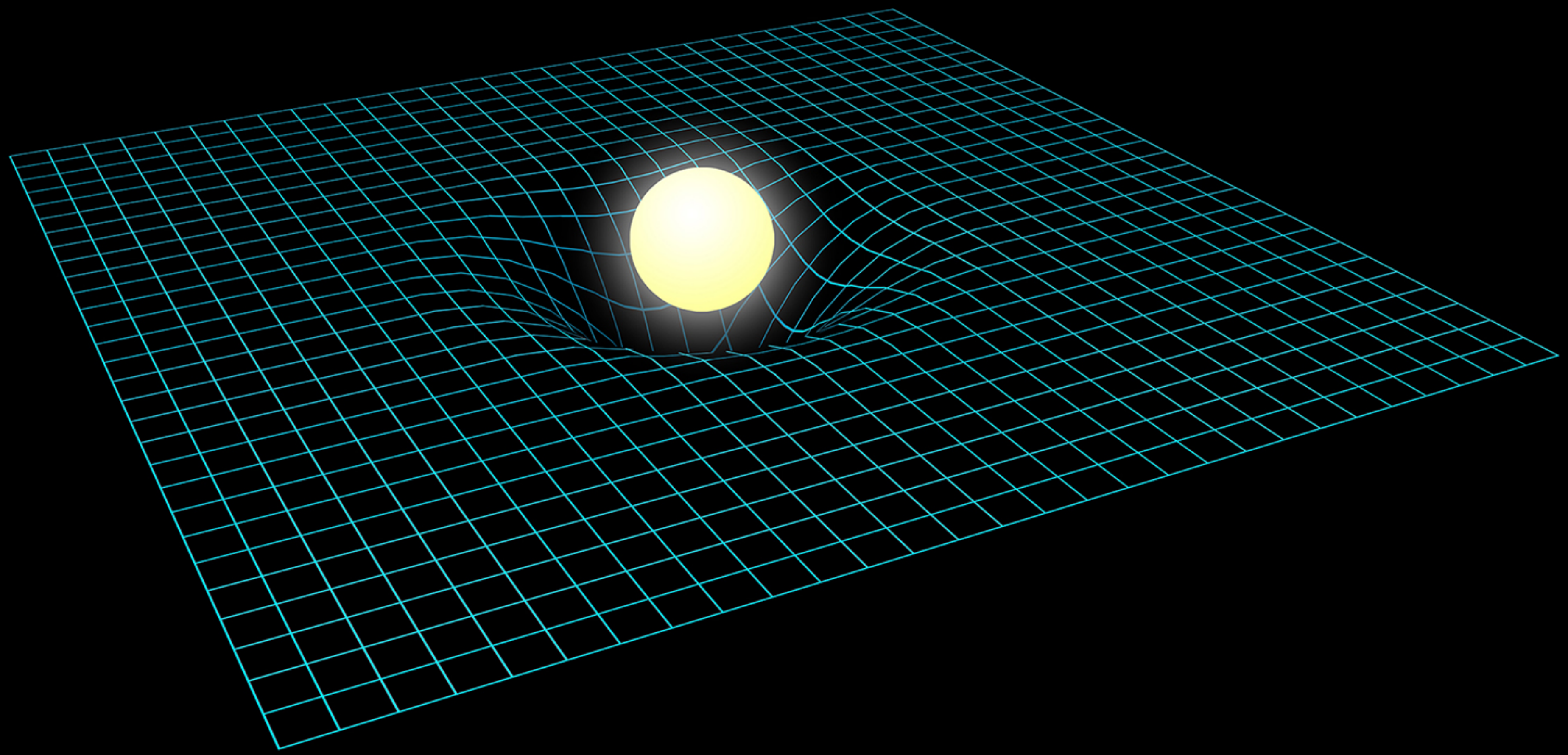

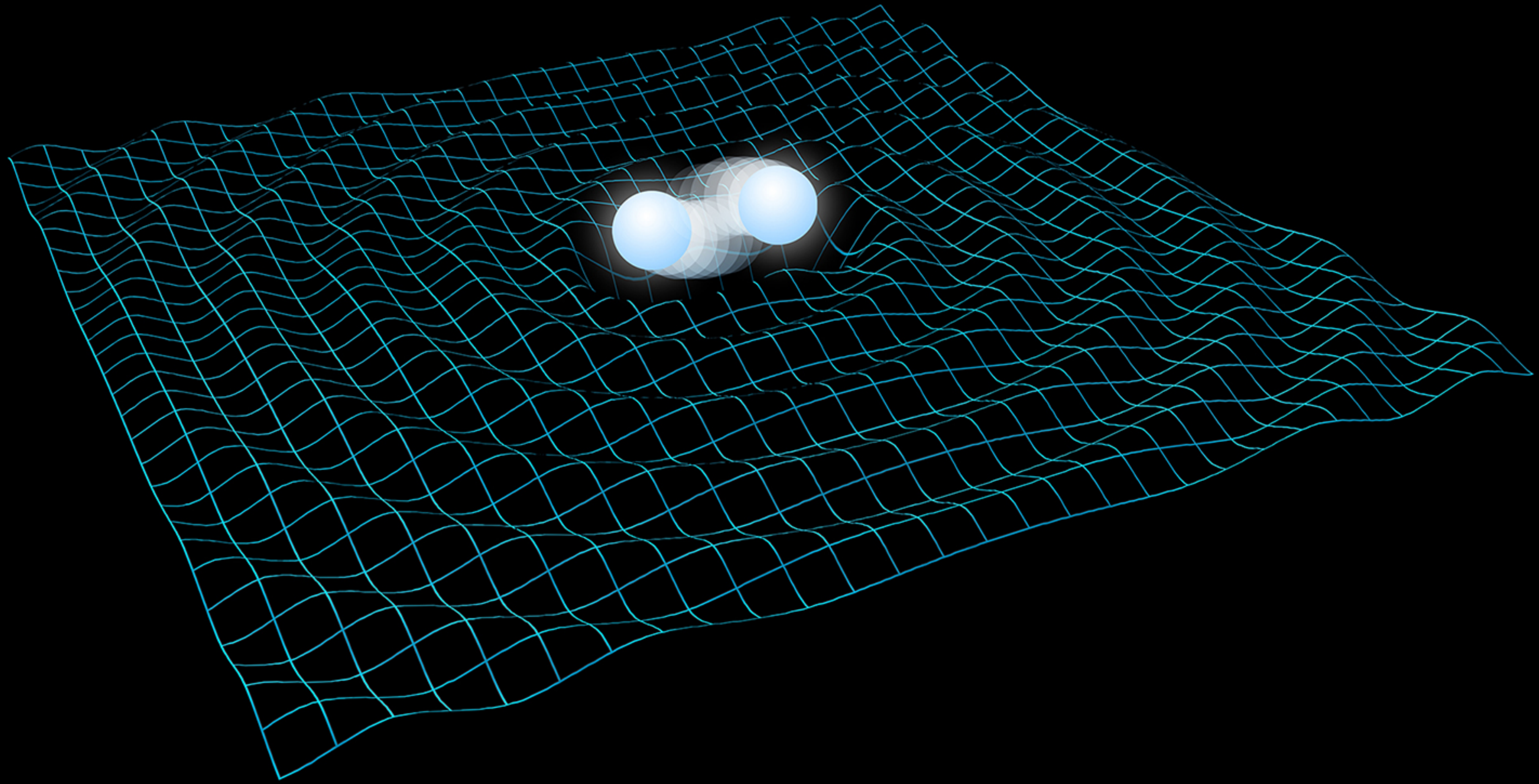

$$G_{\mu\nu} = \frac{8\pi G}{c^4} T_{\mu\nu}$$

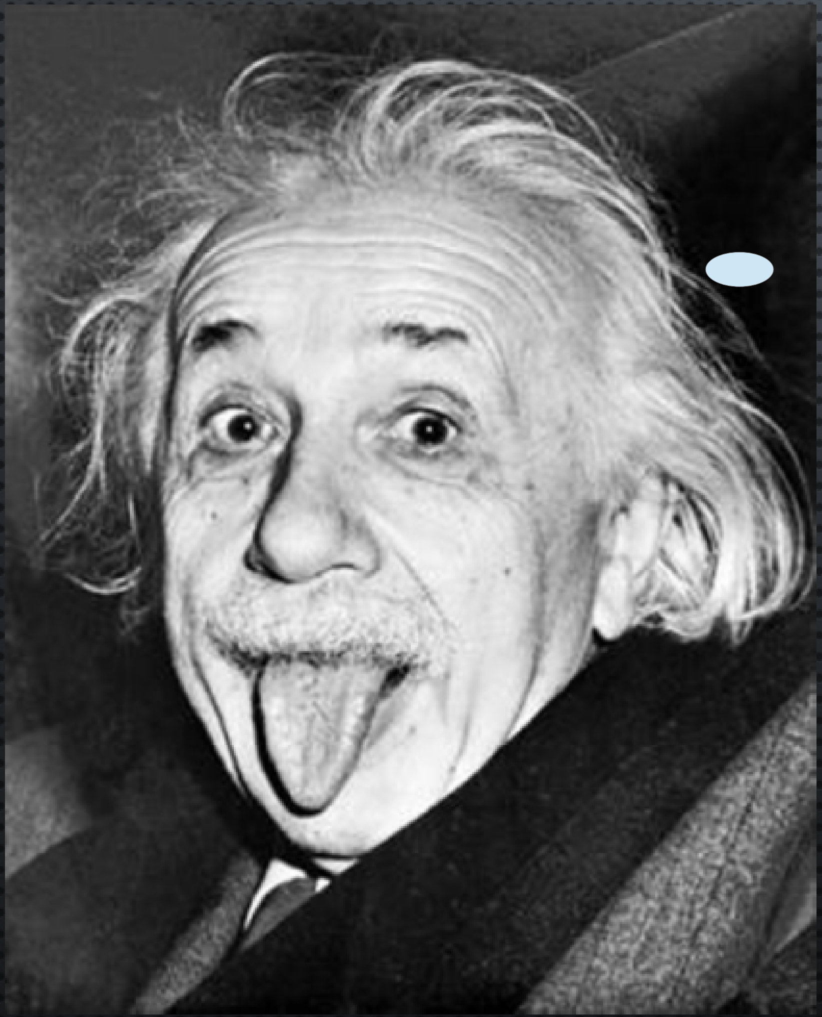

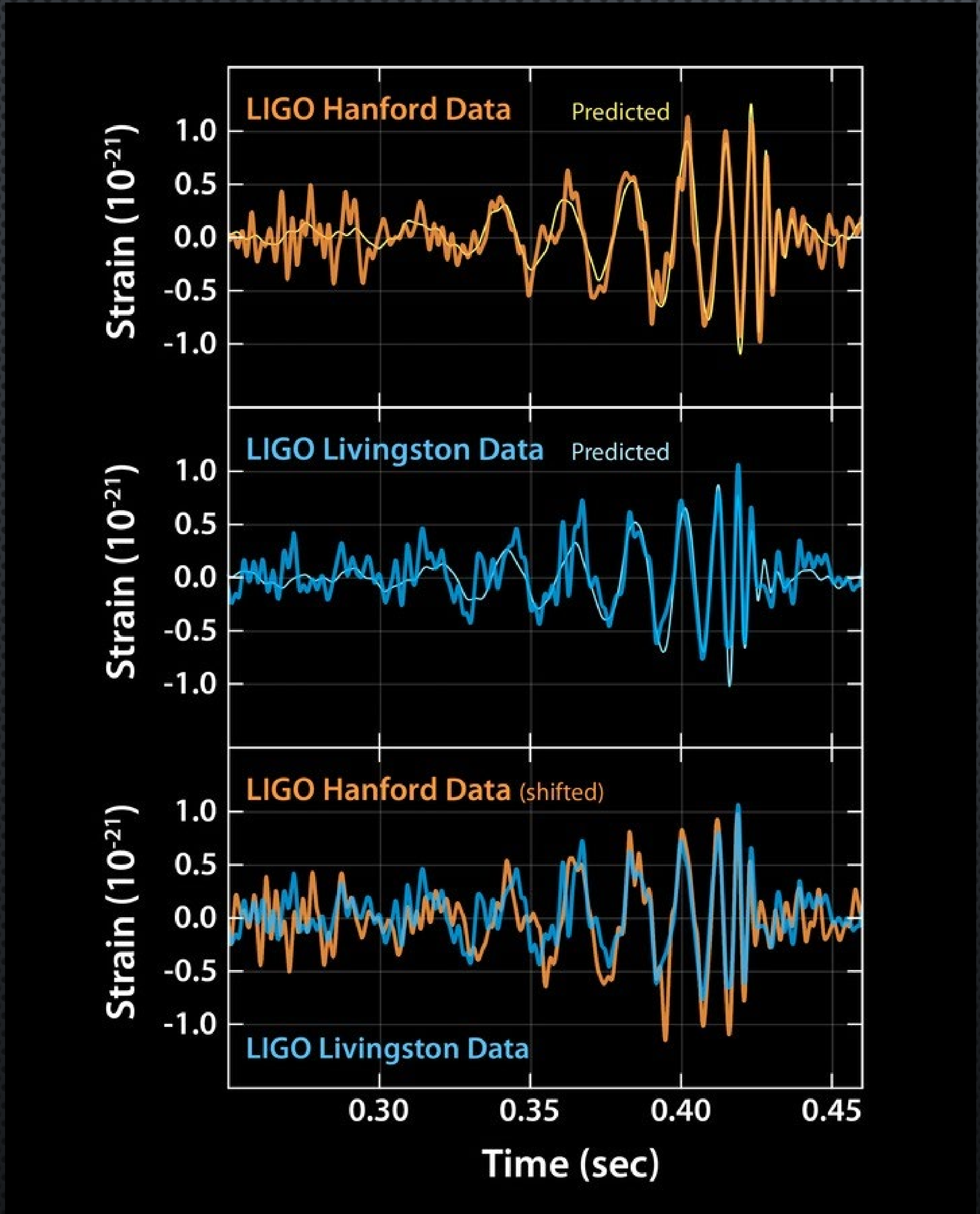

LIGO Hanford Data
Predicted
LIGO Livingston Data
Predicted
LIGO Hanford Data (shifted)
LIGO Livingston Data
Strain (10^{-21})
1.0
0.5
0.0
-0.5
-1.0
0.30
0.35
0.40
0.45
Time (sec)

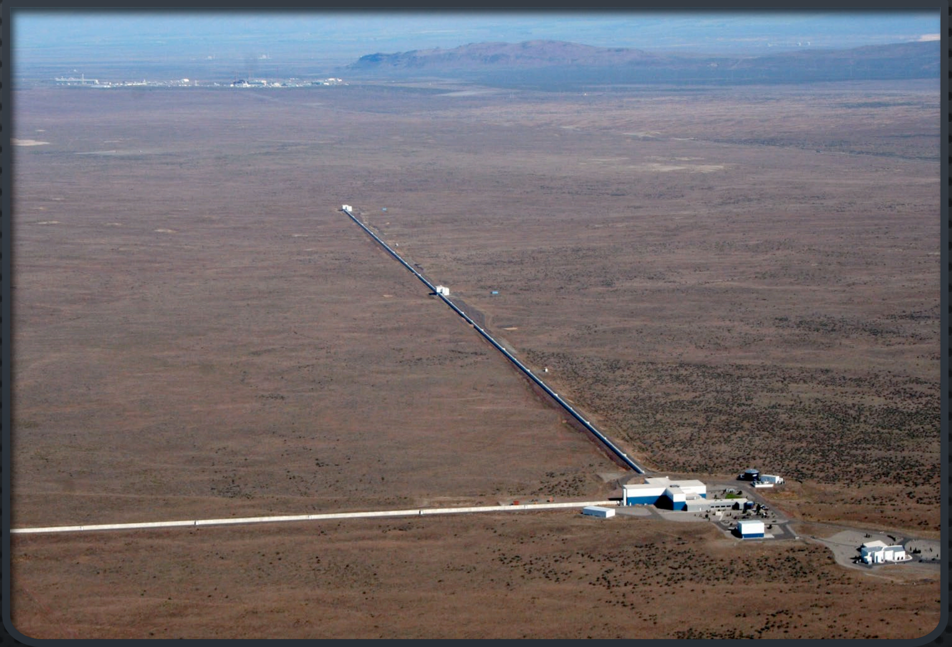

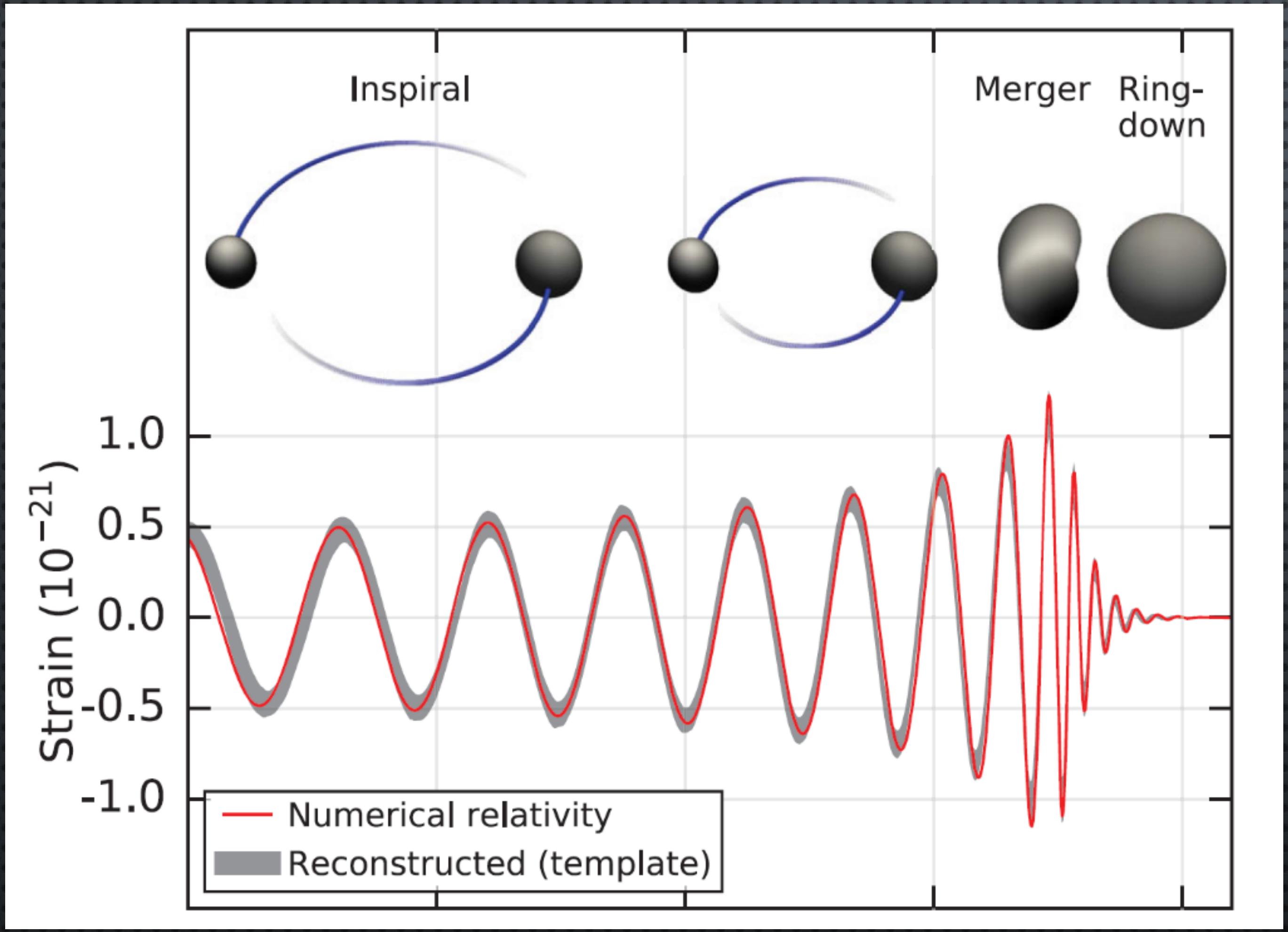

400Mpc

$$29M_\odot + 36M_\odot \rightarrow 62M_\odot$$

Direct detection of gravitational waves

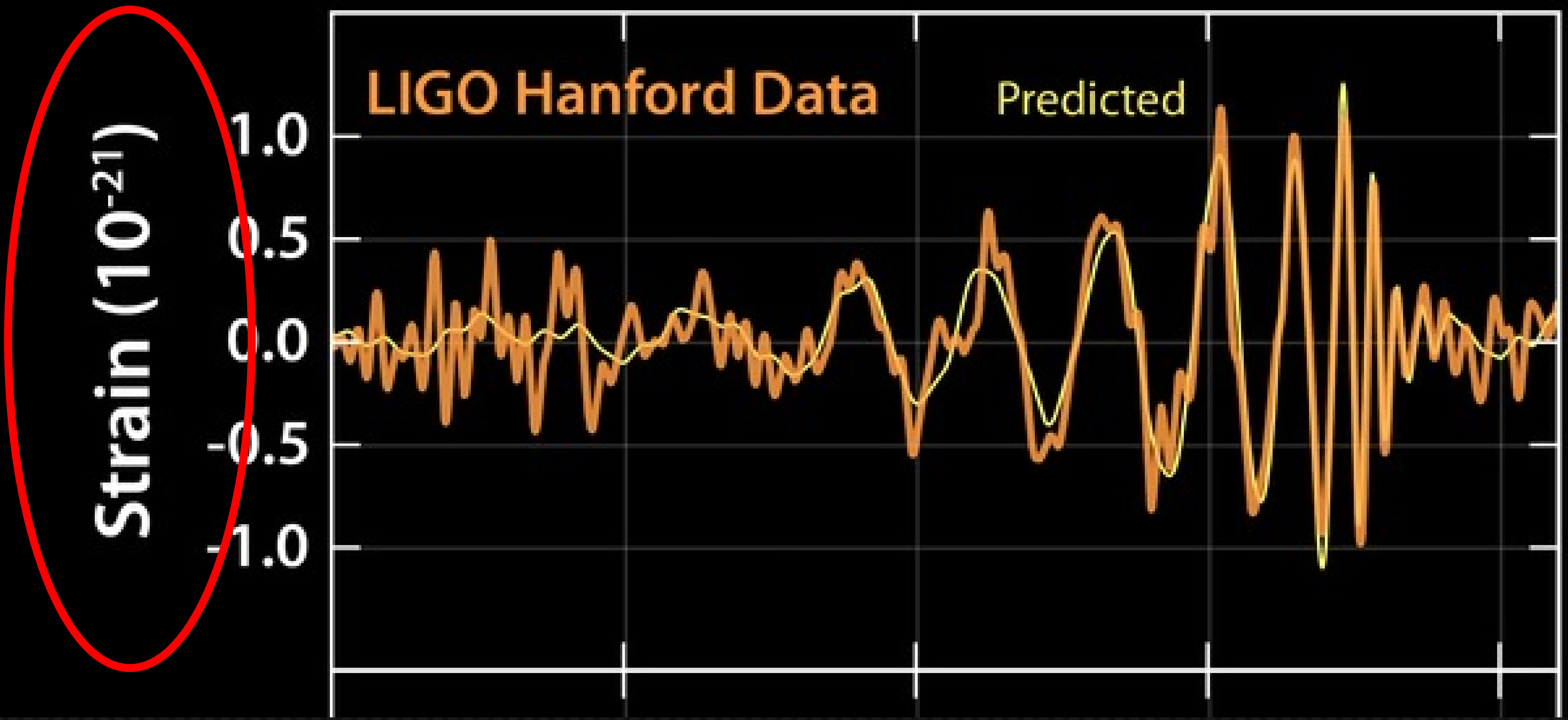
Strain (10^{-21})
1.0
0.5
0.0
-0.5
-1.0
LIGO Hanford Data
Predicted

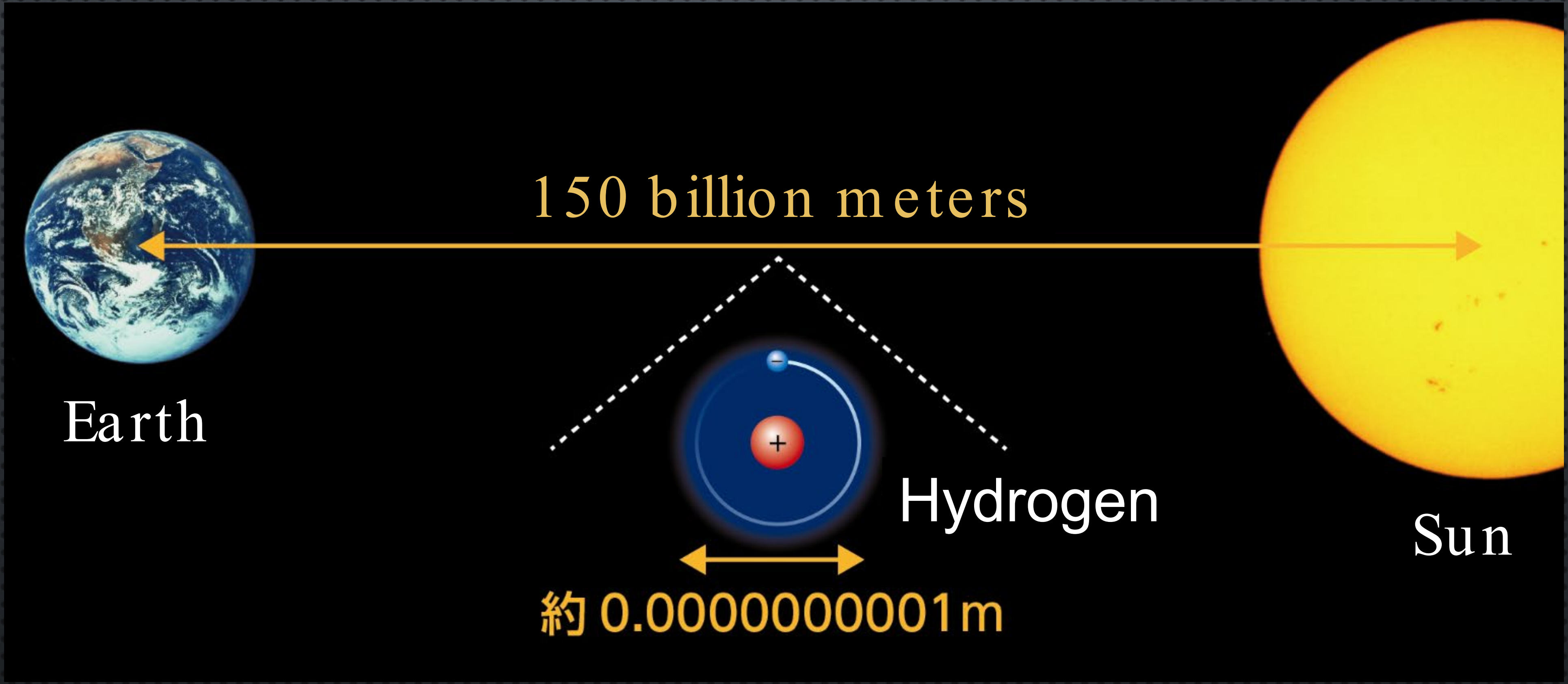

$$h = 10^{-21}$$

Direct detection of gravitational waves

Black hole binaries exist

Direct detection of gravitational waves

Black hole binaries exist

BH with more than 30 solar mass

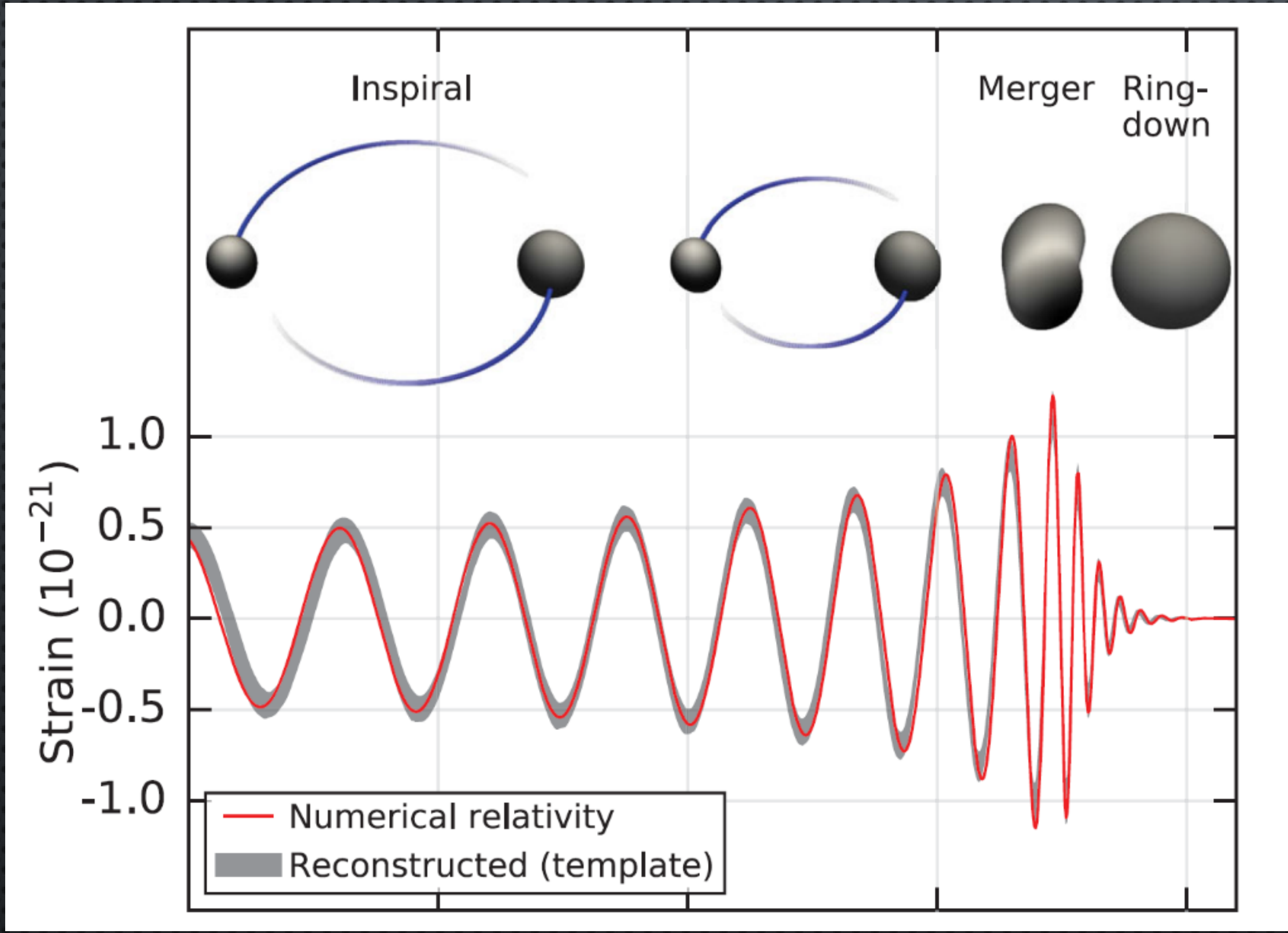

400Mpc

$$29M_\odot + 36M_\odot \to 62M_\odot$$

Gravitational Wave Luminosity

Visible luminosity of the entire Universe

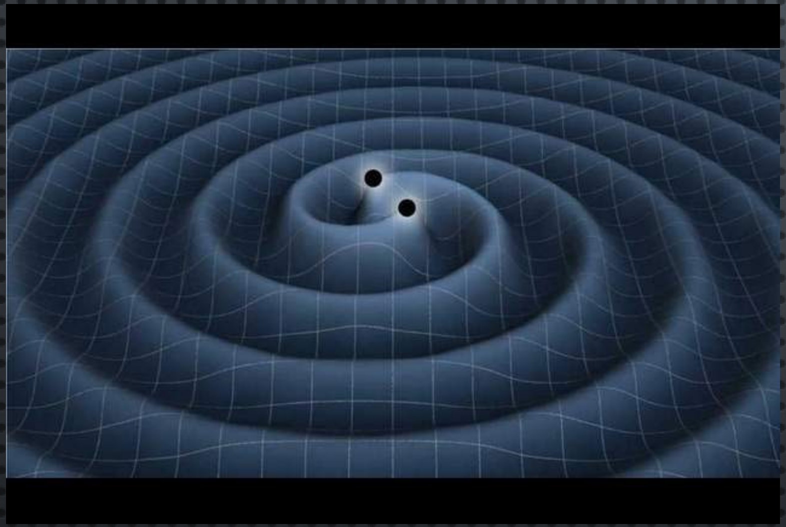

$\geq$

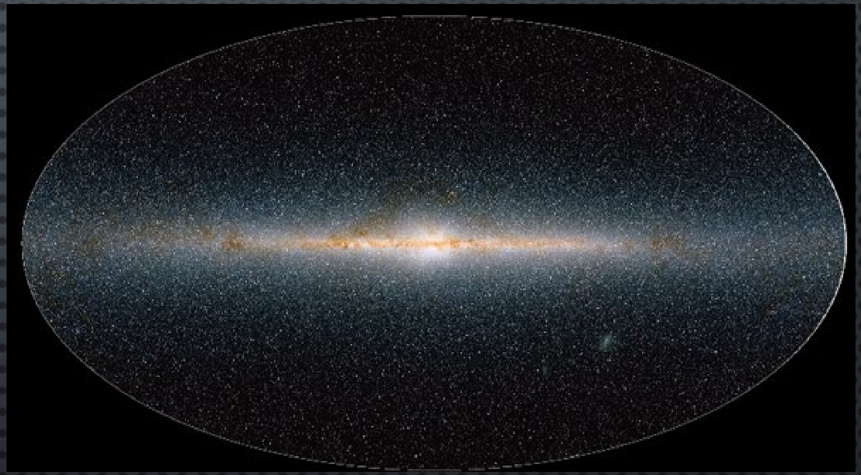

$3.6 \times 10^{49}\,\mathrm{J/s}$

$1 \times 10^{49}\,\mathrm{J/s}$

Masses in the Stellar Graveyard

in Solar Masses

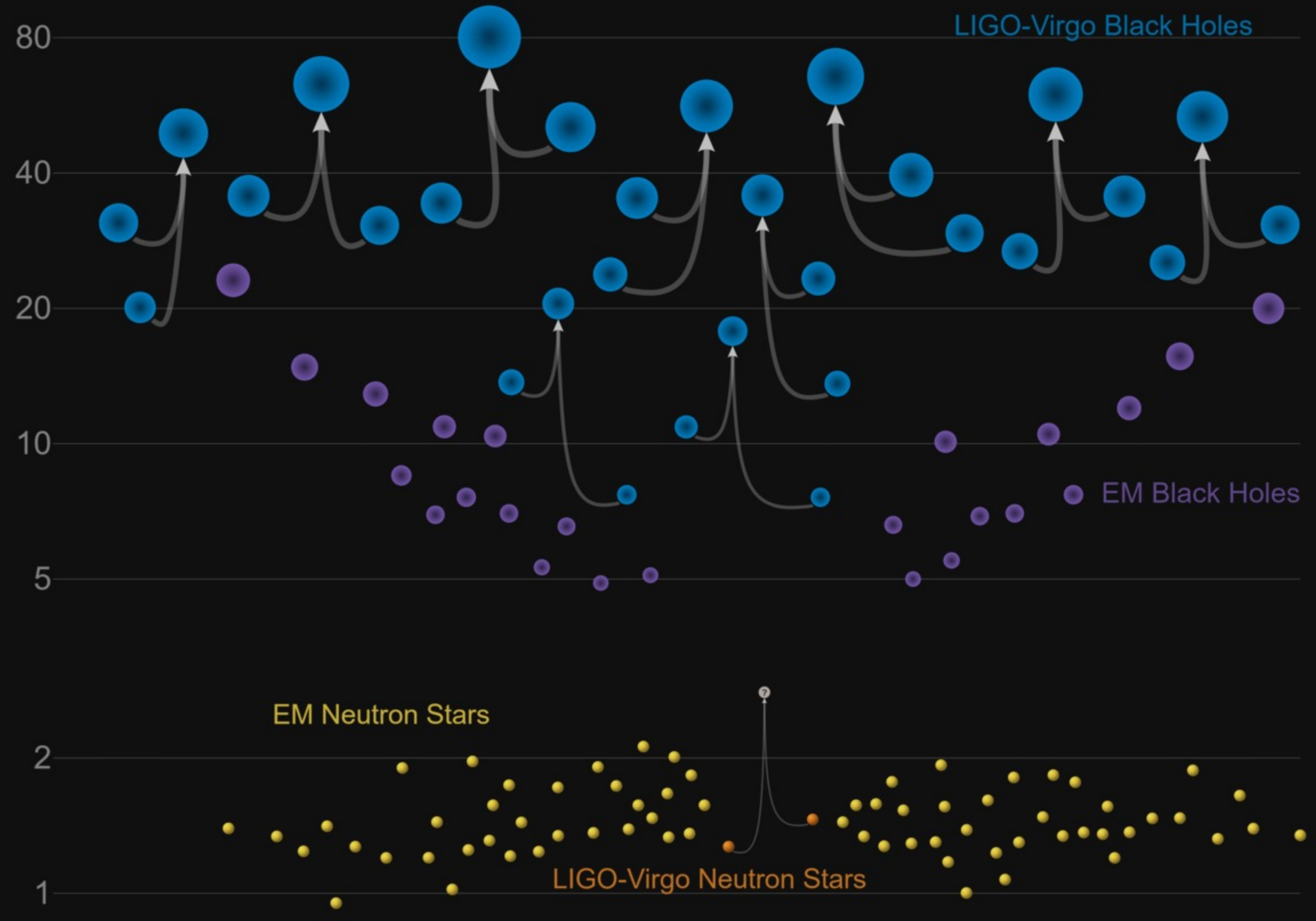

LIGO-Virgo | Frank Elavsky | Northwestern

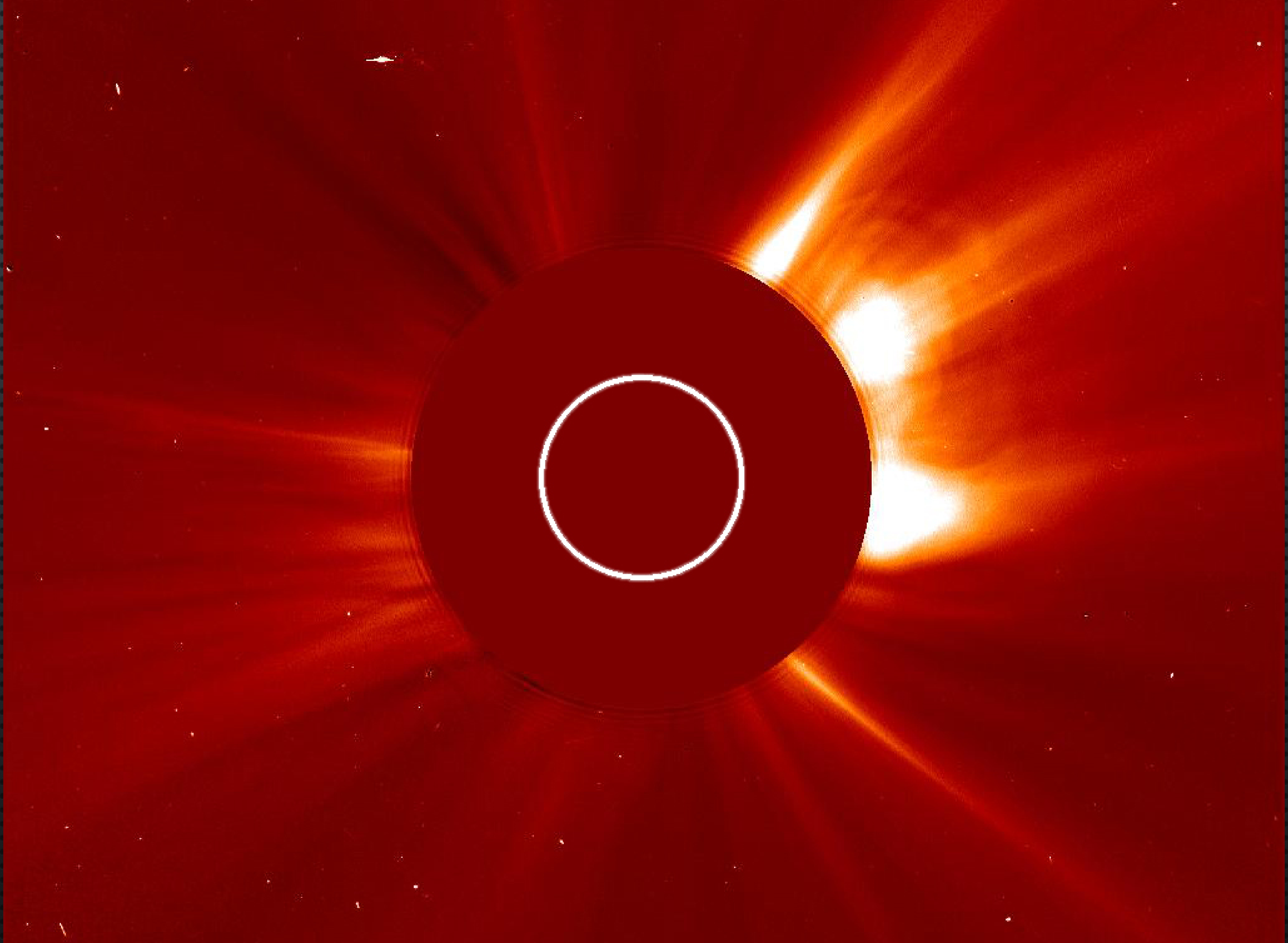

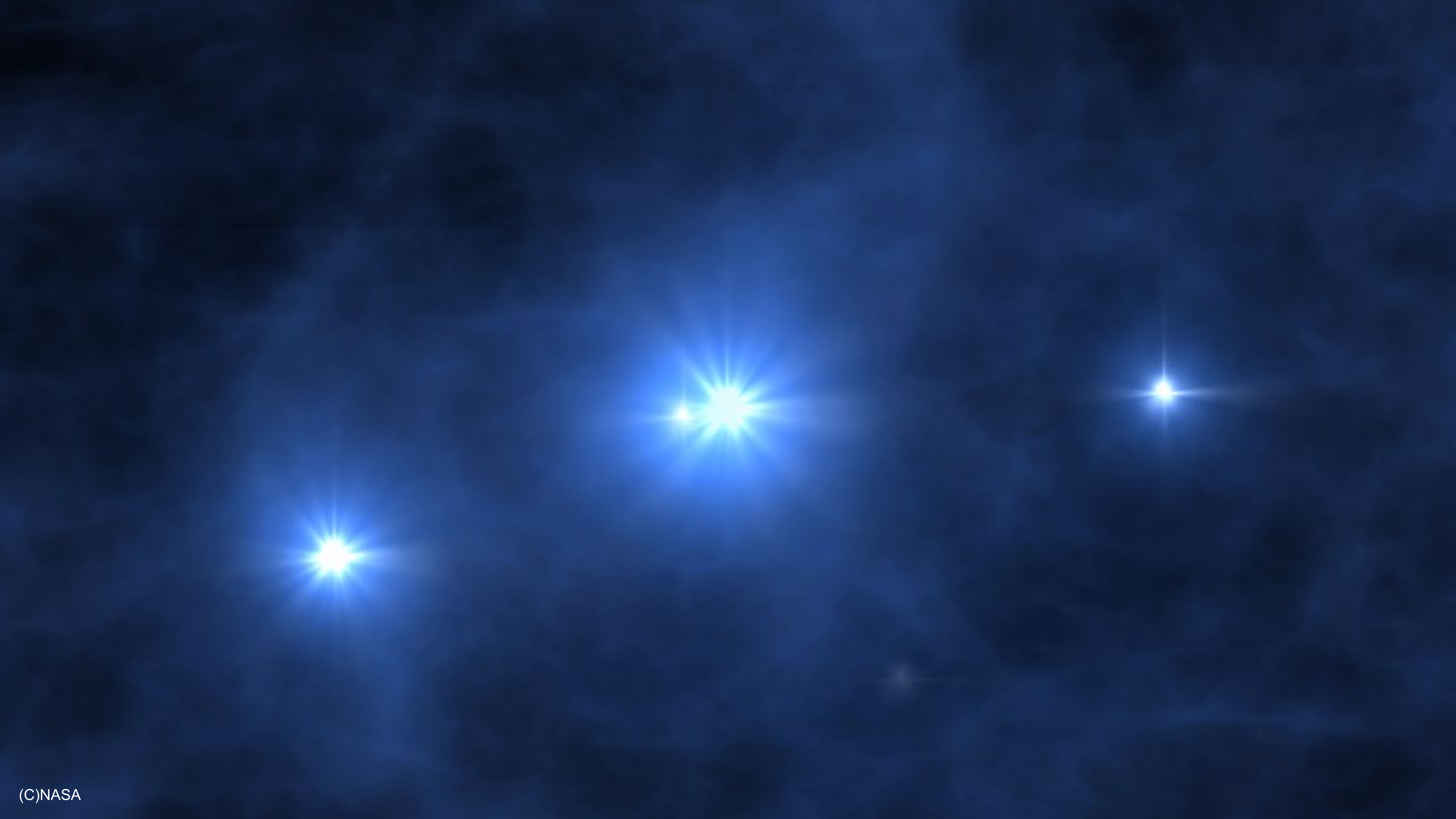

Putative Mass Gaps

$2M_{\odot} \sim 5M_{\odot}$: Largest NS - Smallest BH

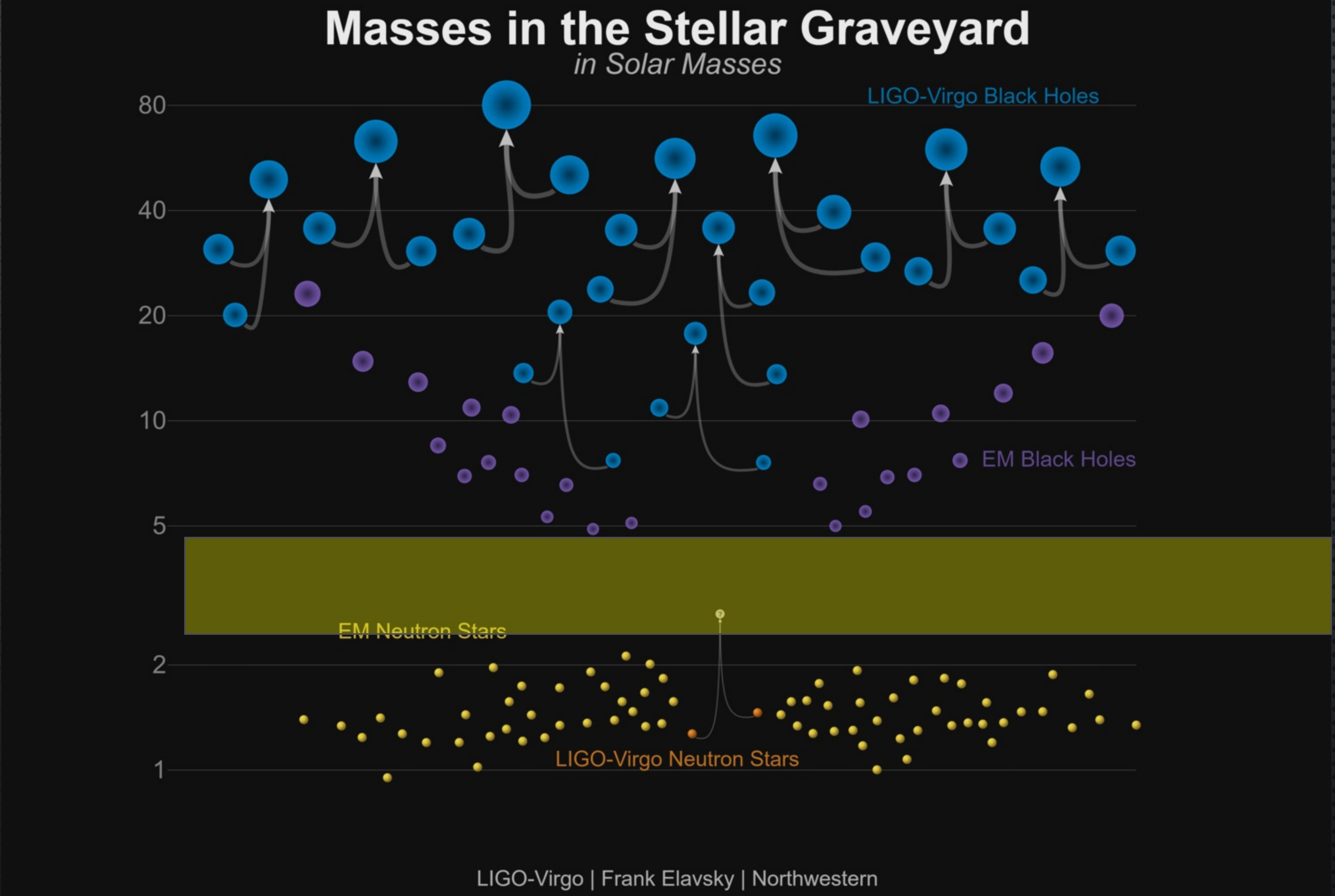
Masses in the Stellar Graveyard
in Solar Masses
80
40
20
10
5
2
1
LIGO-Virgo Black Holes
EM Black Holes
EM Neutron Stars
LIGO-Virgo Neutron Stars
LIGO-Virgo | Frank Elavsky | Northwestern

Putative Mass Gaps

$2M_\odot \sim 5M_\odot$: Largest NS - Smallest BH

$50M_\odot \sim 150M_\odot$:
(Pulsational) Pair-Instability

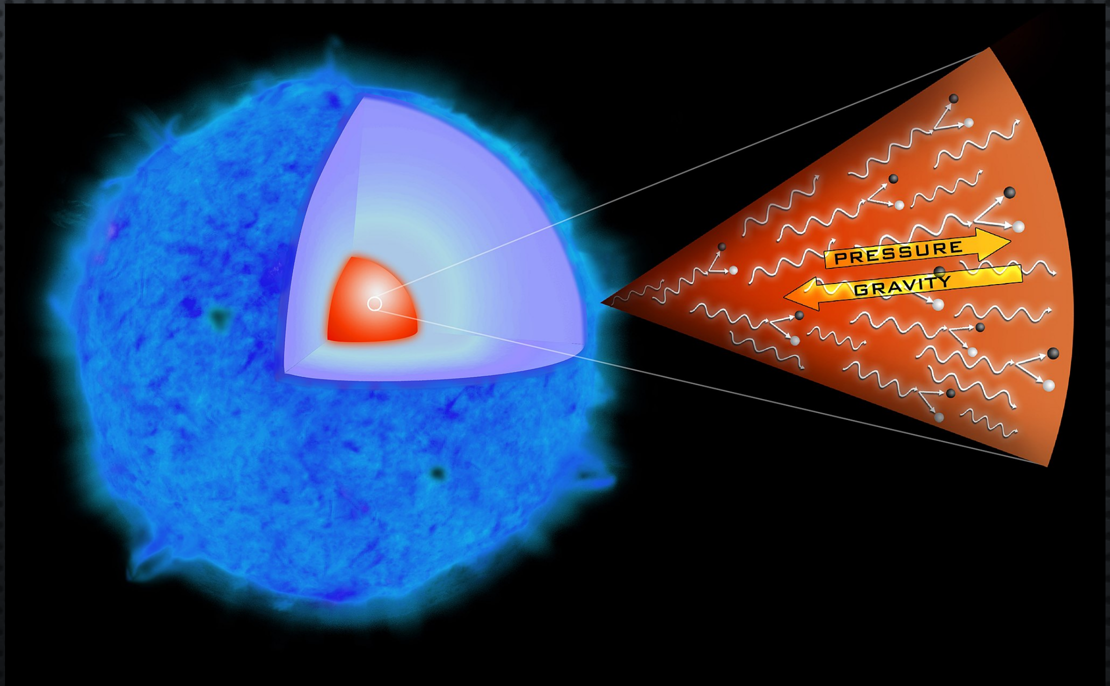

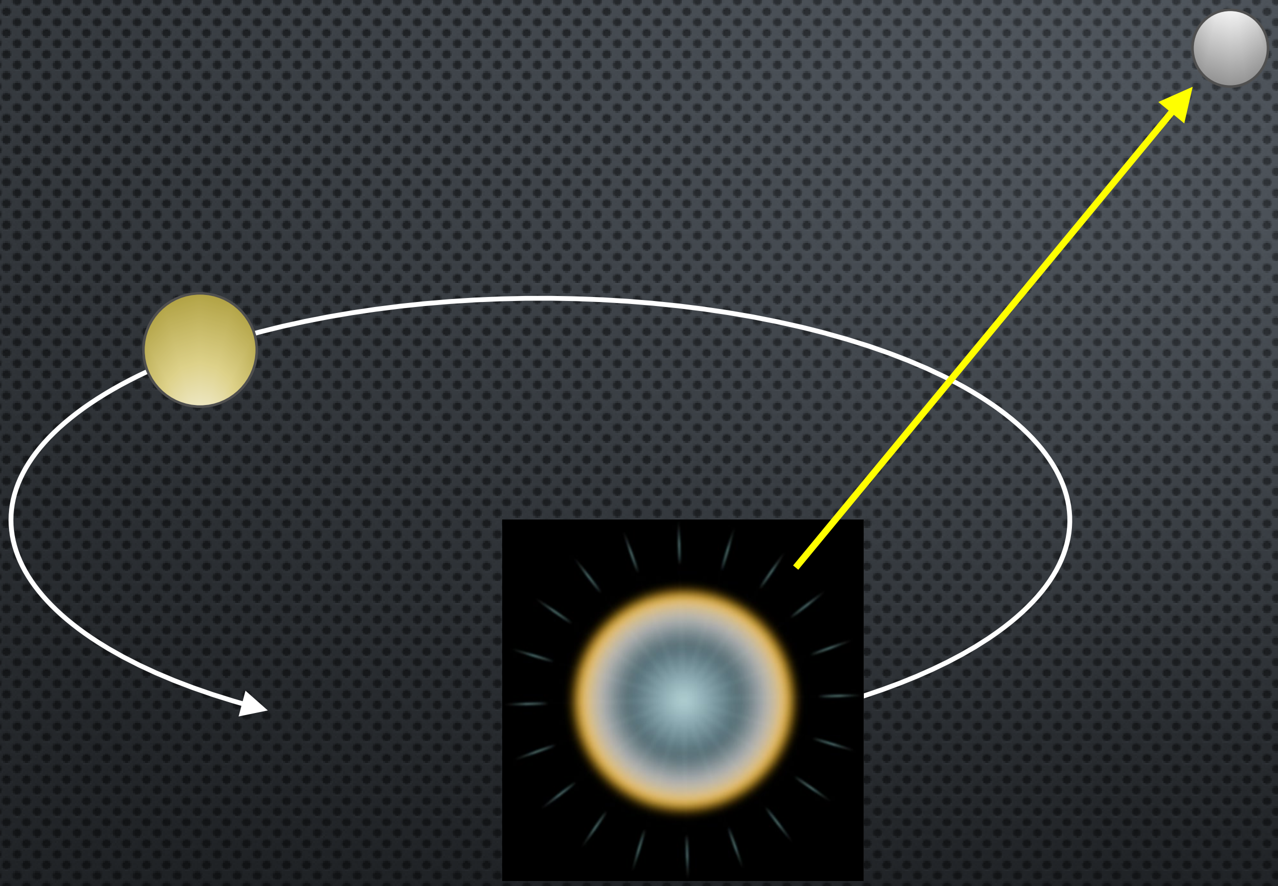

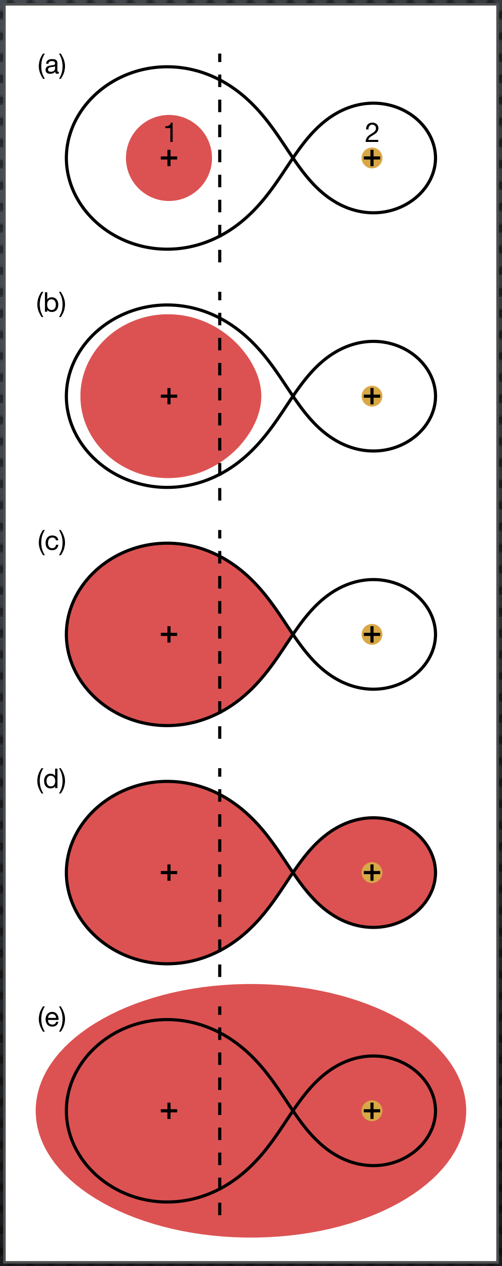
(a)
1
2
(b)
(c)
(d)
(e)

By NASA, The Hubble Heritage Team, STScI, AURA

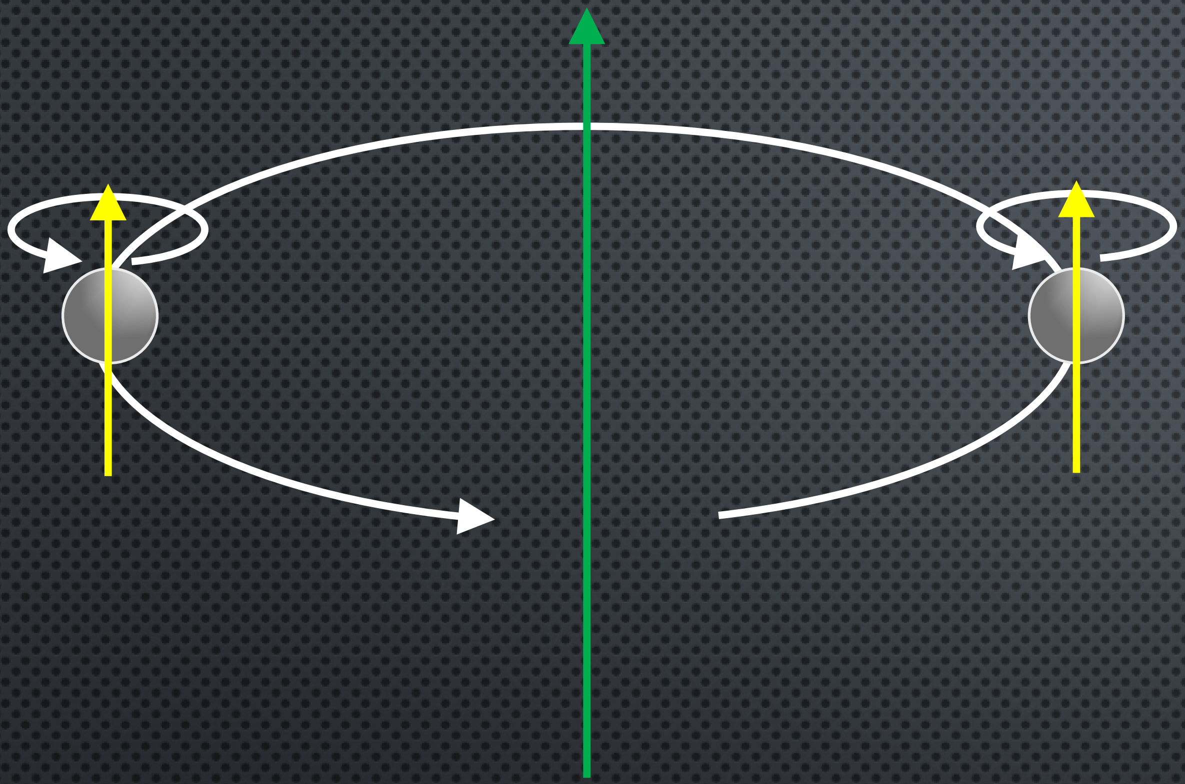

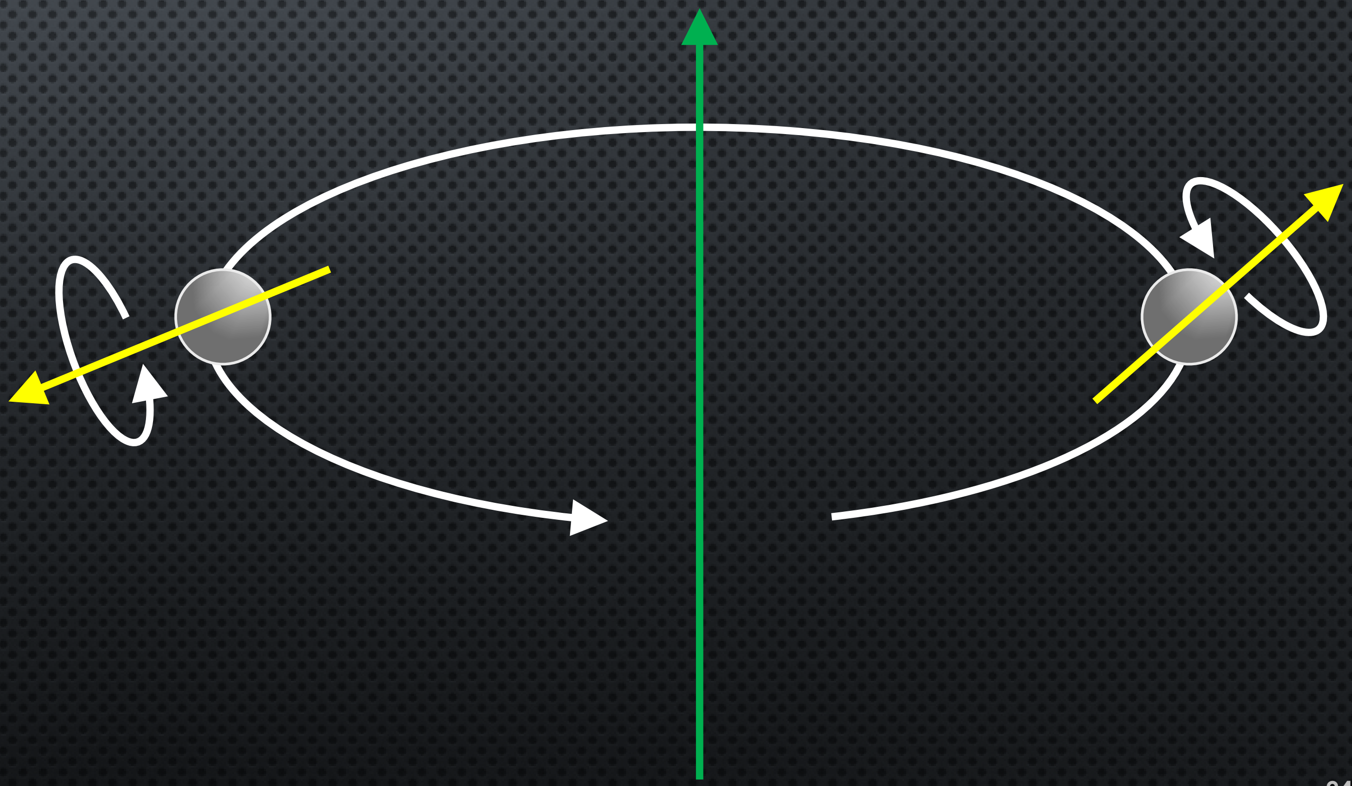

O1, O2 Compact Binary Detections

Event	$m_1/M_\odot$	$m_2/M_\odot$	$\mathcal{M}/M_\odot$	χ_{eff}	$M_f/M_\odot$	a_f	$E_{\mathrm{rad}}/(M_\odot c^2)$	$\ell_{\mathrm{peak}}/(\mathrm{erg\,s^{-1}})$	d_L/Mpc	z	$\Delta\Omega/\mathrm{deg}^2$
GW150914	$35.6^{+4.7}_{-3.1}$	$30.6^{+3.0}_{-4.4}$	$28.6^{+1.7}_{-1.5}$	$-0.01^{+0.12}_{-0.13}$	$63.1^{+3.4}_{-3.0}$	$0.69^{+0.05}_{-0.04}$	$3.1^{+0.4}_{-0.4}$	$3.6^{+0.4}_{-0.4} \times 10^{56}$	440^{+150}_{-170}	$0.09^{+0.03}_{-0.03}$	182
GW151012	$23.2^{+14.9}_{-5.5}$	$13.6^{+4.1}_{-4.8}$	$15.2^{+2.1}_{-1.2}$	$0.05^{+0.31}_{-0.20}$	$35.6^{+10.8}_{-3.8}$	$0.67^{+0.13}_{-0.11}$	$1.6^{+0.6}_{-0.5}$	$3.2^{+0.8}_{-1.7} \times 10^{56}$	1080^{+550}_{-490}	$0.21^{+0.09}_{-0.09}$	1523
GW151226	$13.7^{+8.8}_{-3.2}$	$7.7^{+2.2}_{-2.5}$	$8.9^{+0.3}_{-0.3}$	$0.18^{+0.20}_{-0.12}$	$20.5^{+6.4}_{-1.5}$	$0.74^{+0.07}_{-0.05}$	$1.0^{+0.1}_{-0.2}$	$3.4^{+0.7}_{-1.7} \times 10^{56}$	450^{+180}_{-190}	$0.09^{+0.04}_{-0.04}$	1033
GW170104	$30.8^{+7.3}_{-5.6}$	$20.0^{+4.9}_{-4.6}$	$21.4^{+2.2}_{-1.8}$	$-0.04^{+0.17}_{-0.21}$	$48.9^{+5.1}_{-4.0}$	$0.66^{+0.08}_{-0.11}$	$2.2^{+0.5}_{-0.5}$	$3.3^{+0.6}_{-1.0} \times 10^{56}$	990^{+440}_{-430}	$0.20^{+0.08}_{-0.08}$	921
GW170608	$11.0^{+5.5}_{-1.7}$	$7.6^{+1.4}_{-2.2}$	$7.9^{+0.2}_{-0.2}$	$0.03^{+0.19}_{-0.07}$	$17.8^{+3.4}_{-0.7}$	$0.69^{+0.04}_{-0.04}$	$0.9^{+0.0}_{-0.1}$	$3.5^{+0.4}_{-1.3} \times 10^{56}$	320^{+120}_{-110}	$0.07^{+0.02}_{-0.02}$	392
GW170729	$50.2^{+16.2}_{-10.2}$	$34.0^{+9.1}_{-10.1}$	$35.4^{+6.5}_{-4.8}$	$0.37^{+0.21}_{-0.25}$	$79.5^{+14.7}_{-10.2}$	$0.81^{+0.07}_{-0.13}$	$4.8^{+1.7}_{-1.7}$	$4.2^{+0.9}_{-1.5} \times 10^{56}$	2840^{+1400}_{-1360}	$0.49^{+0.19}_{-0.21}$	1041
GW170809	$35.0^{+8.3}_{-5.9}$	$23.8^{+5.1}_{-5.2}$	$24.9^{+2.1}_{-1.7}$	$0.08^{+0.17}_{-0.17}$	$56.3^{+5.2}_{-3.8}$	$0.70^{+0.08}_{-0.09}$	$2.7^{+0.6}_{-0.6}$	$3.5^{+0.6}_{-0.9} \times 10^{56}$	1030^{+320}_{-390}	$0.20^{+0.05}_{-0.07}$	308
GW170814	$30.6^{+5.6}_{-3.0}$	$25.2^{+2.8}_{-4.0}$	$24.1^{+1.4}_{-1.1}$	$0.07^{+0.12}_{-0.12}$	$53.2^{+3.2}_{-2.4}$	$0.72^{+0.07}_{-0.05}$	$2.7^{+0.4}_{-0.3}$	$3.7^{+0.4}_{-0.5} \times 10^{56}$	600^{+150}_{-220}	$0.12^{+0.03}_{-0.04}$	87
GW170817	$1.46^{+0.12}_{-0.10}$	$1.27^{+0.09}_{-0.09}$	$1.186^{+0.001}_{-0.001}$	$0.00^{+0.02}_{-0.01}$	≤ 2.8	≤ 0.89	≥ 0.04	$\geq 0.1 \times 10^{56}$	40^{+7}_{-15}	$0.01^{+0.00}_{-0.00}$	16
GW170818	$35.4^{+7.5}_{-4.7}$	$26.7^{+4.3}_{-5.2}$	$26.5^{+2.1}_{-1.7}$	$-0.09^{+0.18}_{-0.21}$	$59.4^{+4.9}_{-3.8}$	$0.67^{+0.07}_{-0.08}$	$2.7^{+0.5}_{-0.5}$	$3.4^{+0.5}_{-0.7} \times 10^{56}$	1060^{+420}_{-380}	$0.21^{+0.07}_{-0.07}$	39
GW170823	$39.5^{+11.2}_{-6.7}$	$29.0^{+6.7}_{-7.8}$	$29.2^{+4.6}_{-3.6}$	$0.09^{+0.22}_{-0.26}$	$65.4^{+10.1}_{-7.4}$	$0.72^{+0.09}_{-0.12}$	$3.3^{+1.0}_{-0.9}$	$3.6^{+0.7}_{-1.1} \times 10^{56}$	1940^{+970}_{-900}	$0.35^{+0.15}_{-0.15}$	1666

Phys. Rev. X **9**, 031040 (2019)

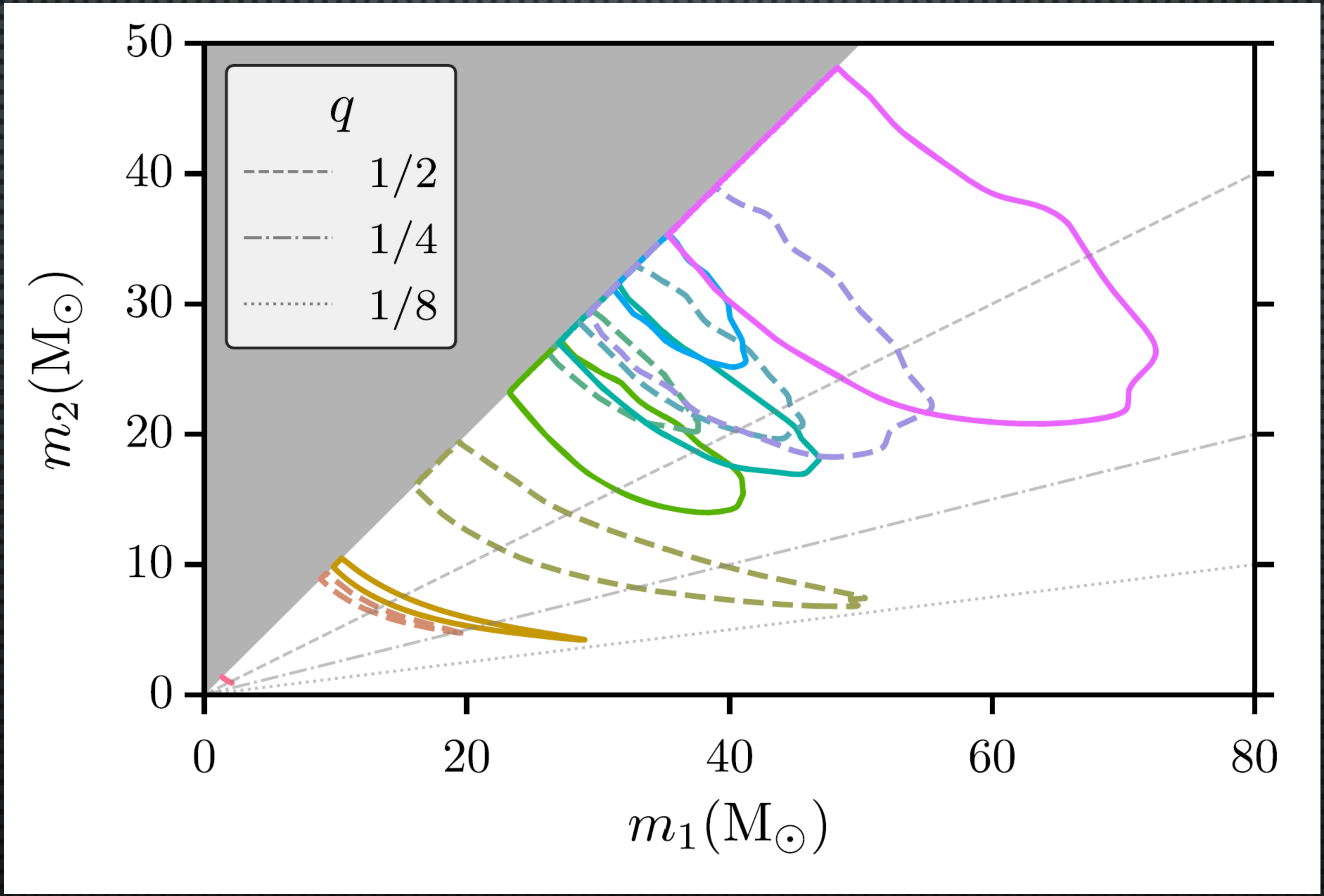

q
1/2
1/4
1/8
50
40
30
20
10
0
0
20
40
60
80
$m_2(\mathrm{M}_\odot)$
$m_1(\mathrm{M}_\odot)$

THE ASTROPHYSICAL JOURNAL LETTERS, 882:L24 (30pp), 2019 September 10 https://doi.org/10.3847/2041-8213/ab3800

CrossMark

Binary Black Hole Population Properties Inferred from the First and Second Observing Runs of Advanced LIGO and Advanced Virgo

B. P. Abbott[1], R. Abbott[1], T. D. Abbott[2], S. Abraham[3], F. Acernese[4,5], K. Ackley[6], C. Adams[7], R. X. Adhikari[1], V. B. Adya[8,9], C. Affeldt[8,9], M. Agathos[10], K. Agatsuma[11], N. Aggarwal[12], O. D. Aguiar[13], L. Aiello[14,15], A. Ain[3], P. Ajith[16], G. Allen[17], A. Allocca[18,19], M. A. Aloy[20], P. A. Altin[21], A. Amato[22], A. Ananyeva[1], S. B. Anderson[1], W. G. Anderson[23], S. V. Angelova[24], S. Antier[25], S. Appert[1], K. Arai[1], M. C. Araya[1], J. S. Areeda[26], M. Arène[27], N. Arnaud[25,28], K. G. Arun[29], S. Ascenzi[30,31], G. Ashton[6], S. M. Aston[7], P. Astone[32], F. Aubin[33], P. Aufmuth[9], K. AultONeal[34], C. Austin[2], V. Avendano[35], A. Avila-Alvarez[26]

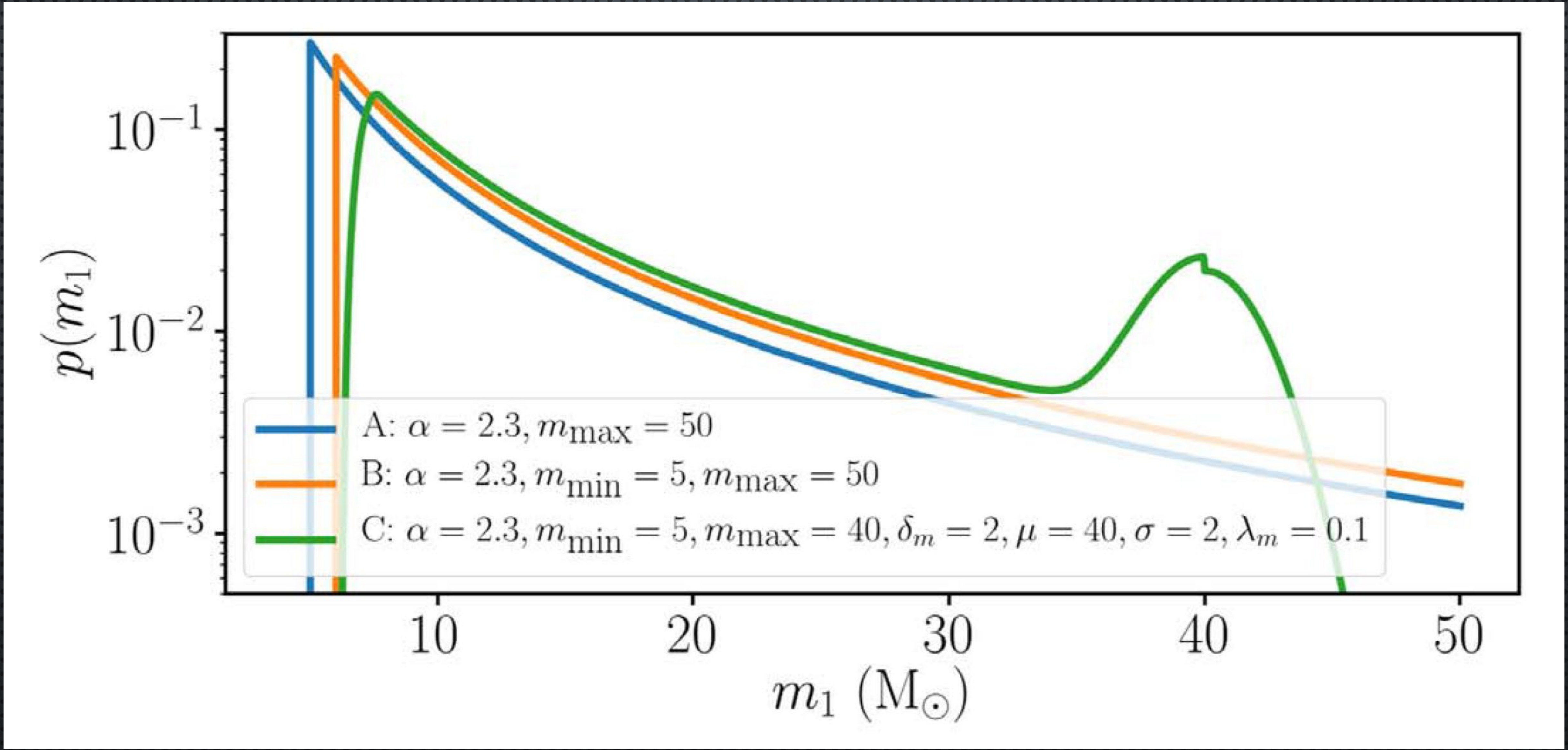
$p(m_1)$
10^{-1}
10^{-2}
10^{-3}
A: $\alpha = 2.3, m_{\max} = 50$
B: $\alpha = 2.3, m_{\min} = 5, m_{\max} = 50$
C: $\alpha = 2.3, m_{\min} = 5, m_{\max} = 40, \delta_m = 2, \mu = 40, \sigma = 2, \lambda_m = 0.1$
10
20
30
40
50
m_1 ($M_\odot$)

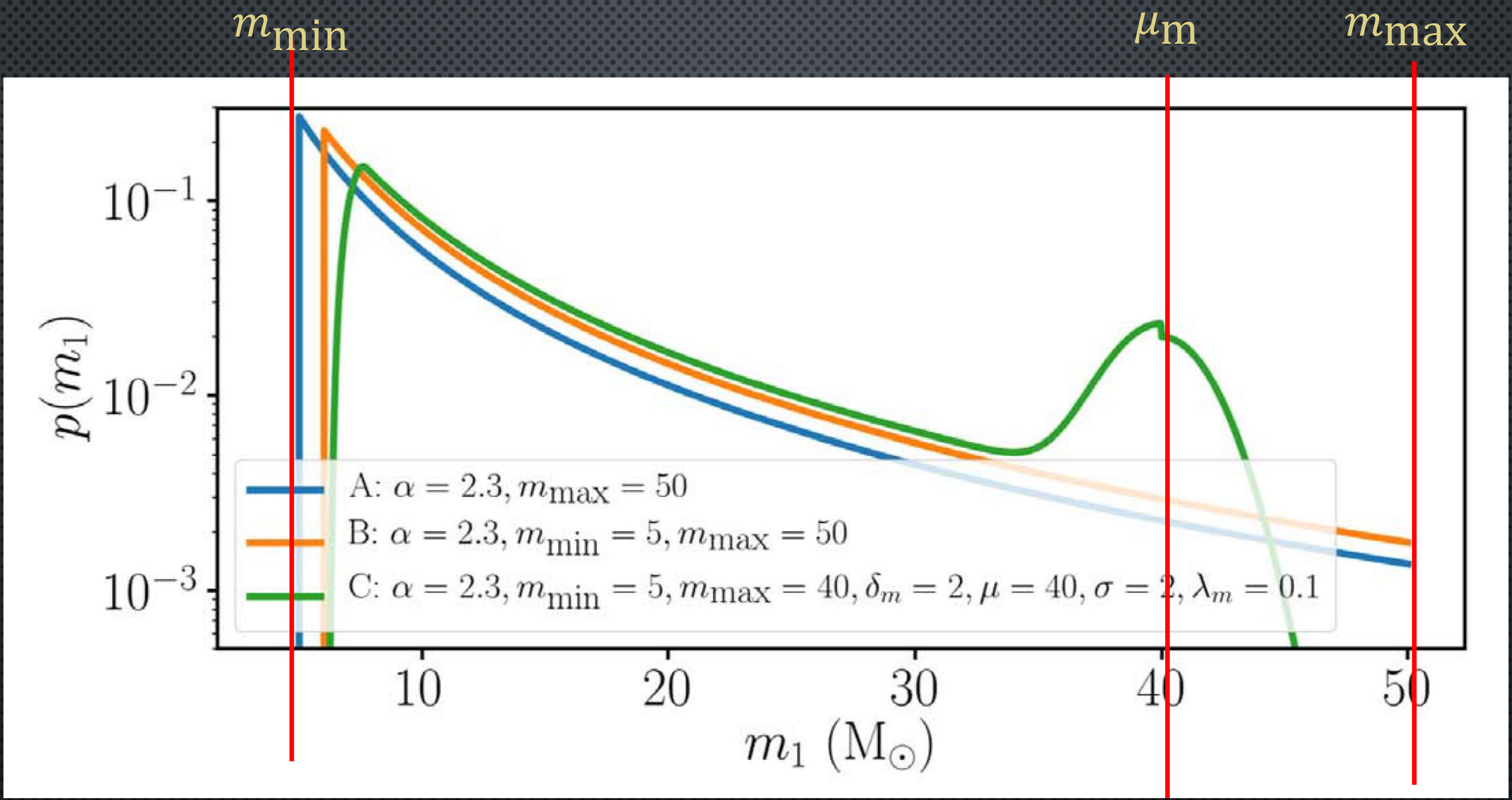
m_{min}
μ_m
m_{max}
10^{-1}
10^{-2}
10^{-3}
$p(m_1)$
A: $\alpha = 2.3, m_{max} = 50$
B: $\alpha = 2.3, m_{min} = 5, m_{max} = 50$
C: $\alpha = 2.3, m_{min} = 5, m_{max} = 40, \delta_m = 2, \mu = 40, \sigma = 2, \lambda_m = 0.1$
10
20
30
40
50
m_1 ($M_\odot$)

a: Spin magnitude

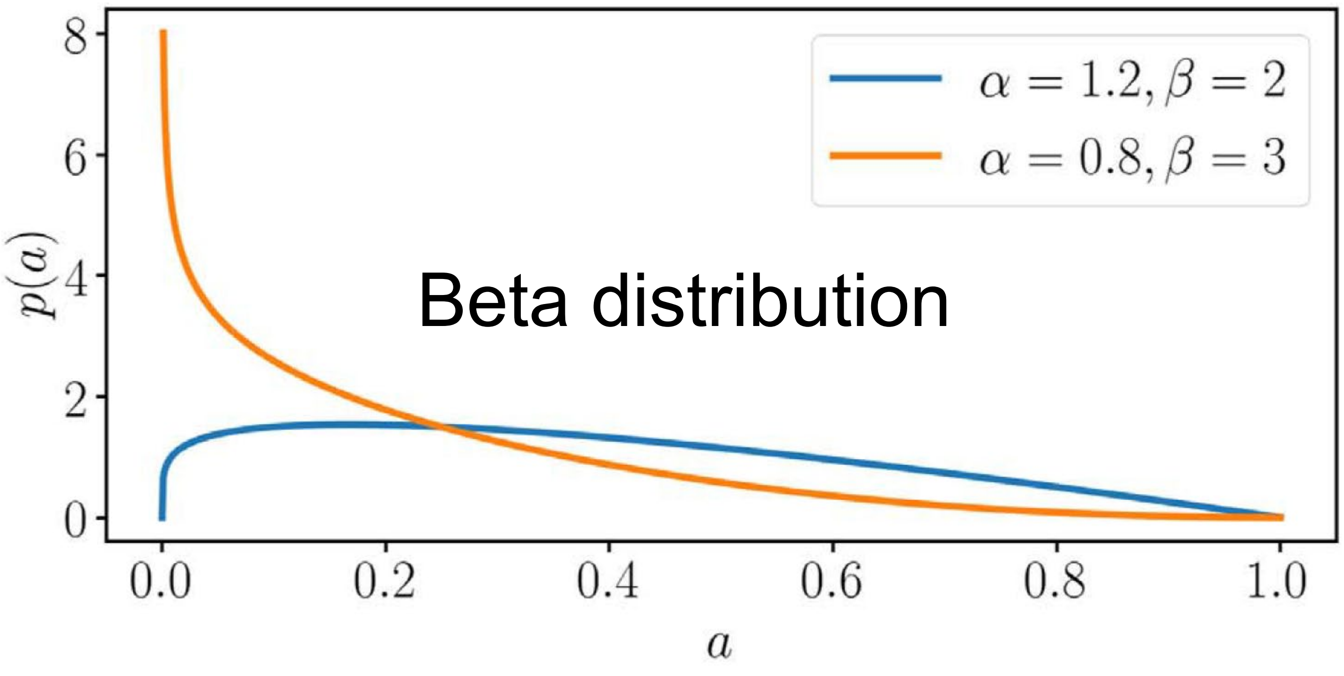

t_1, t_2: Tilt of spin

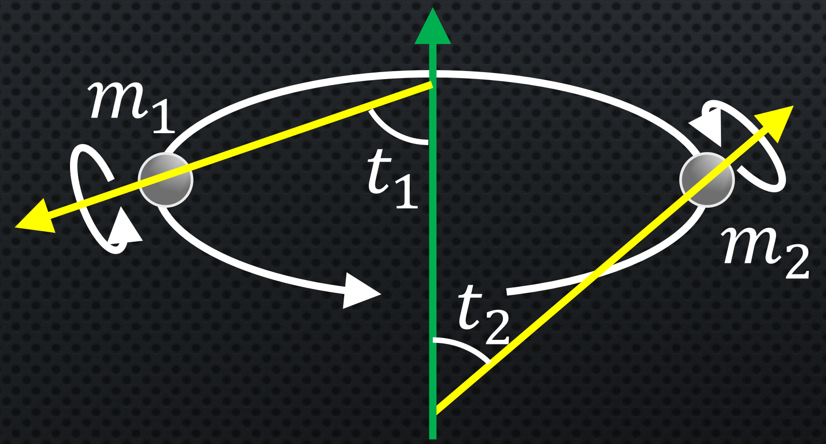

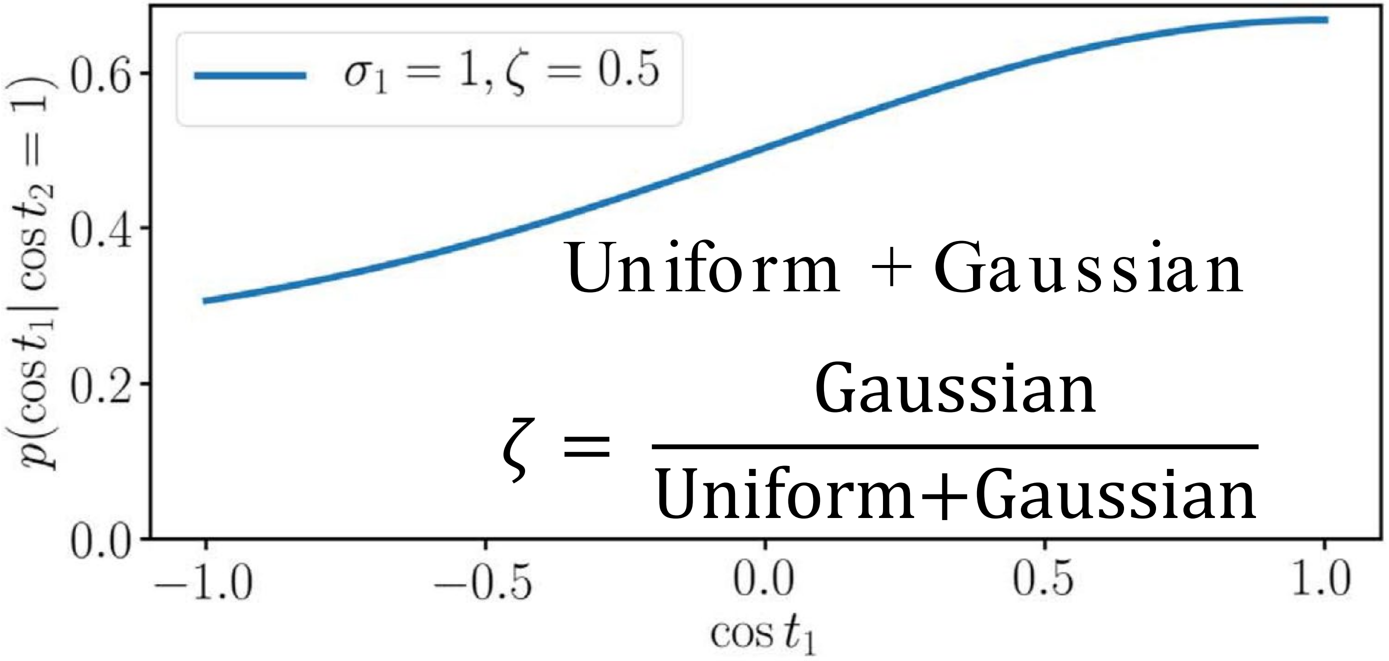

Model parameters

$$\theta = \{\alpha, m_{\mathrm{max}}, m_{\mathrm{min}}, \beta_q, \lambda_{\mathrm{m}}, \mu_{\mathrm{m}}, \sigma_{\mathrm{m}}, \delta_{\mathrm{m}}, \zeta, \sigma_i, \mathrm{E}[a], \mathrm{Var}[a], \lambda\}$$

Likelihood of observed events

$$\mathcal{L}(\{d_i\}|\theta)$$

d_i : i-th detection

Bayesian inference of model parameters

$$\mathcal{L}(\theta|\{d_i\}) = \frac{\mathcal{L}(\{d_i\}|\theta)\mathcal{L}(\theta)}{\mathcal{L}(\{d_i\})}$$

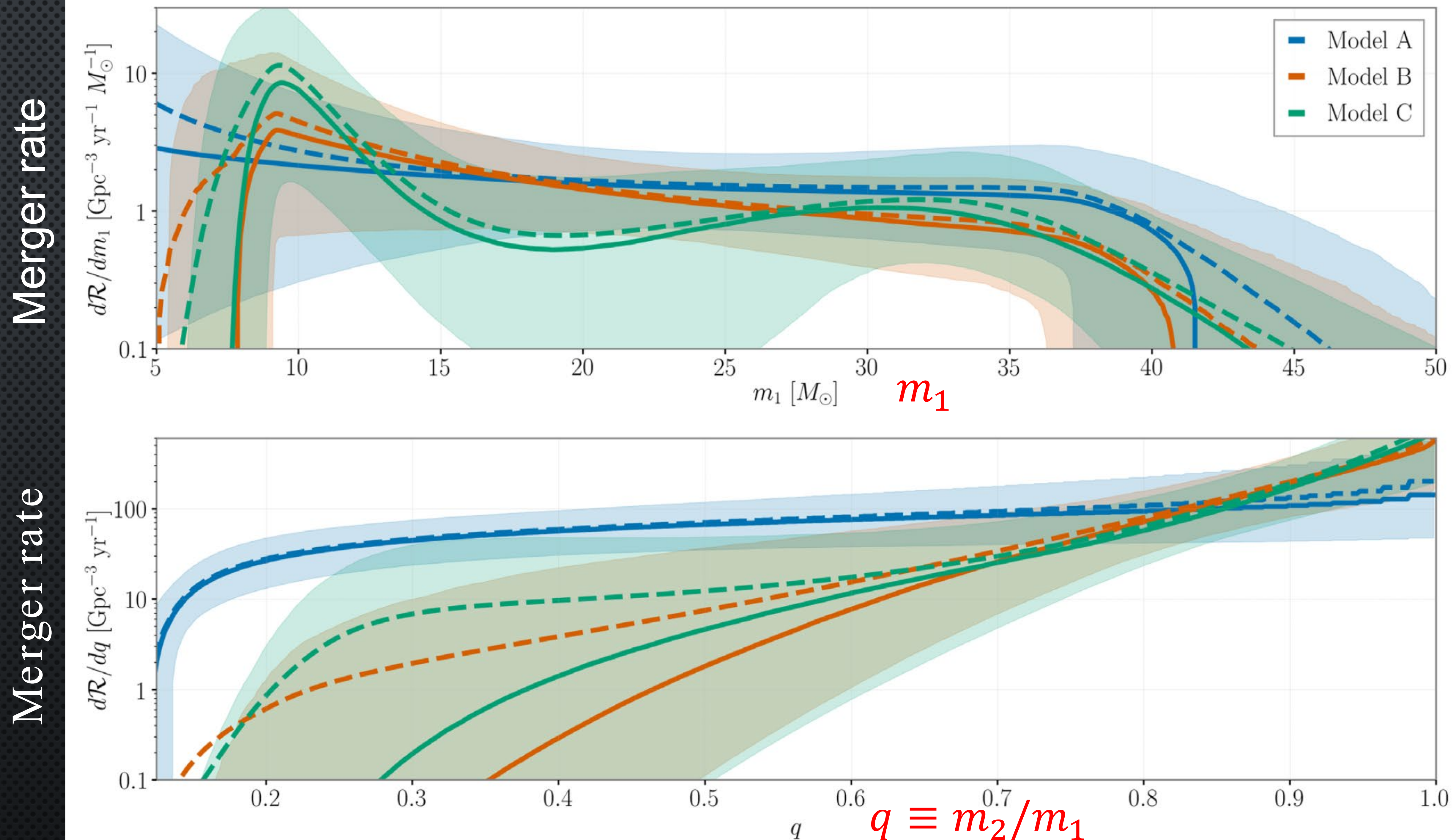

Merger rate
Merger rate
Model A
Model B
Model C
$d\mathcal{R}/dm_1$ [Gpc^{-3} yr^{-1} $M_\odot^{-1}$]
m_1 [$M_\odot$]
m_1
$d\mathcal{R}/dq$ [Gpc^{-3} yr^{-1}]
q
$q \equiv m_2/m_1$

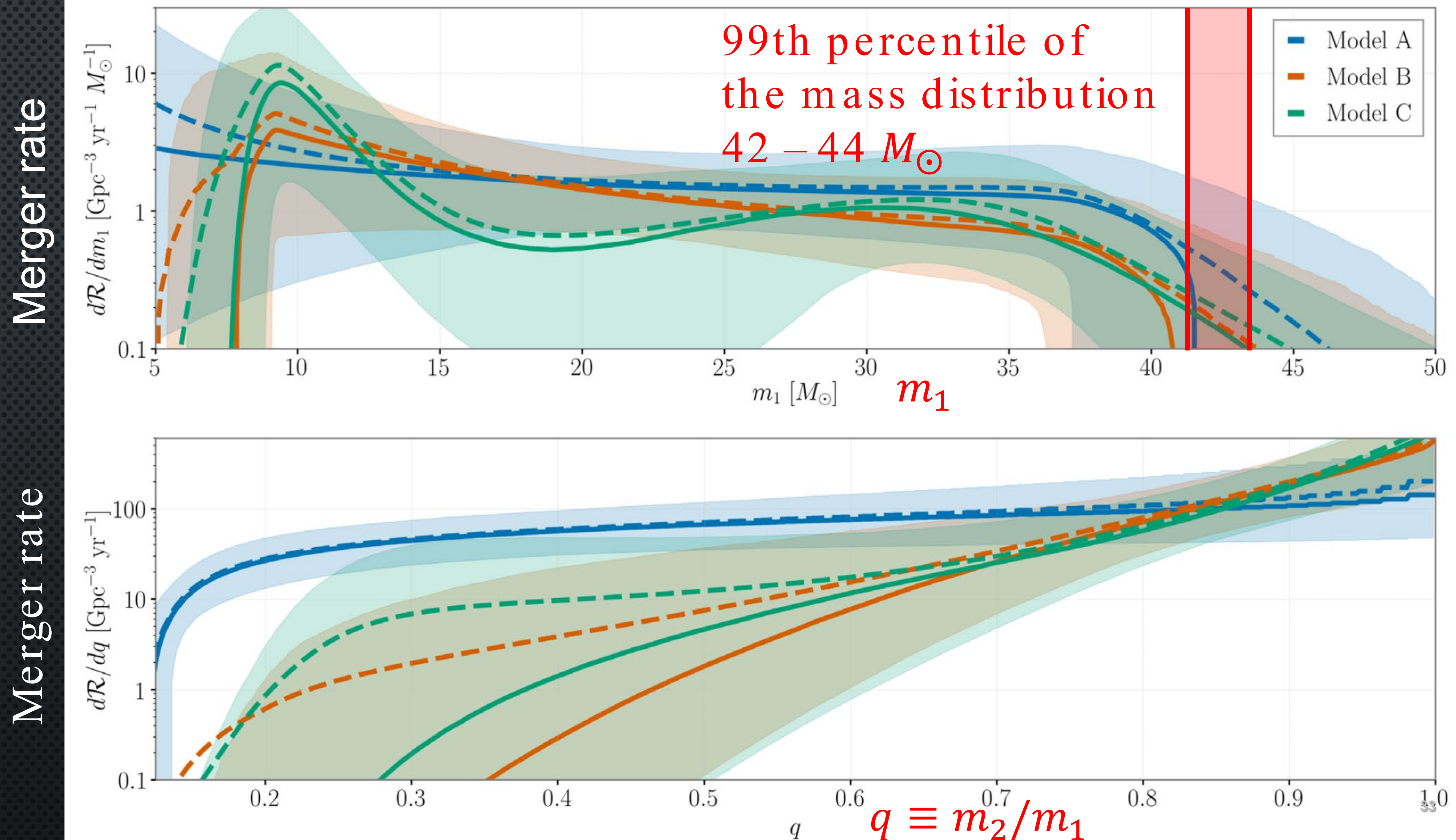
Merger rate
Merger rate
99th percentile of
the mass distribution
42 – 44 $M_\odot$
Model A
Model B
Model C
$d\mathcal{R}/dm_1$ [Gpc^{-3} yr^{-1} $M_\odot^{-1}$]
m_1 [$M_\odot$]
m_1
$d\mathcal{R}/dq$ [Gpc^{-3} yr^{-1}]
q
$q \equiv m_2/m_1$

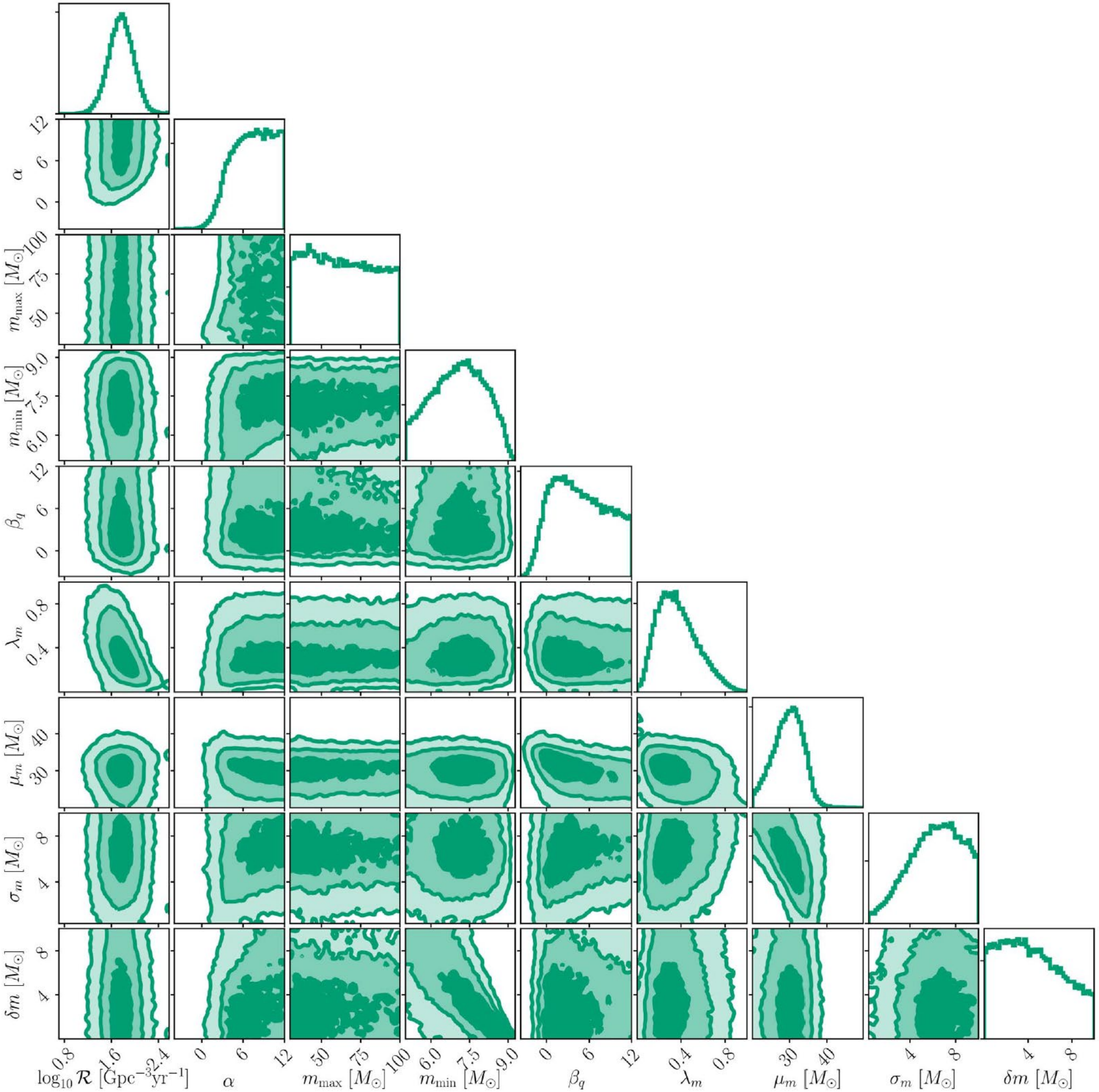

$\log_{10}\mathcal{R}\ [\mathrm{Gpc}^{-3}\mathrm{yr}^{-1}]$
α
$m_{\rm max}\ [M_\odot]$
$m_{\rm min}\ [M_\odot]$
β_q
λ_m
$\mu_m\ [M_\odot]$
$\sigma_m\ [M_\odot]$
$\delta m\ [M_\odot]$

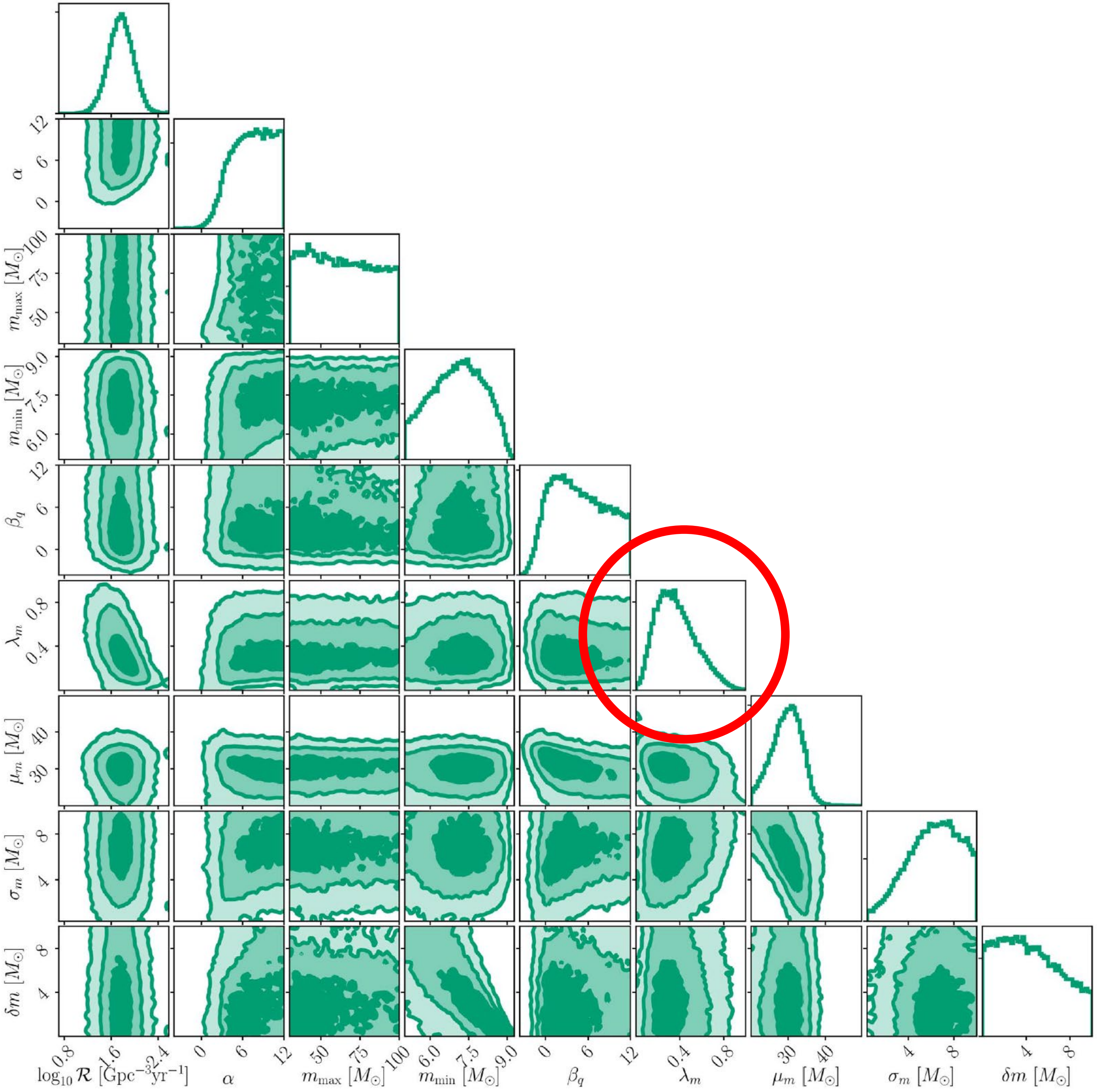
$\log_{10}\mathcal{R}$ [Gpc^{-3}yr^{-1}]
α
$m_{\max}$ [$M_\odot$]
$m_{\min}$ [$M_\odot$]
β_q
λ_m
μ_m [$M_\odot$]
σ_m [$M_\odot$]
δm [$M_\odot$]

Ratio of the Gaussian component in mass spectrum

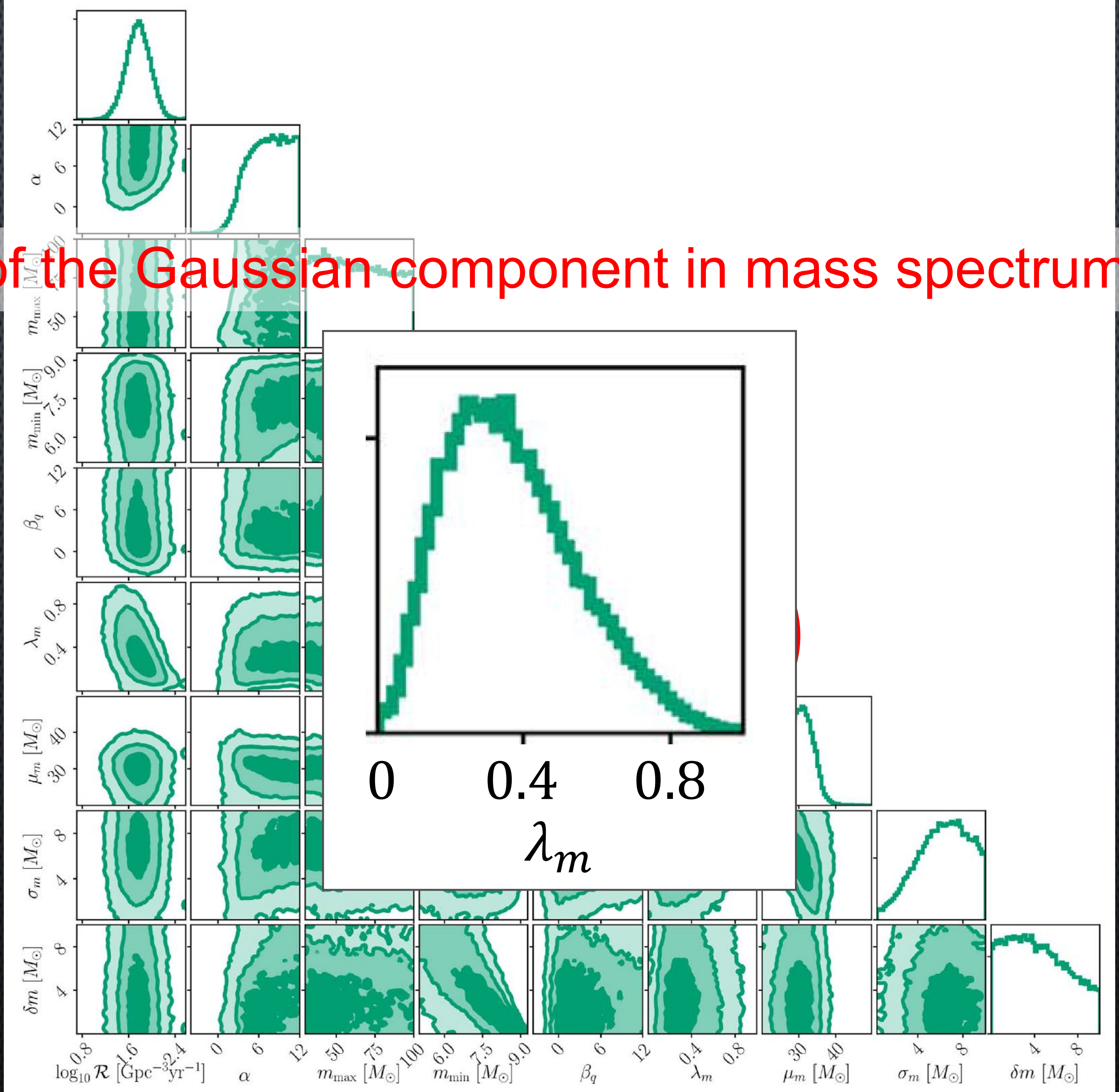

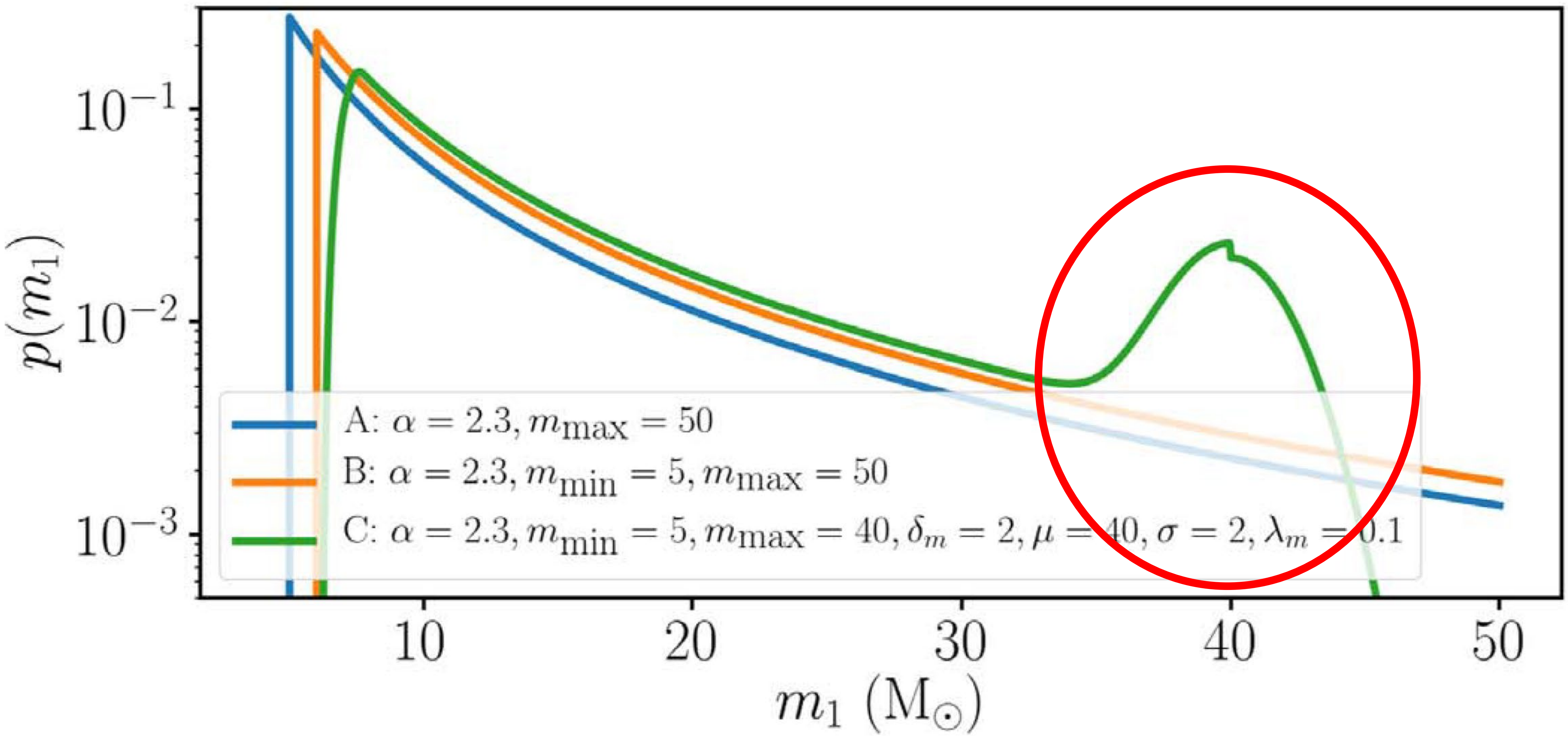

$p(m_1)$
10^{-1}
10^{-2}
10^{-3}
A: $\alpha = 2.3, m_{\max} = 50$
B: $\alpha = 2.3, m_{\min} = 5, m_{\max} = 50$
C: $\alpha = 2.3, m_{\min} = 5, m_{\max} = 40, \delta_m = 2, \mu = 40, \sigma = 2, \lambda_m = 0.1$
10
20
30
40
50
m_1 ($M_\odot$)

Ratio of the Gaussian component in mass spectrum

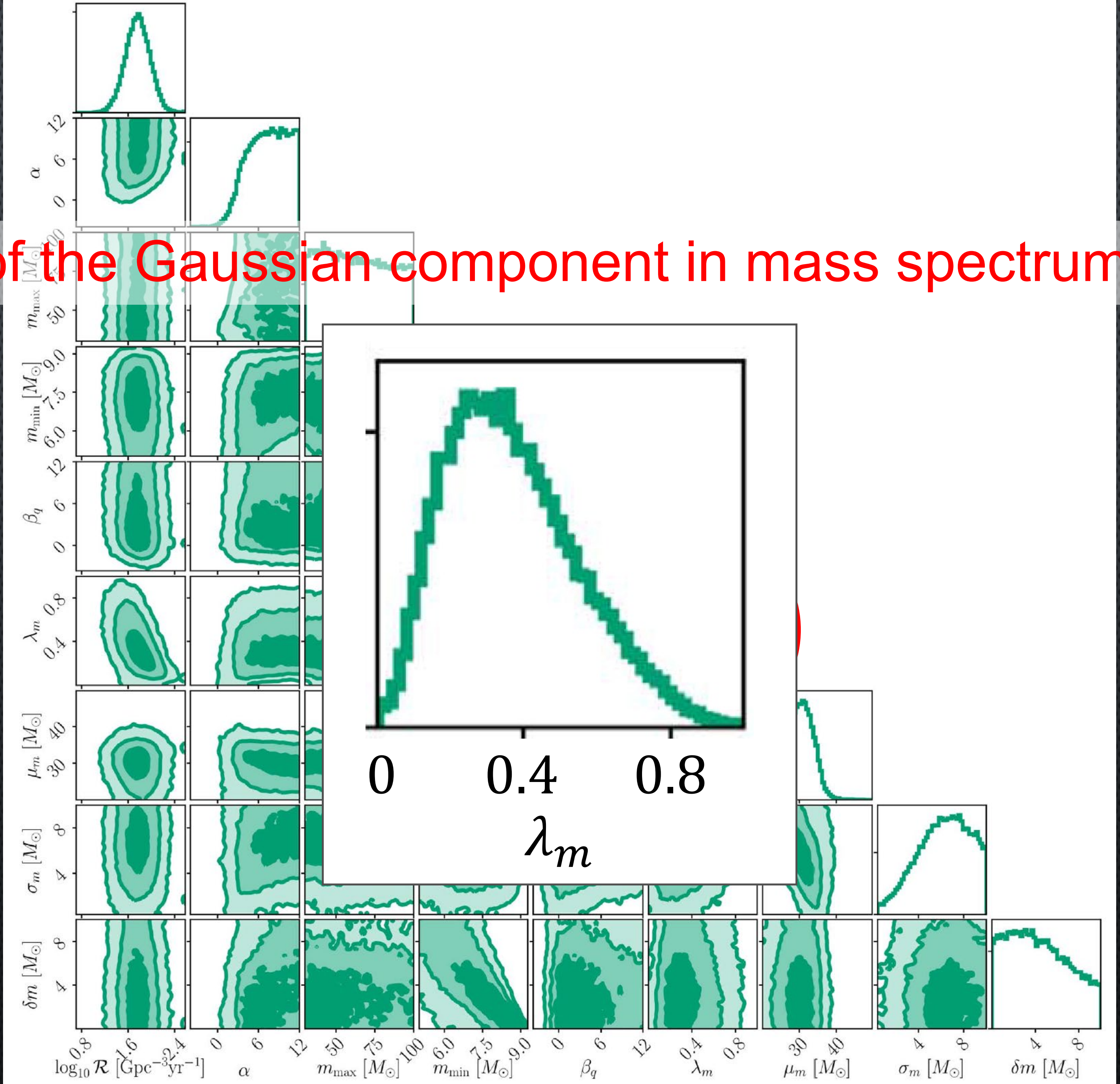

Parametrized Models

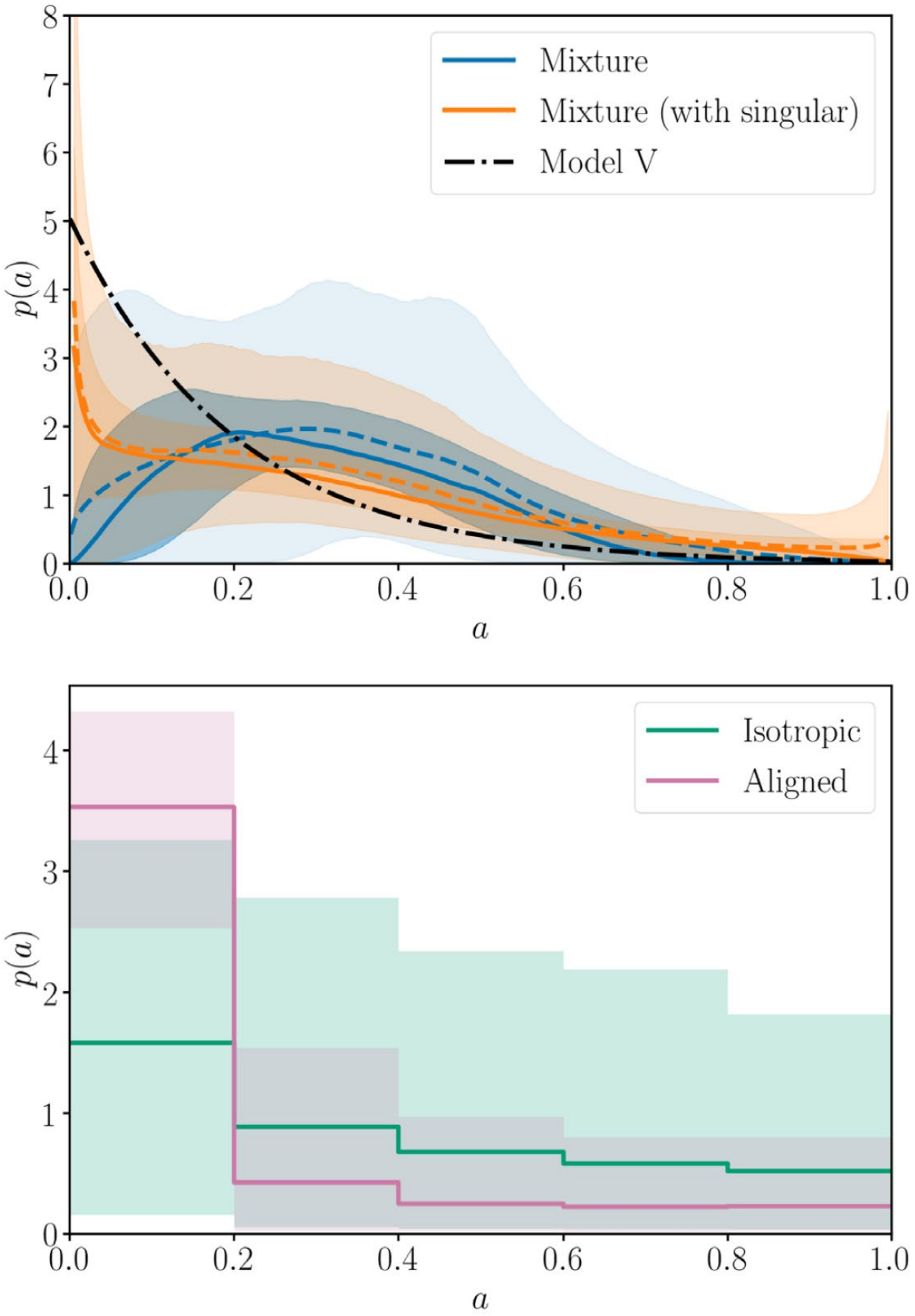

χ_{eff} measurements

Effective Spin Parameter

$$\chi_{\mathrm{eff}} \equiv \frac{m_1 a_1 \cos t_1 + m_2 a_2 \cos t_2}{m_1 + m_2}$$

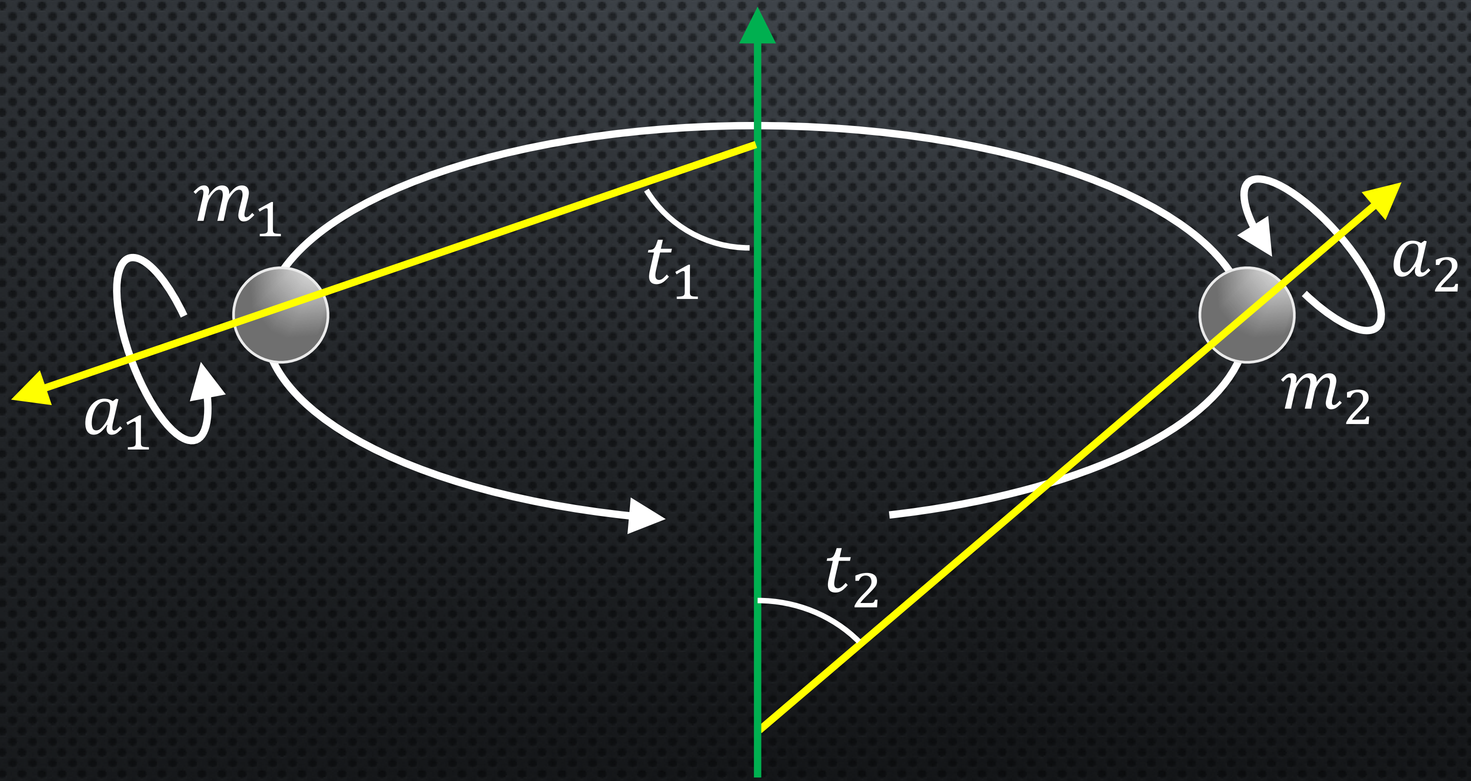

χ_{eff} distribution

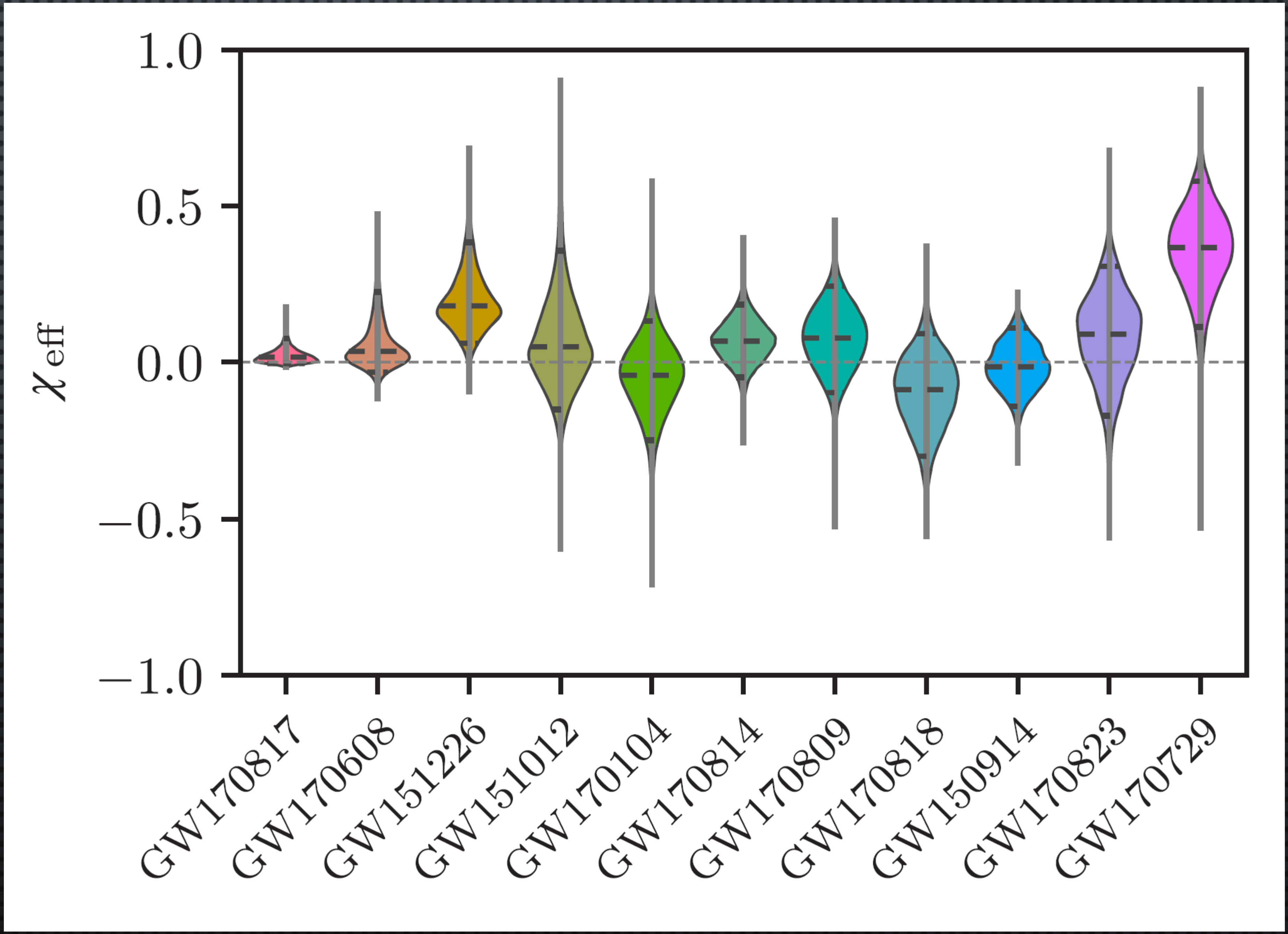

PHYS. REV. X 9, 031040 (2019)

Parametrized Models

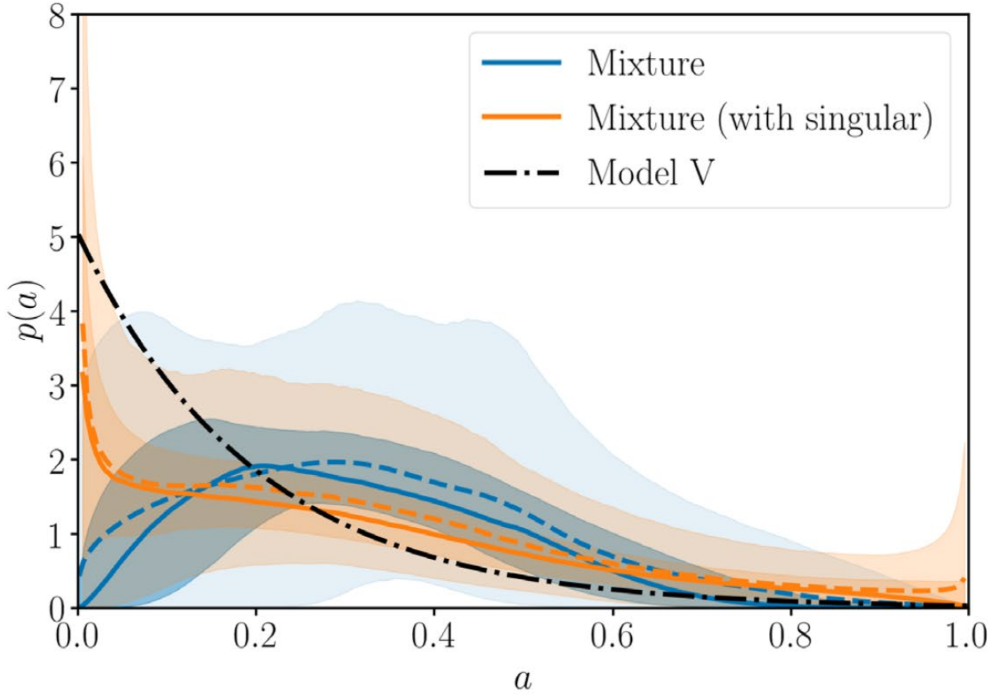

χ_{eff} measurements

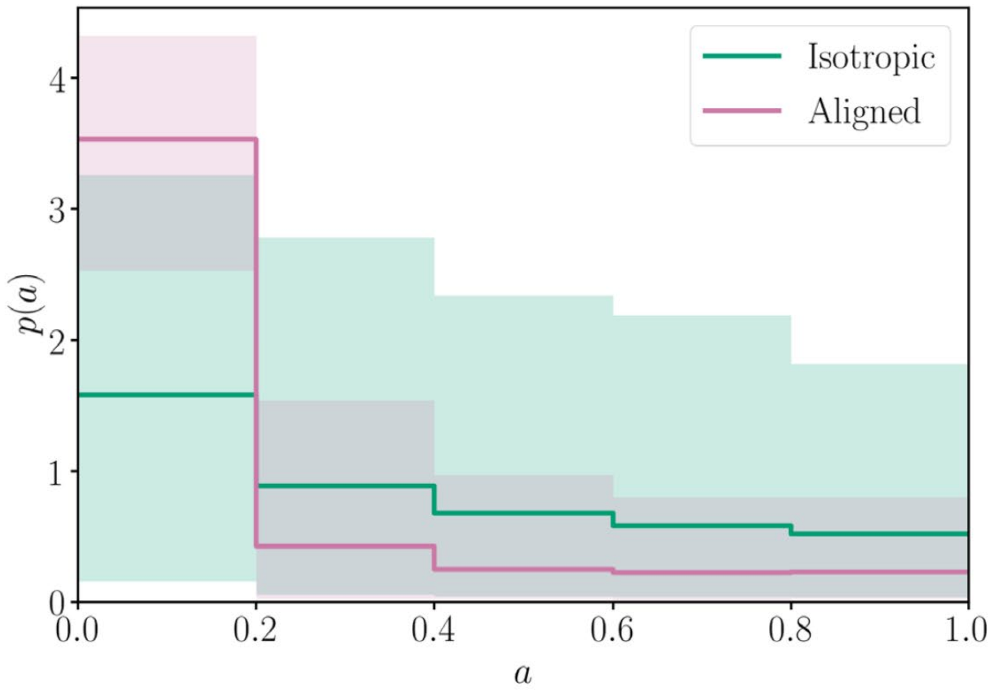

Spin tilt distribution

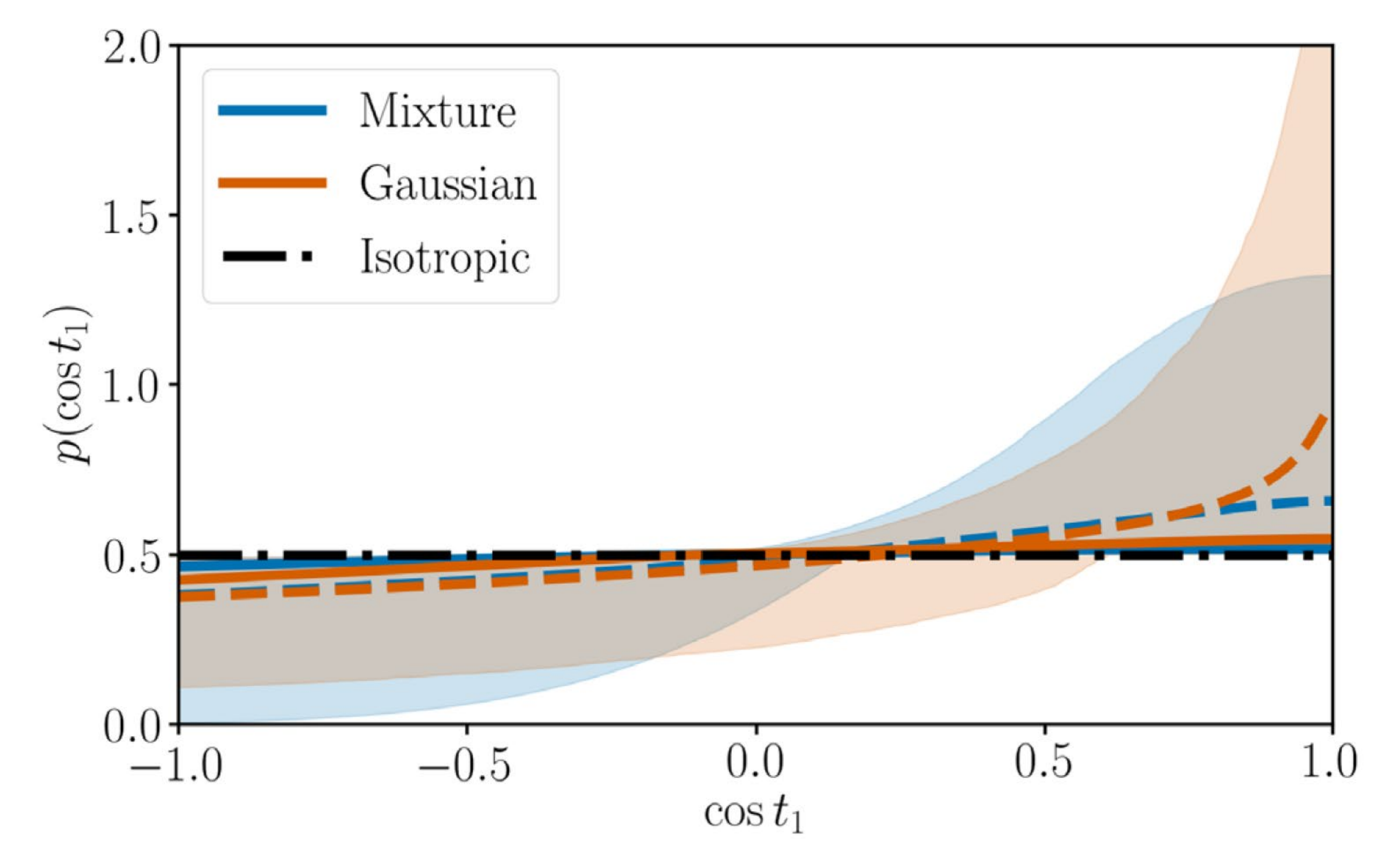

GW170817

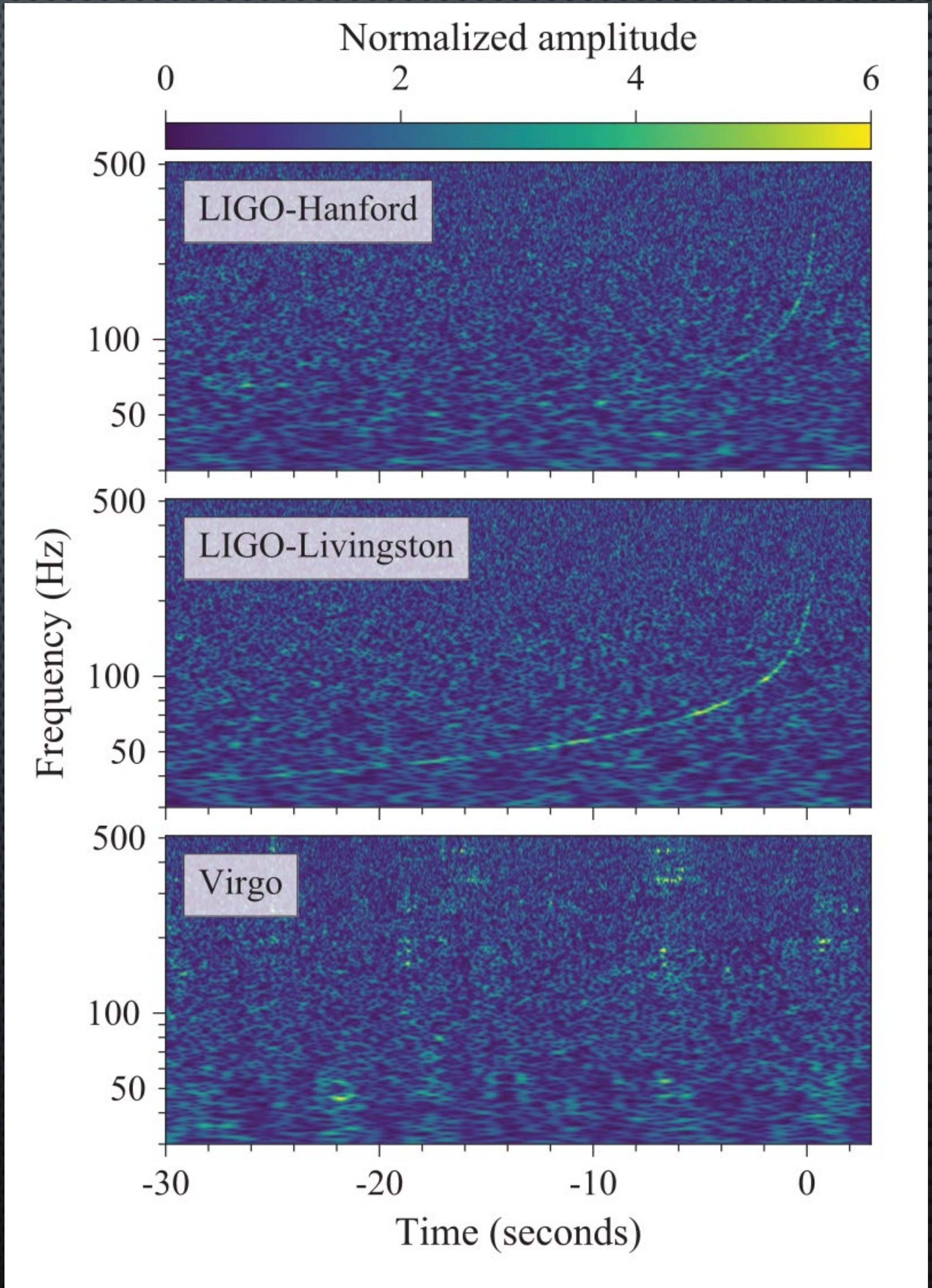

PRL 119, 161101(2017)


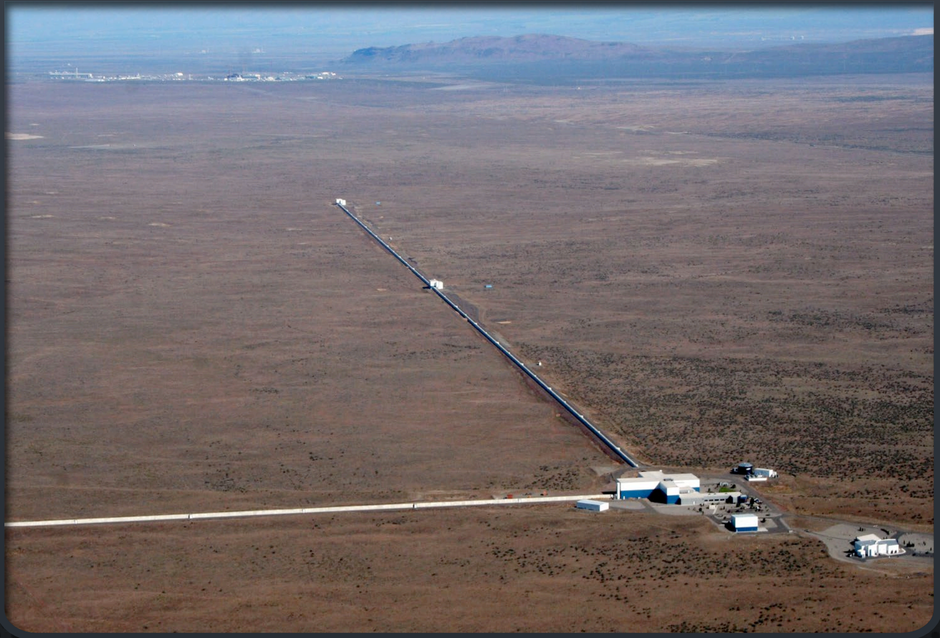


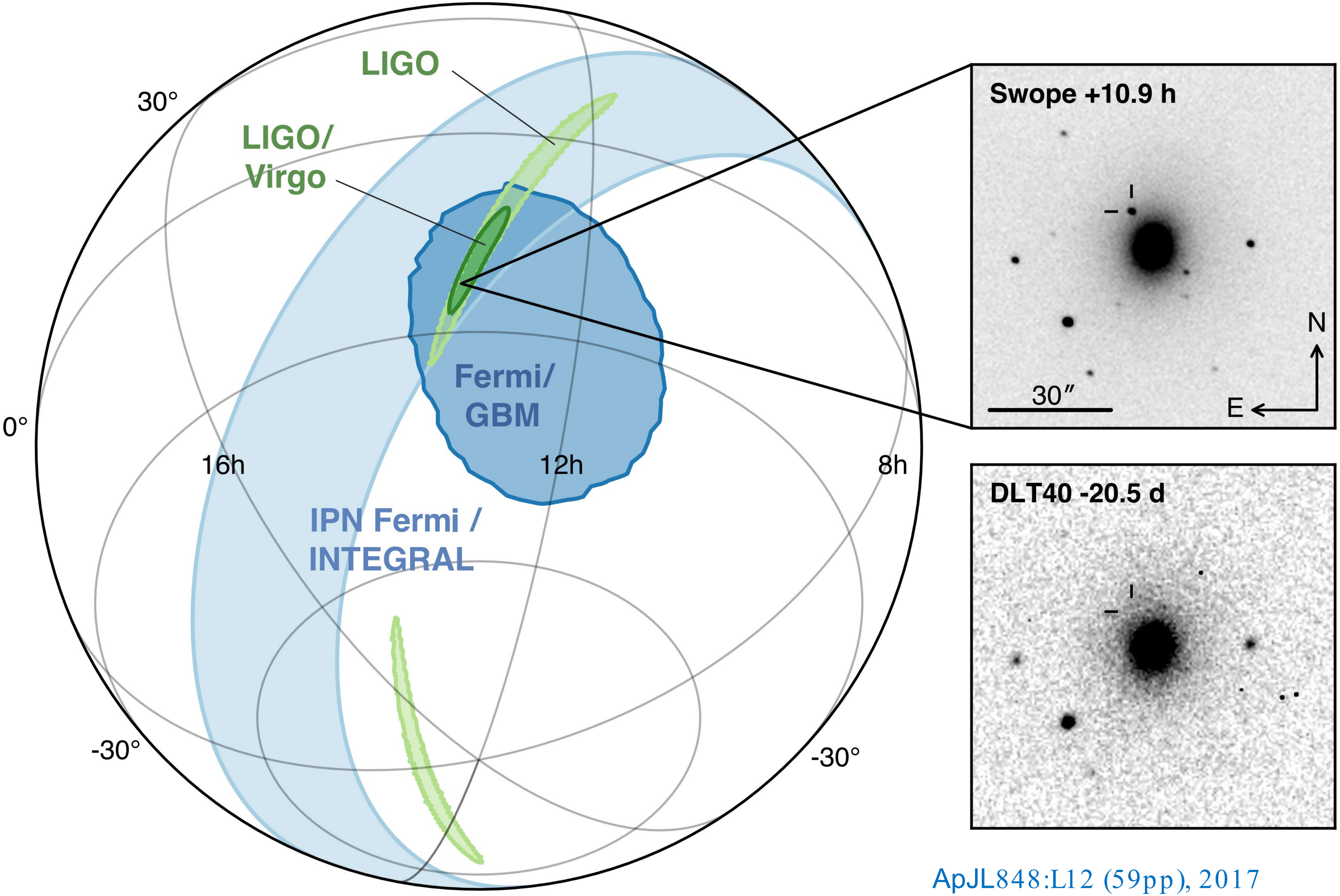

ApJL848:L12 (59pp), 2017

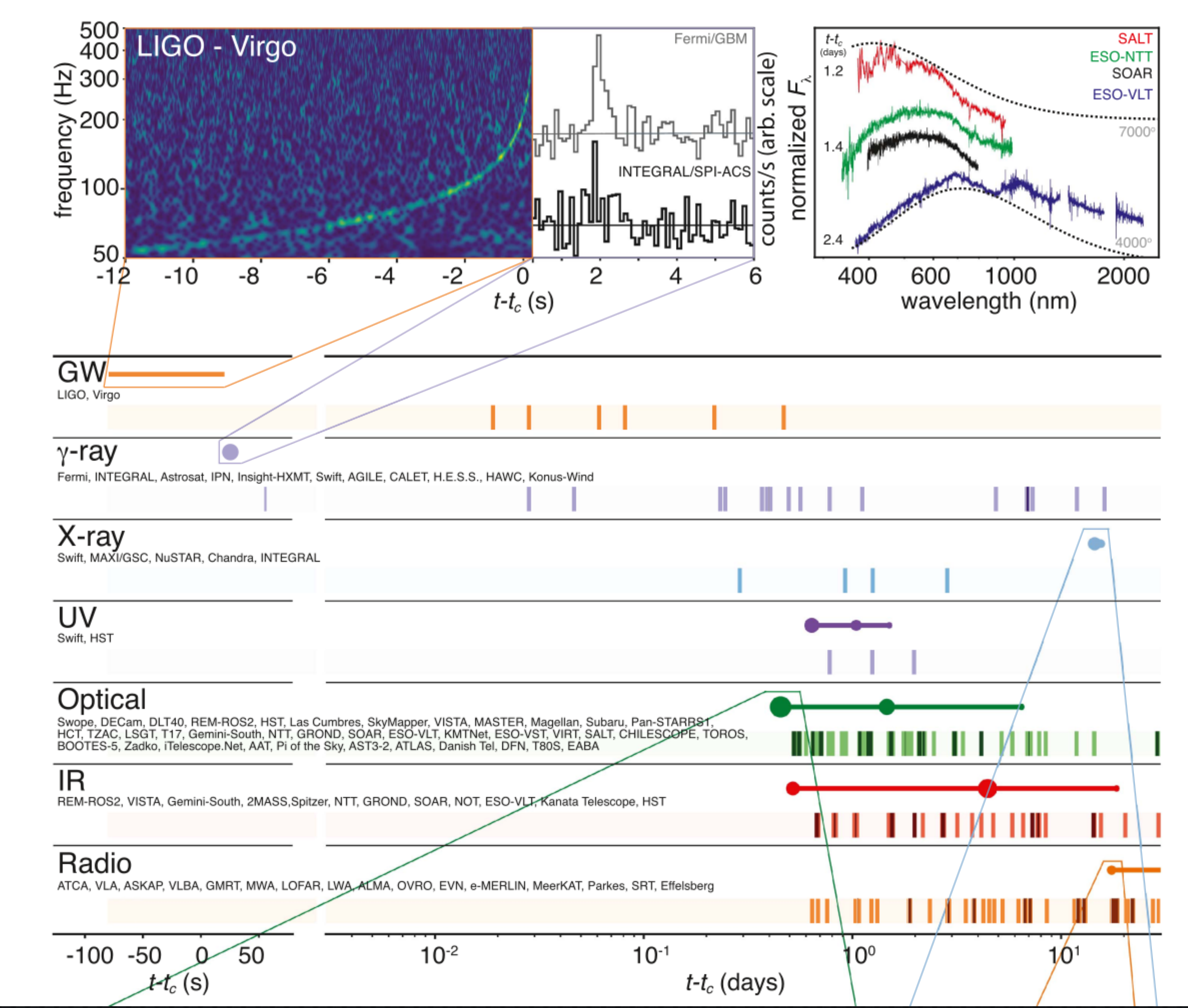

ApJL848:L12 (59pp), 2017

Properties of neutron stars in GW170817

	Low-spin prior ($\chi \leq 0.05$)	High-spin prior ($\chi \leq 0.89$)
Binary inclination θ_{JN}	146^{+25}_{-27} deg	152^{+21}_{-27} deg
Binary inclination θ_{JN} using EM distance constraint [108]	151^{+15}_{-11} deg	153^{+15}_{-11} deg
Detector-frame chirp mass $\mathcal{M}^{\mathrm{det}}$	$1.1975^{+0.0001}_{-0.0001}$ $M_\odot$	$1.1976^{+0.0004}_{-0.0002}$ $M_\odot$
Chirp mass $\mathcal{M}$	$1.186^{+0.001}_{-0.001}$ $M_\odot$	$1.186^{+0.001}_{-0.001}$ $M_\odot$
Primary mass m_1	(1.36, 1.60) $M_\odot$	(1.36, 1.89) $M_\odot$
Secondary mass m_2	(1.16, 1.36) $M_\odot$	(1.00, 1.36) $M_\odot$
Total mass m	$2.73^{+0.04}_{-0.01}$ $M_\odot$	$2.77^{+0.22}_{-0.05}$ $M_\odot$
Mass ratio q	(0.73, 1.00)	(0.53, 1.00)
Effective spin χ_{eff}	$0.00^{+0.02}_{-0.01}$	$0.02^{+0.08}_{-0.02}$
Primary dimensionless spin χ_1	(0.00, 0.04)	(0.00, 0.50)
Secondary dimensionless spin χ_2	(0.00, 0.04)	(0.00, 0.61)
Tidal deformability $\tilde{\Lambda}$ with flat prior	300^{+500}_{-190} (symmetric)/300^{+420}_{-230} (HPD)	(0, 630)

PHYSICAL REVIEW X 9, 011001 (2019)

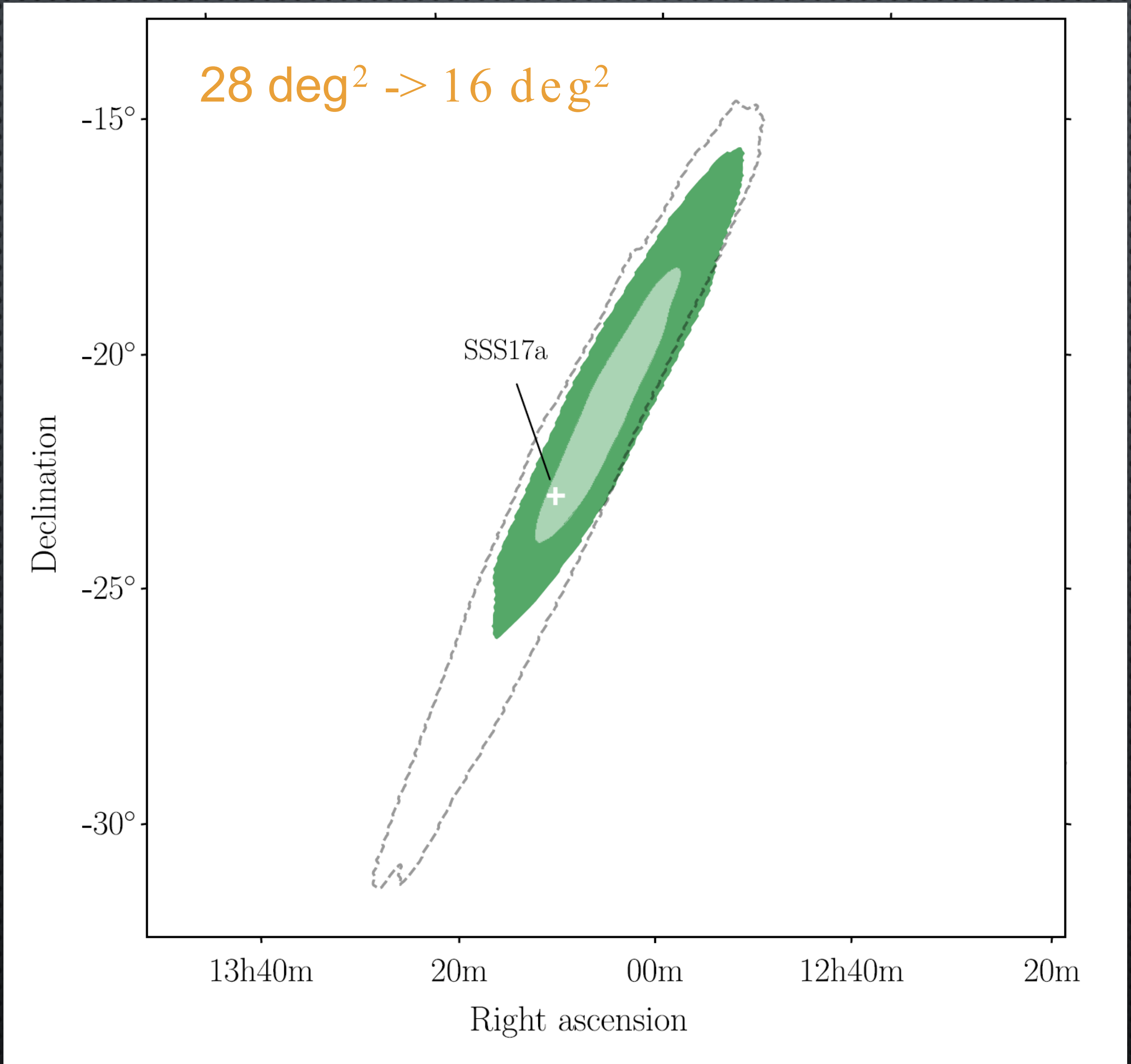
28 deg² -> 16 deg²
-15°
-20°
-25°
-30°
Declination
SSS17a
13h40m
20m
00m
12h40m
20m
Right ascension

Prior for spin

Dimension less spin parameter: $\chi \equiv |c\vec{S}/(Gm^2)|$

High Spin Prior

$$\chi < 0.89$$

Low Spin Prior

$$\chi < 0.05$$

Mass posterior

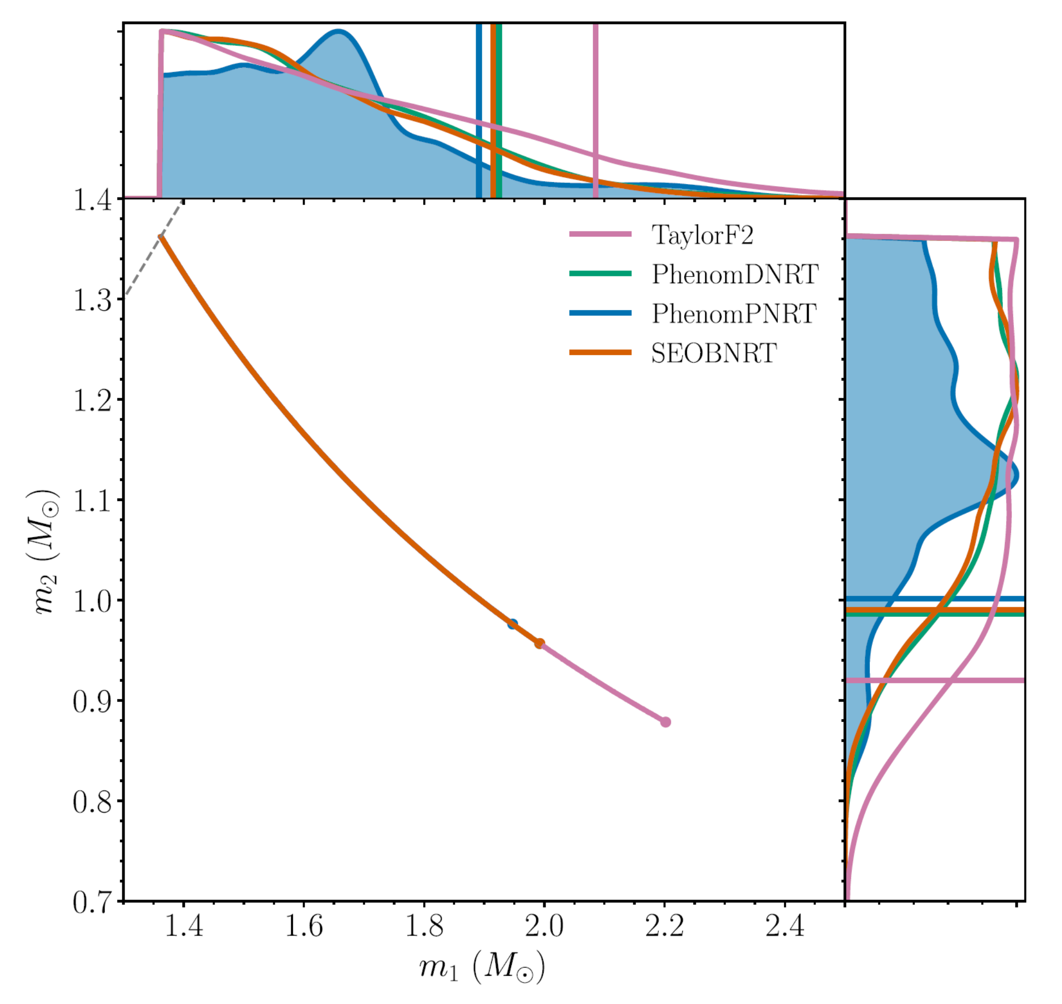

High Spin

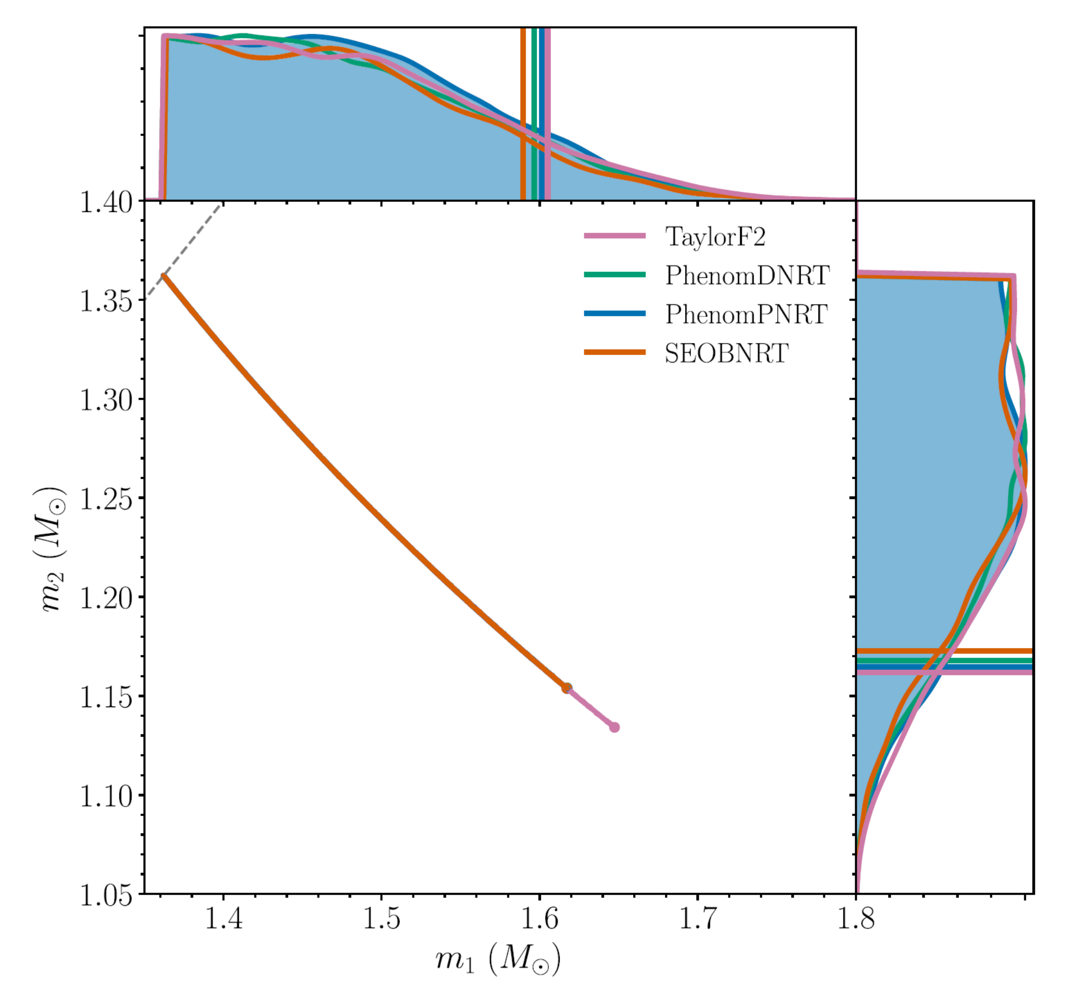

Low Spin

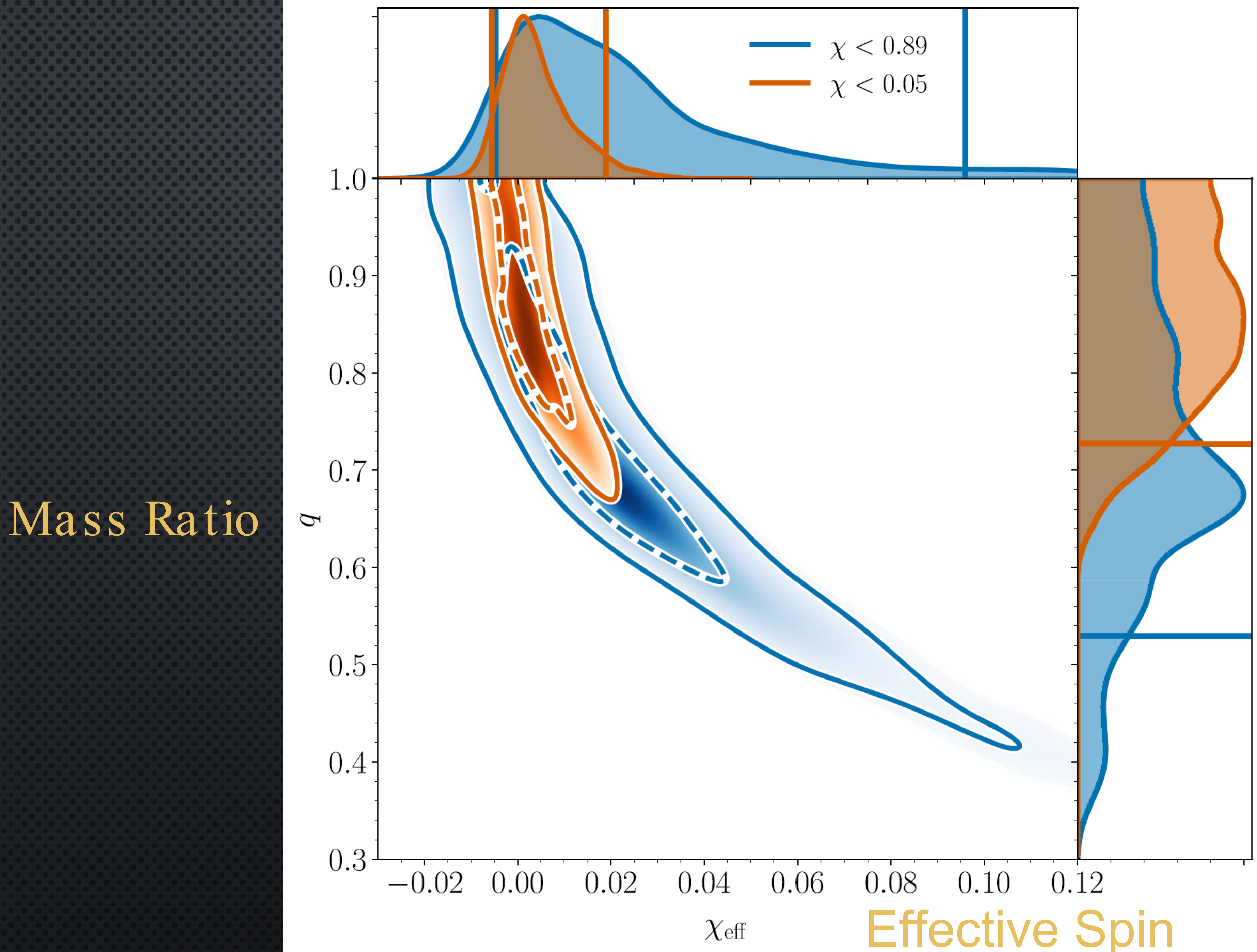
Mass Ratio
$\chi < 0.89$
$\chi < 0.05$
1.0
0.9
0.8
0.7
0.6
0.5
0.4
0.3
q
−0.02
0.00
0.02
0.04
0.06
0.08
0.10
0.12
$\chi_{\rm eff}$
Effective Spin

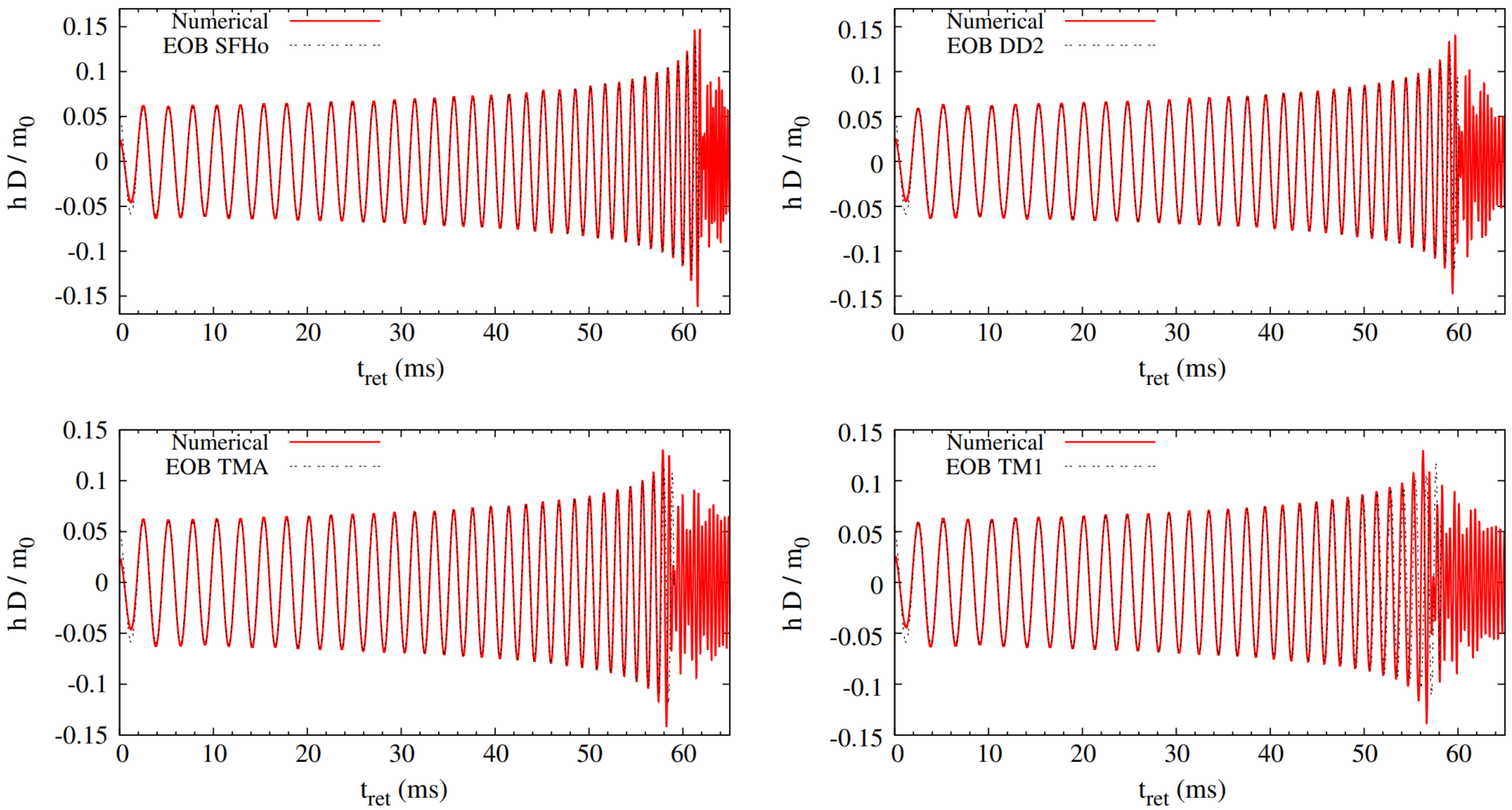

K. Hotokezaka et. al., *Phys. Rev. D* **93**, 064082 (2016)

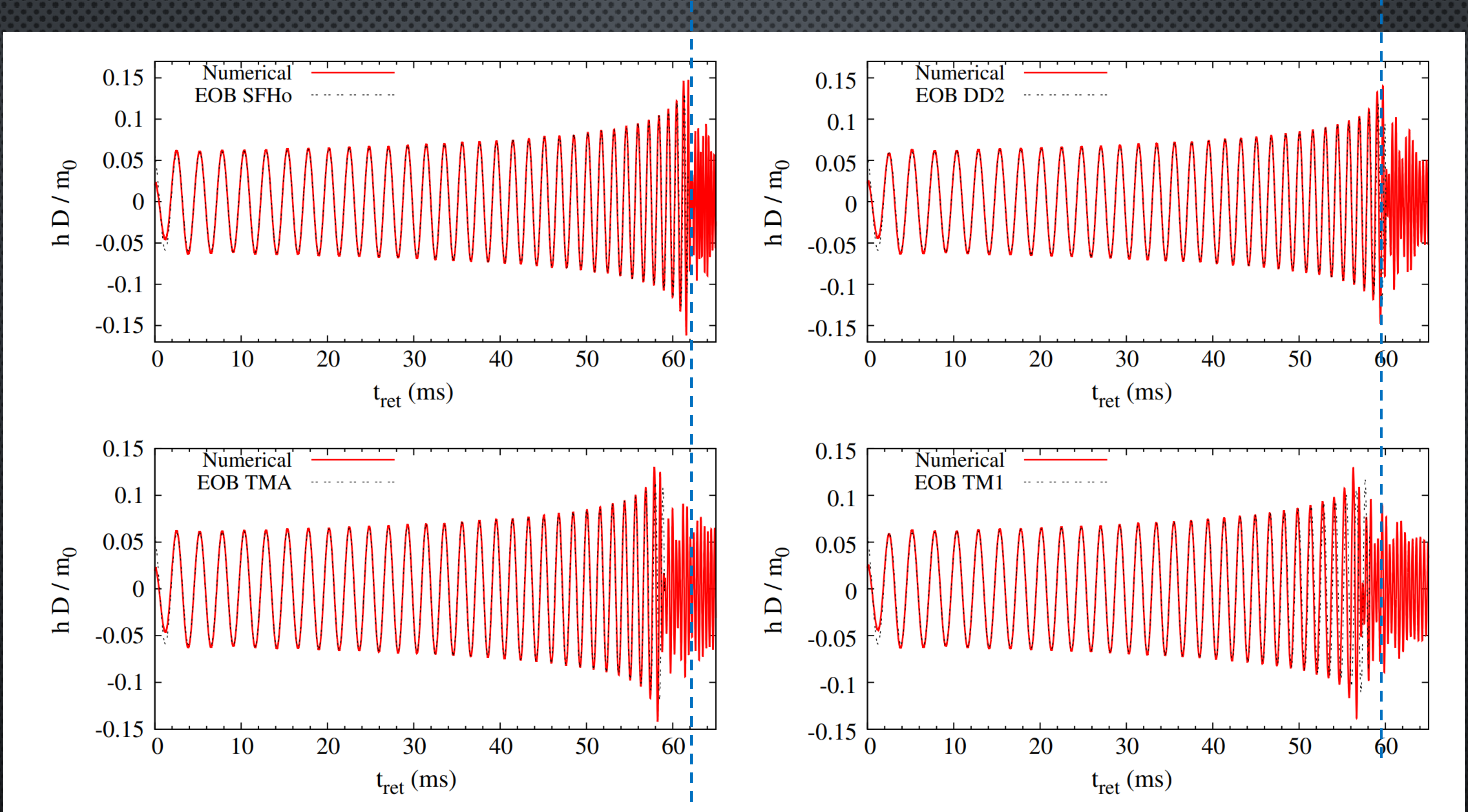

K. Hotokezaka et. al., *Phys. Rev. D* **93**, 064082 (2016)

Tidal deformability

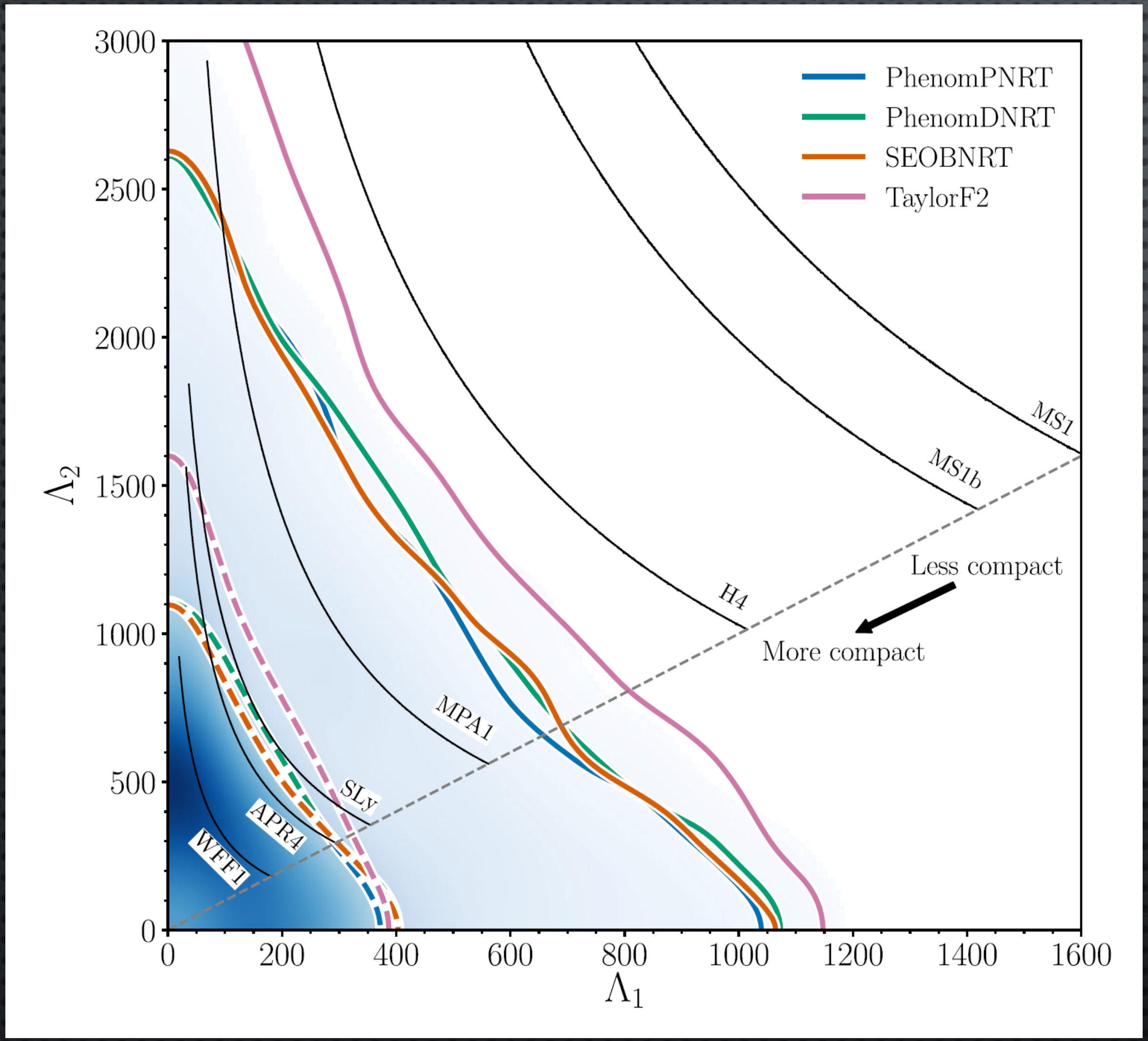

High Spin

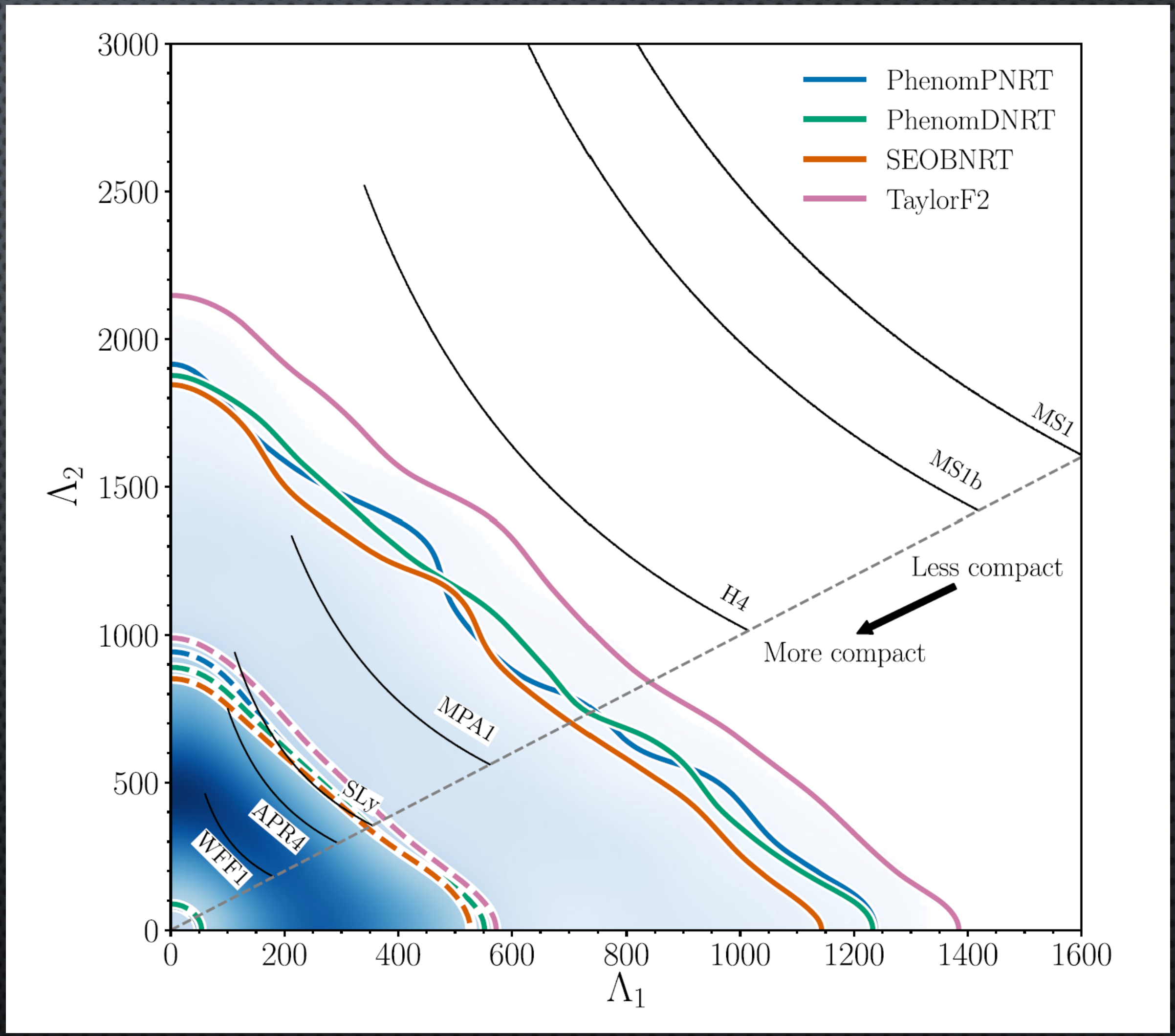

Low Spin

Multi-Messenger Astronomy

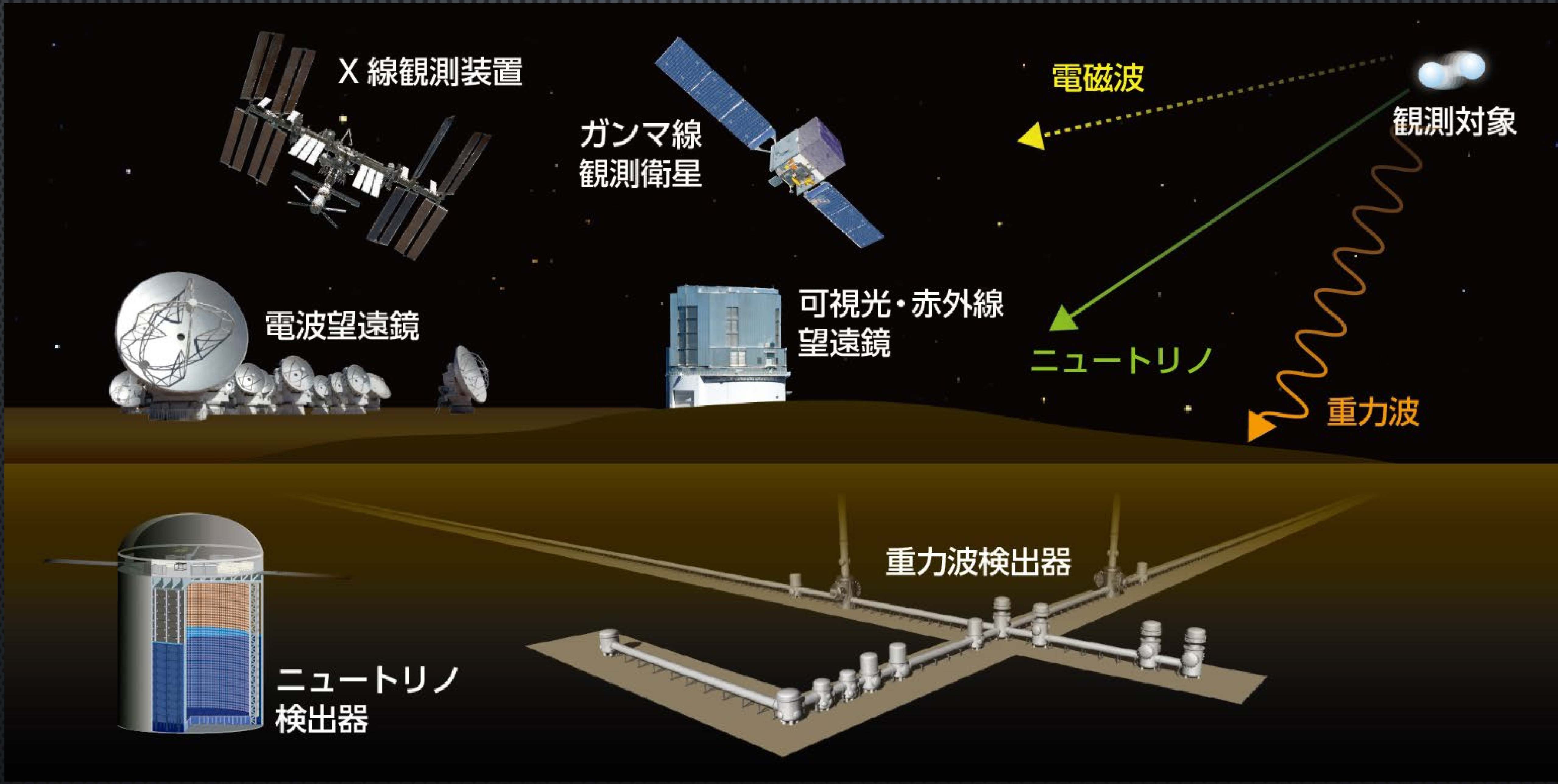

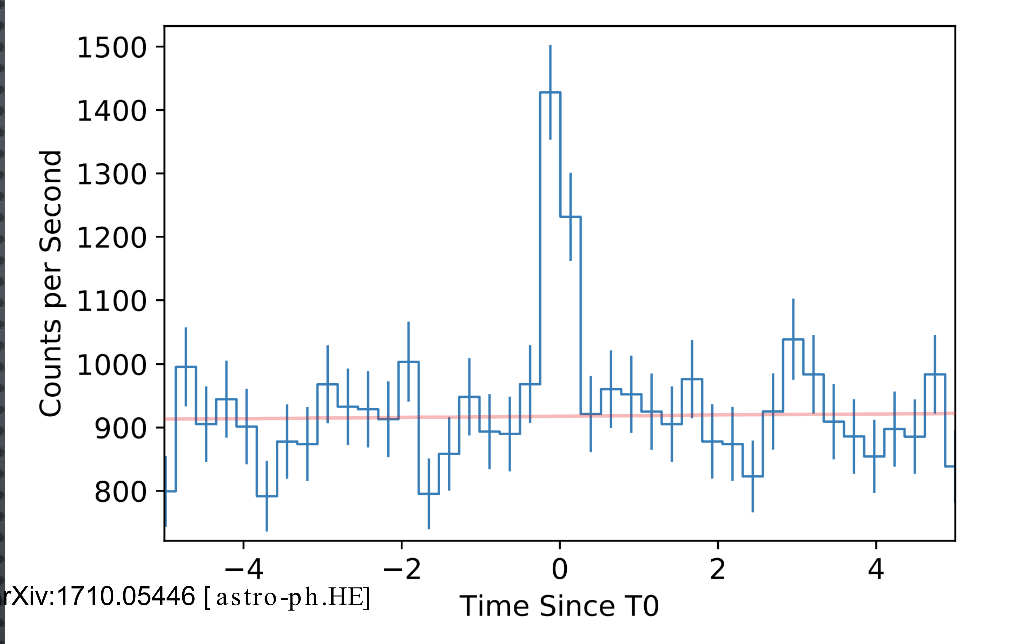

$$\Delta t = 1.7 \text{ sec} \longrightarrow |c_{GW} - 1| < 10^{-15}$$

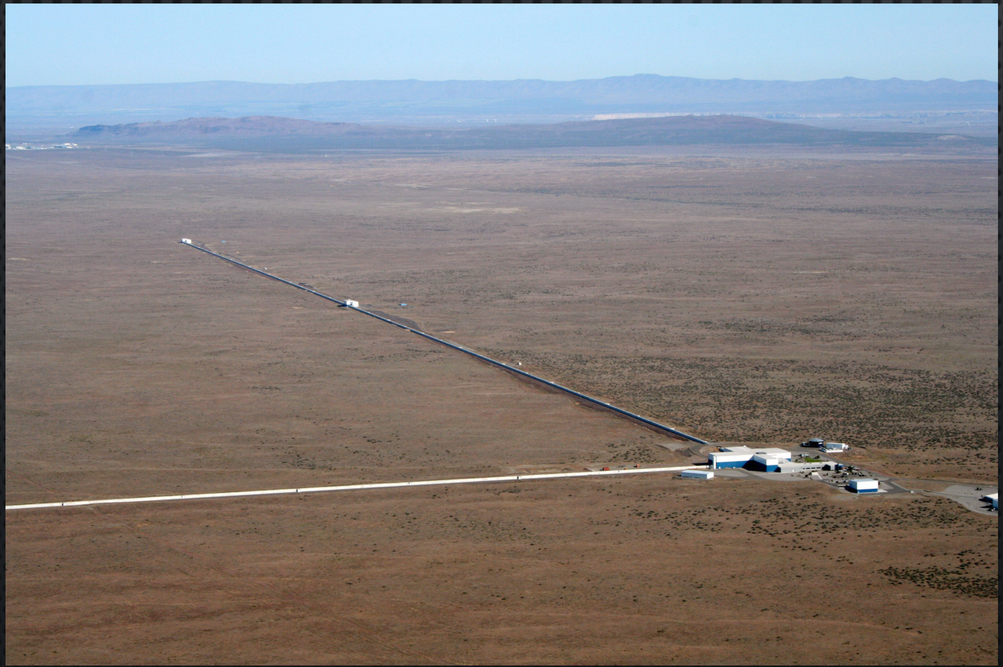

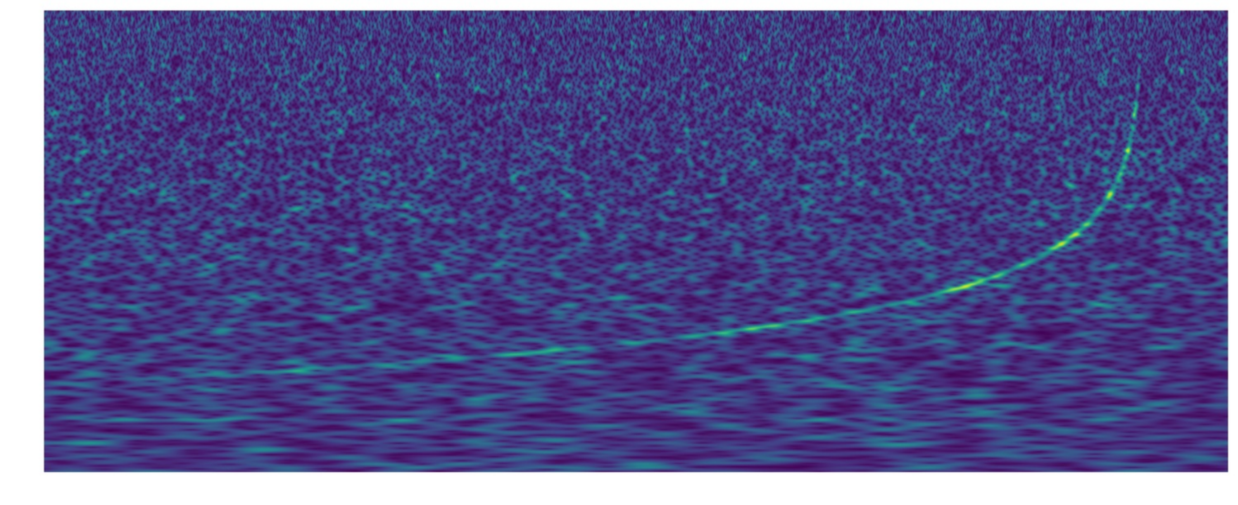

Hubble Constant

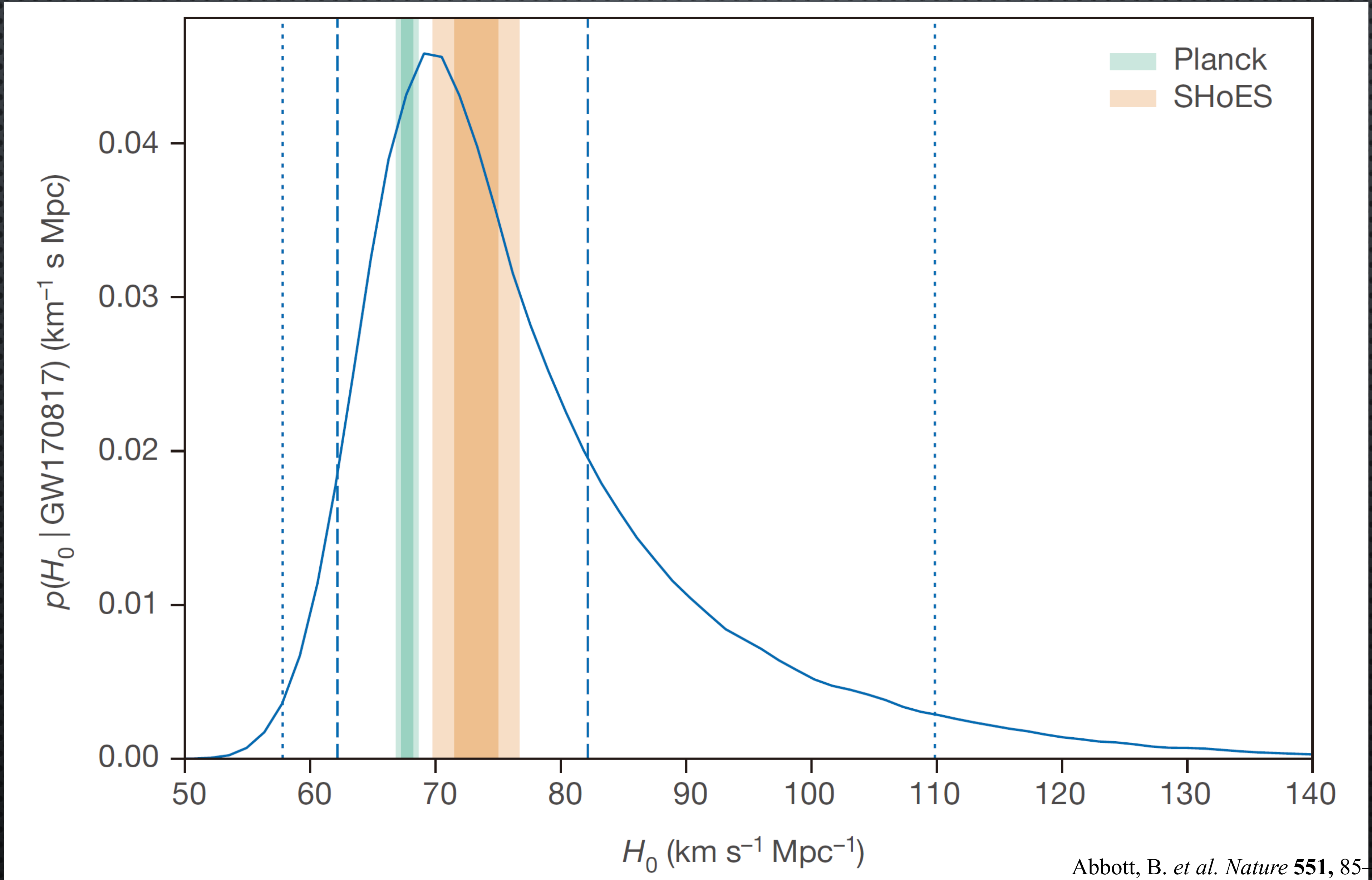

Abbott, B. *et al. Nature* **551,** 85–88 (2017)

2017/8/18-19

2017/8/24-25

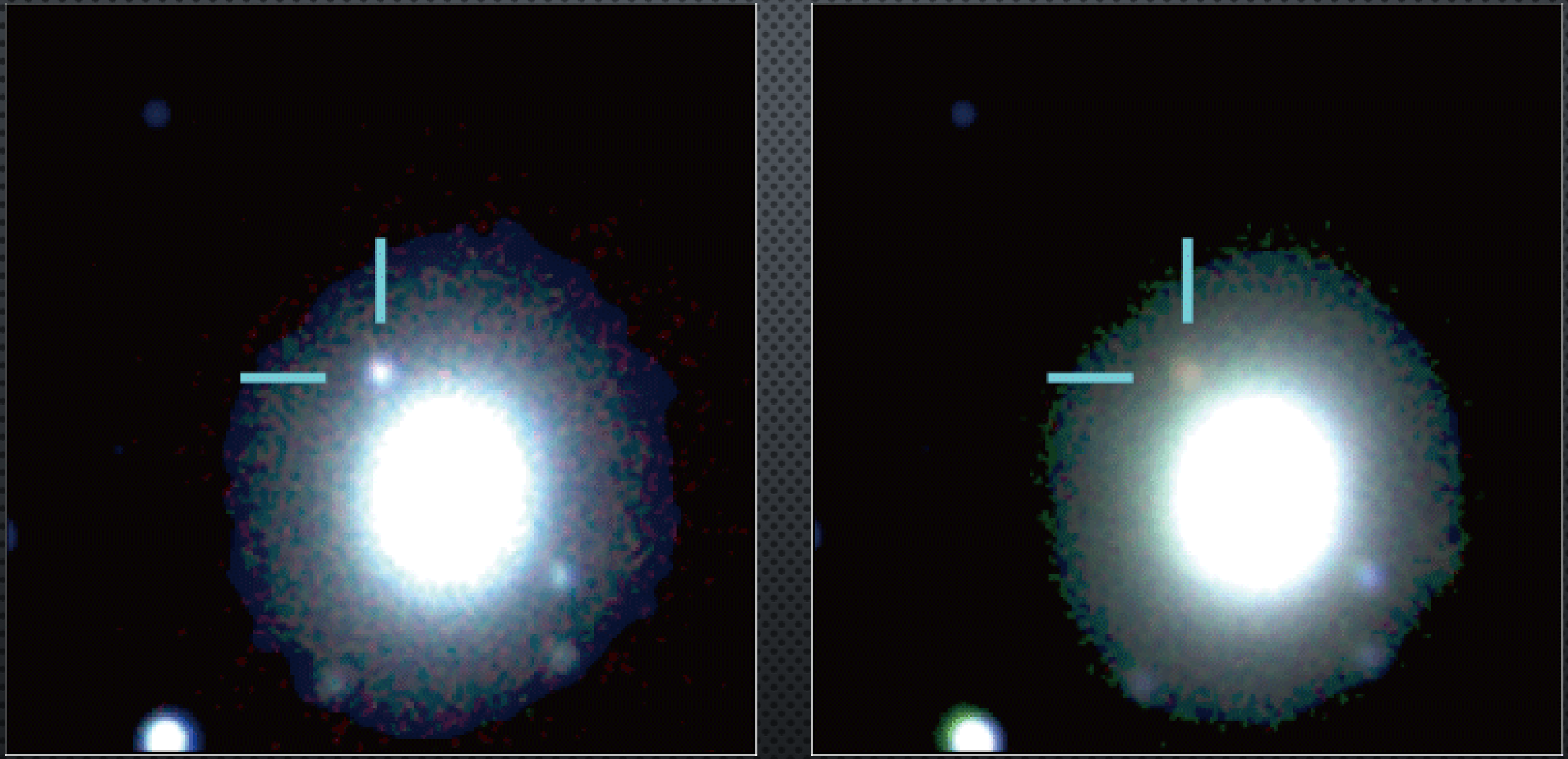

NGC 4993

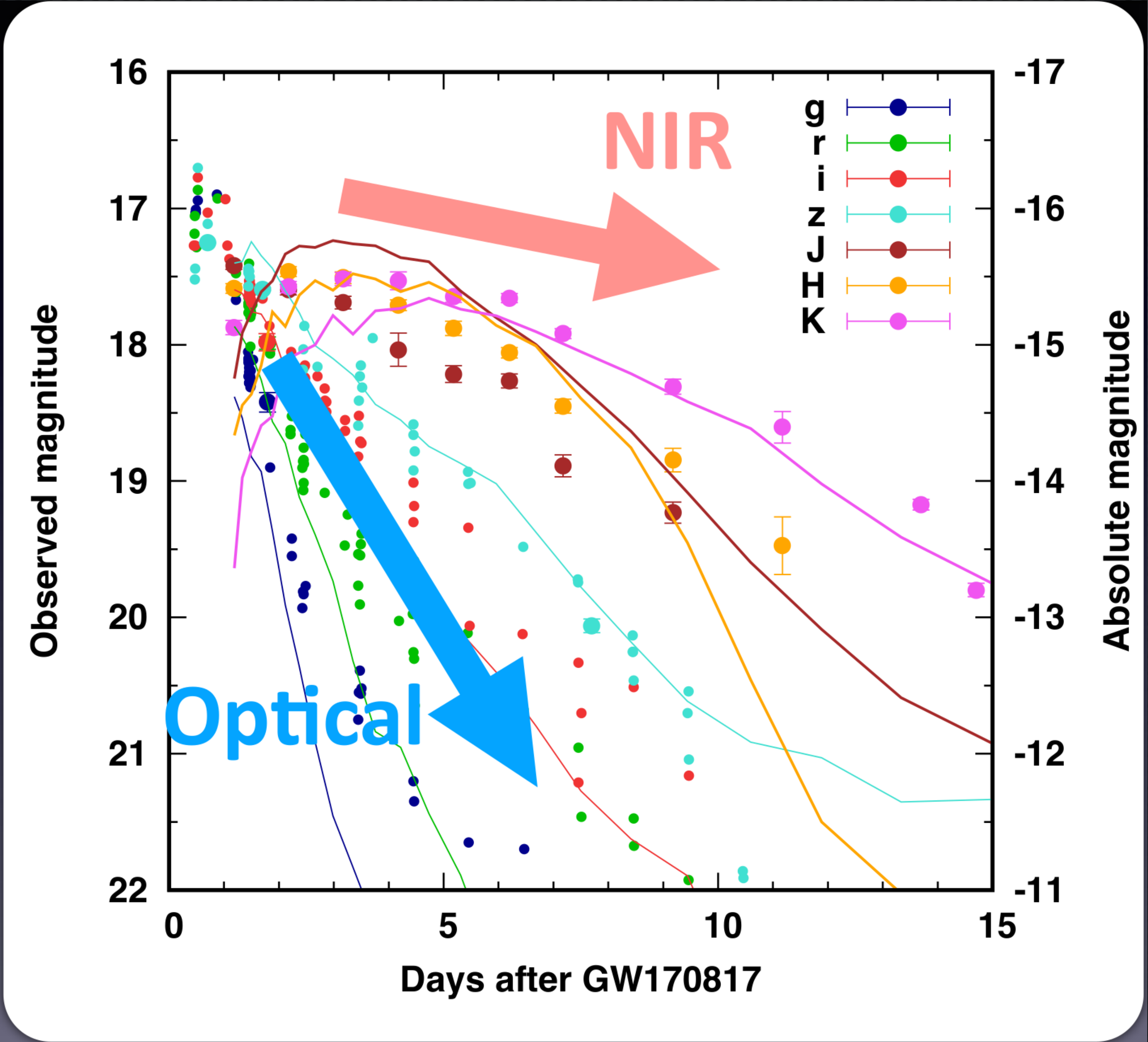

NIR
Optical
g
r
i
z
J
H
K
Observed magnitude
Absolute magnitude
Days after GW170817
16
17
18
19
20
21
22
-17
-16
-15
-14
-13
-12
-11
0
5
10
15

(C) M. Tanaka

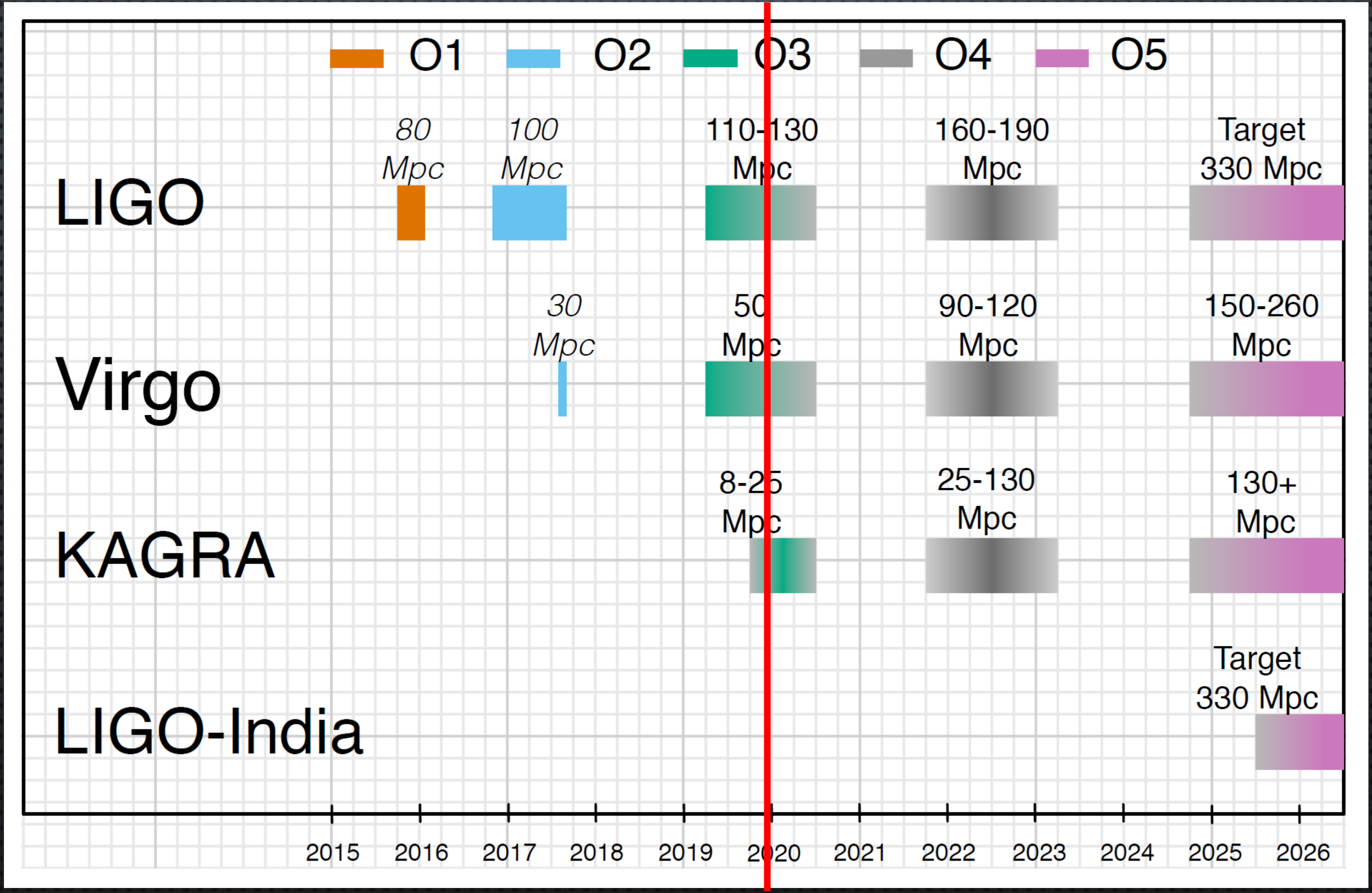

O1
O2
O3
O4
O5
LIGO
Virgo
KAGRA
LIGO-India
80 Mpc
100 Mpc
110-130 Mpc
160-190 Mpc
Target 330 Mpc
30 Mpc
50 Mpc
90-120 Mpc
150-260 Mpc
8-25 Mpc
25-130 Mpc
130+ Mpc
Target 330 Mpc
2015
2016
2017
2018
2019
2020
2021
2022
2023
2024
2025
2026

Now

O3 Open Public Alerts

Black hole + Black hole: 25

Neutron star + Neutron star: 6

Black hole + Neutron star: 5

Mass Gap: 2

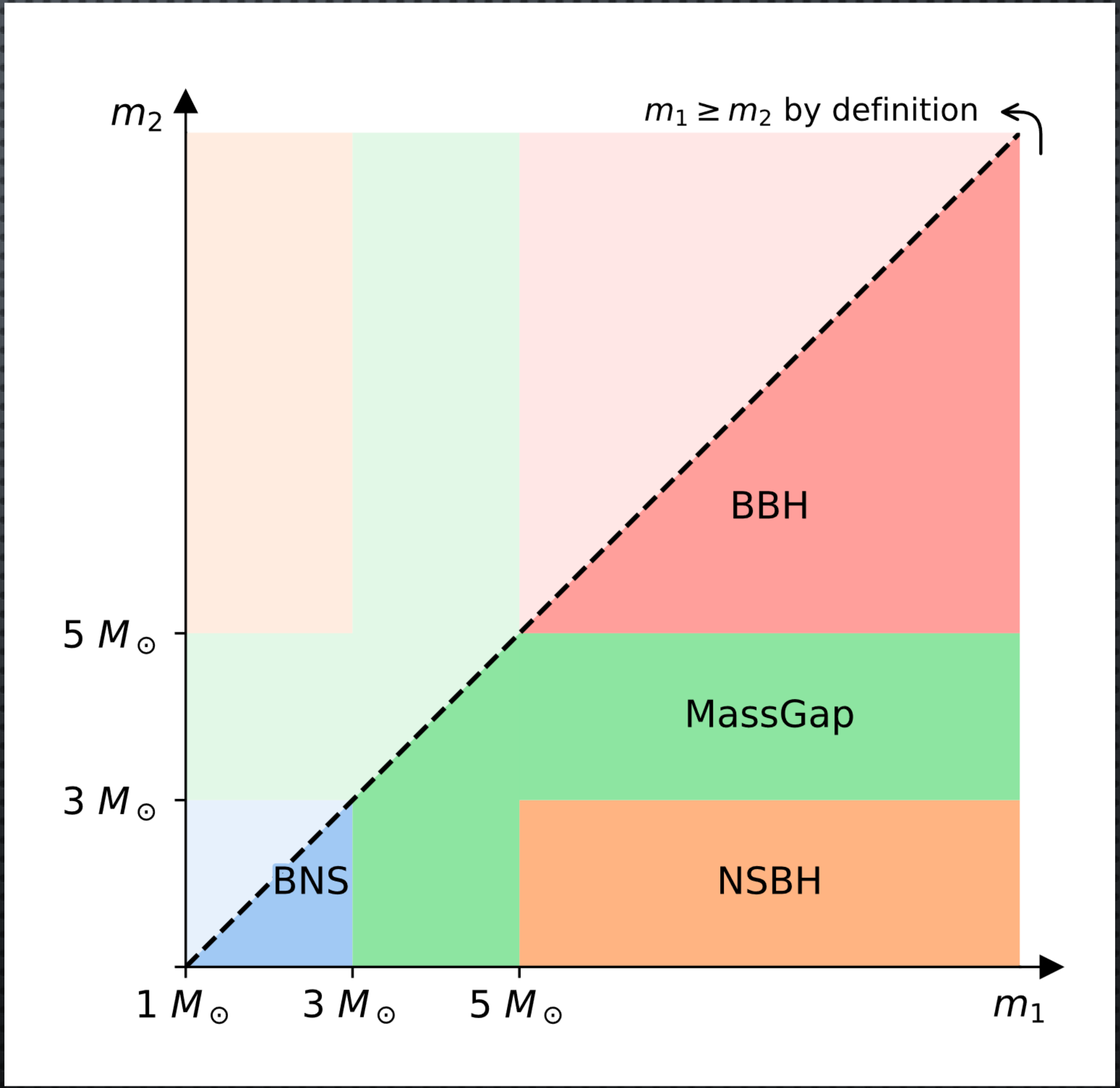

The KAGRA Project

- Over 300 collaborators
- Over 70 institutes from around the world

KAGRA Interferometer

Resonant Sideband Extraction (RSE)

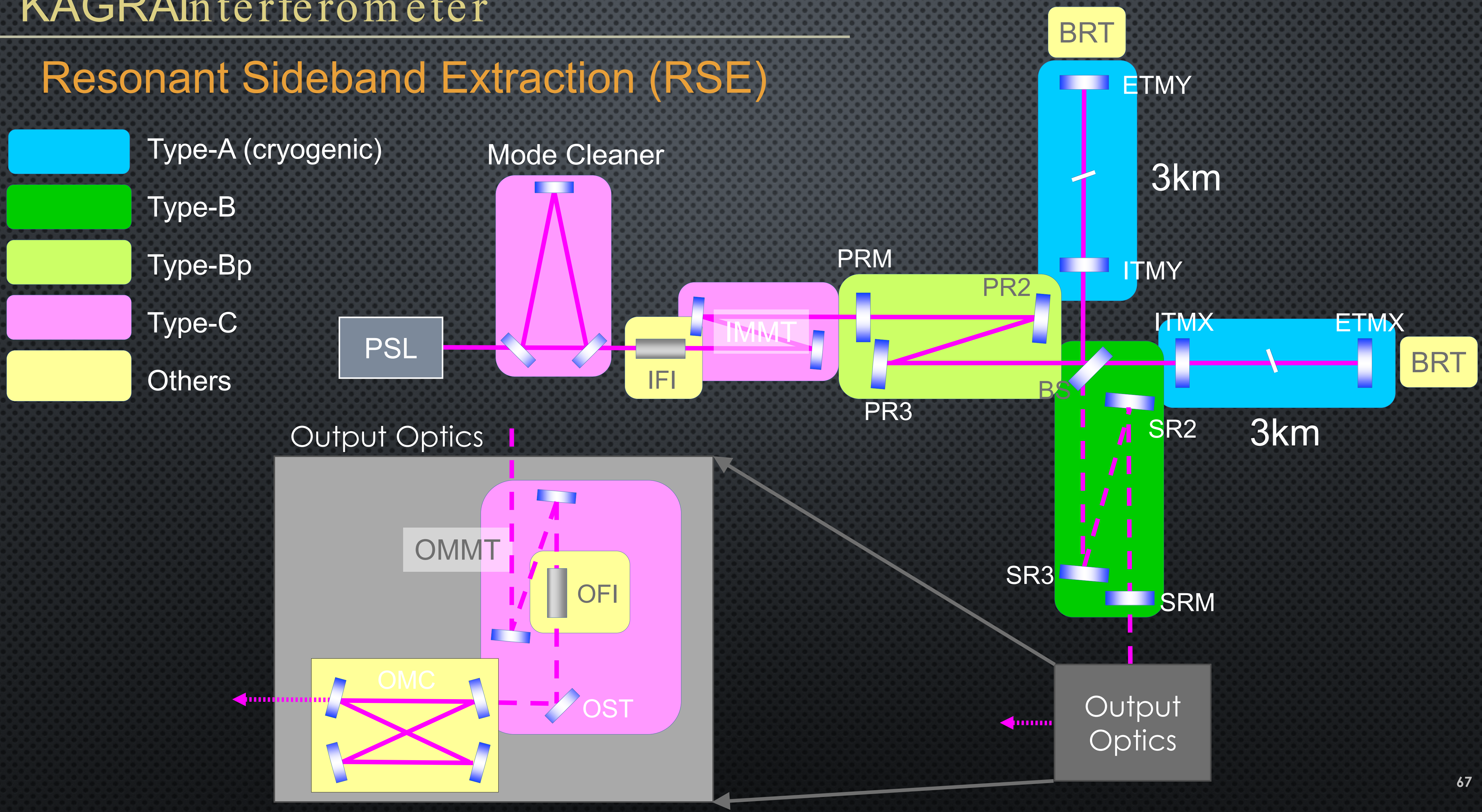

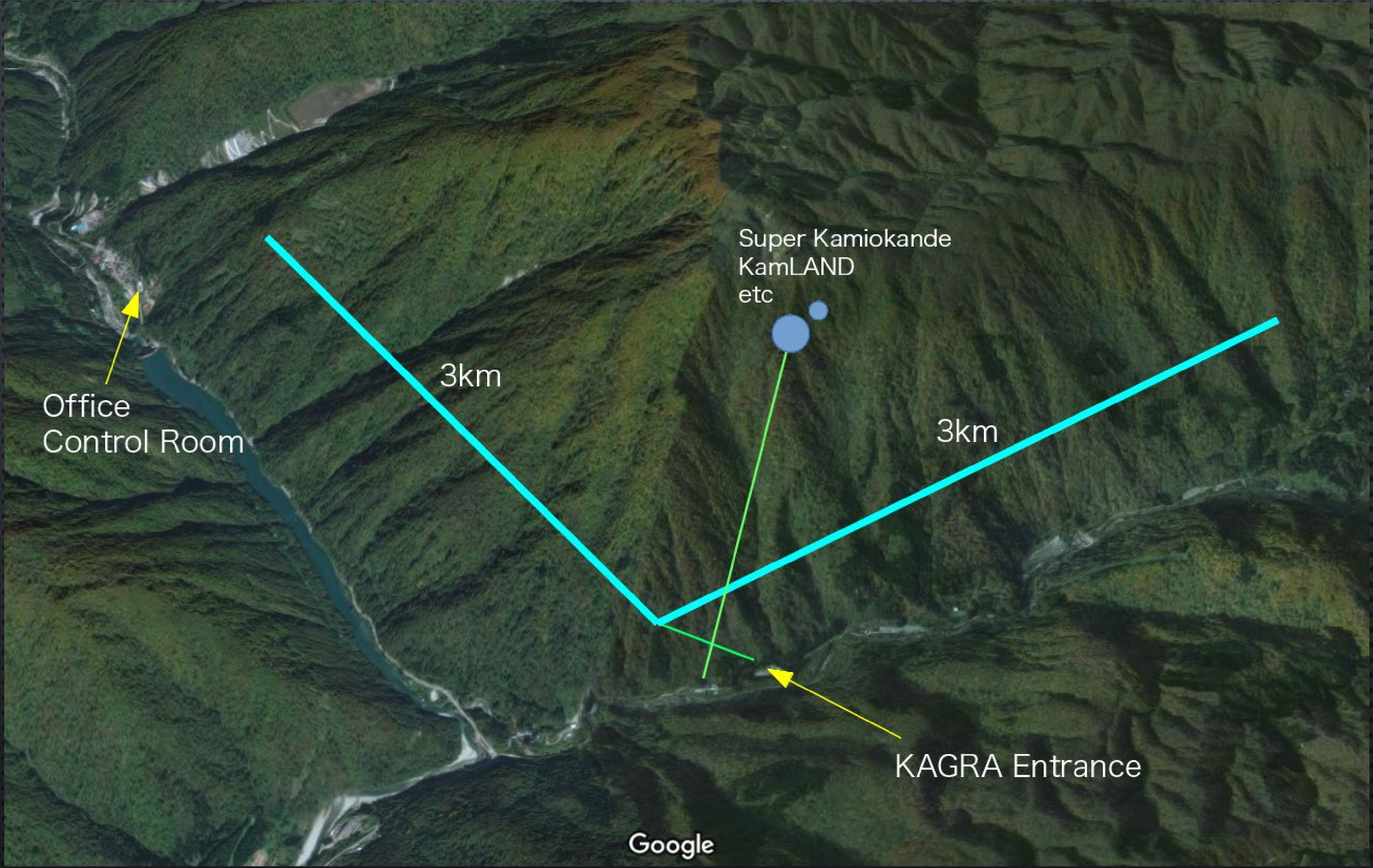
Super Kamiokande
KamLAND
etc
3km
3km
Office
Control Room
KAGRA Entrance
Google


重力波
大型低温重力波望遠鏡 -かぐら-
国際重力波観測網
KAGRAの構成
安全

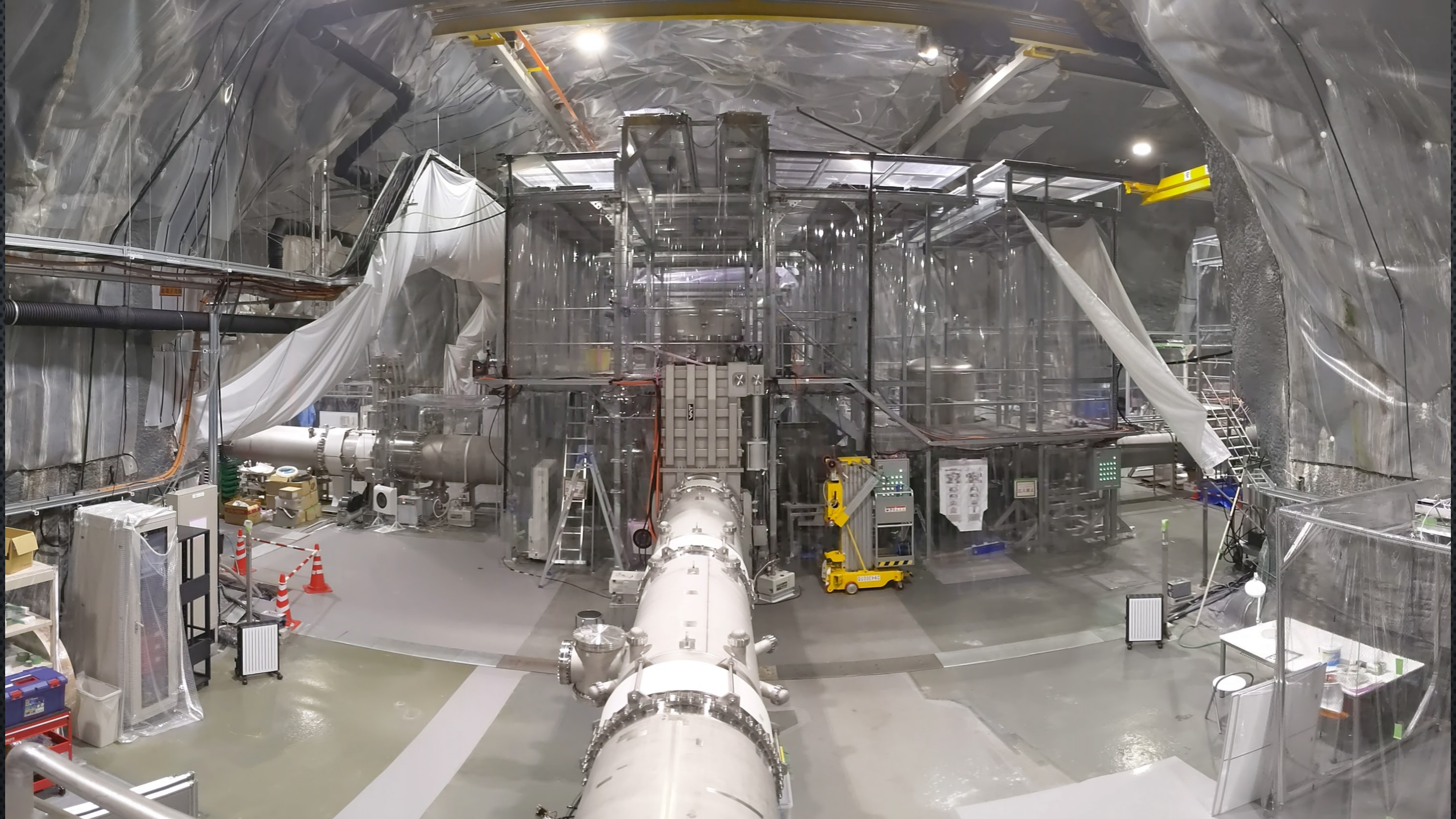

Beam Splitter Suspension

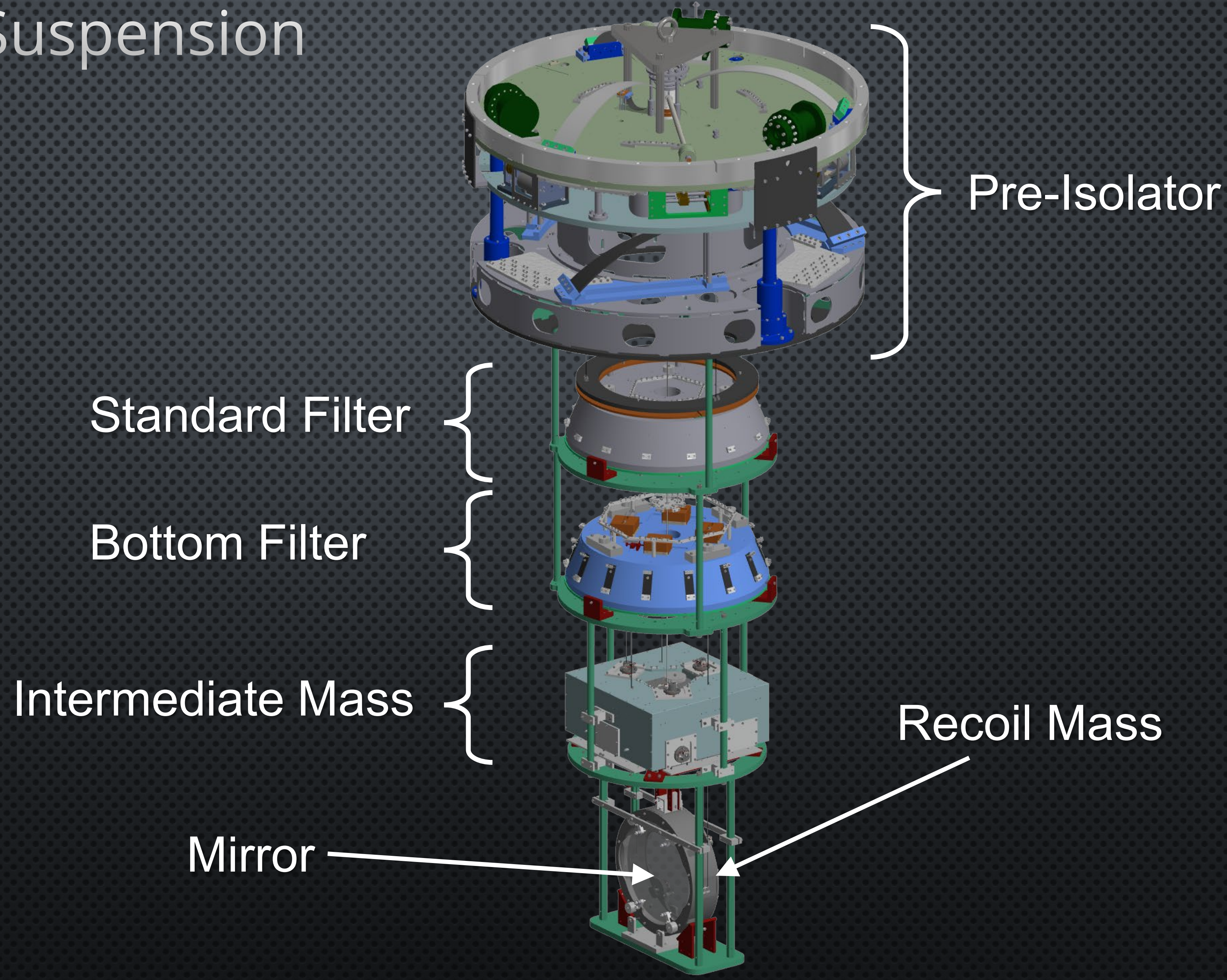

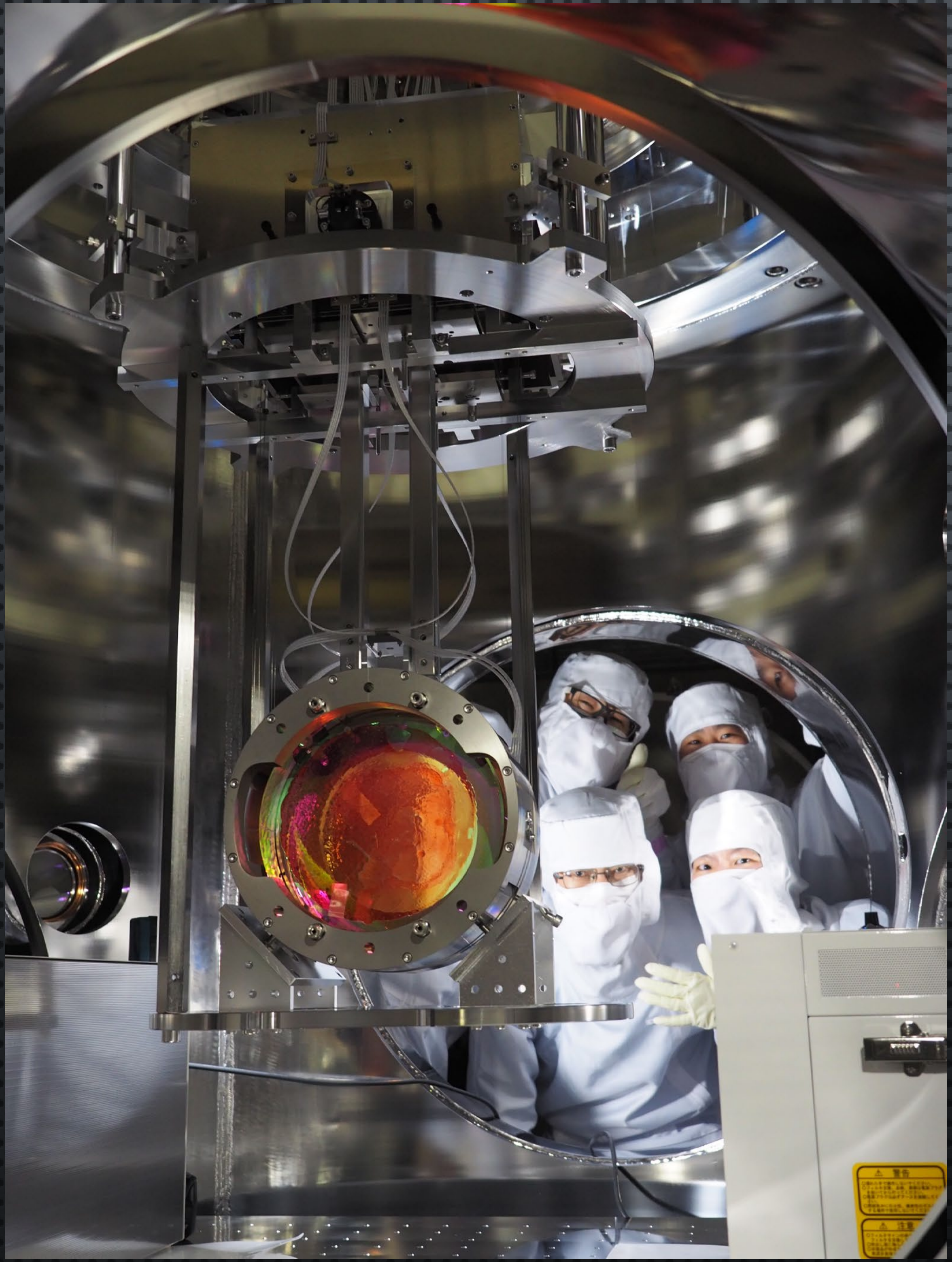

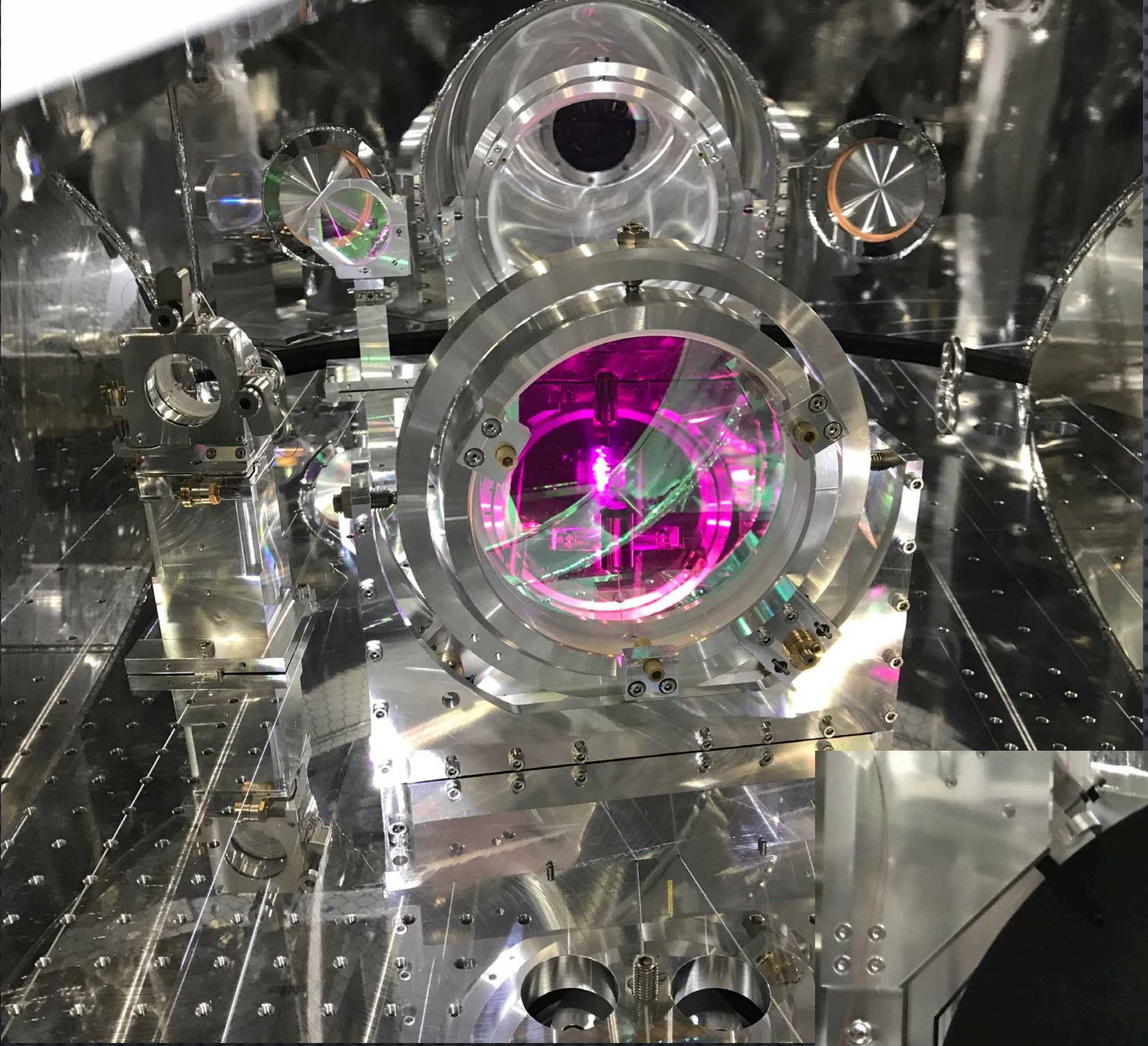
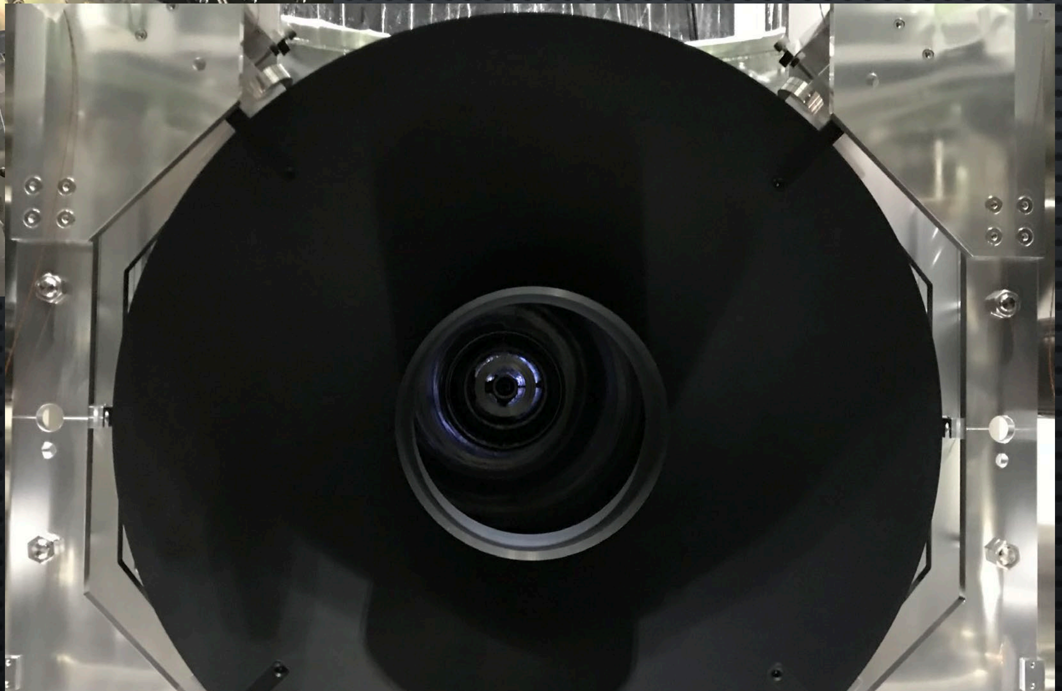
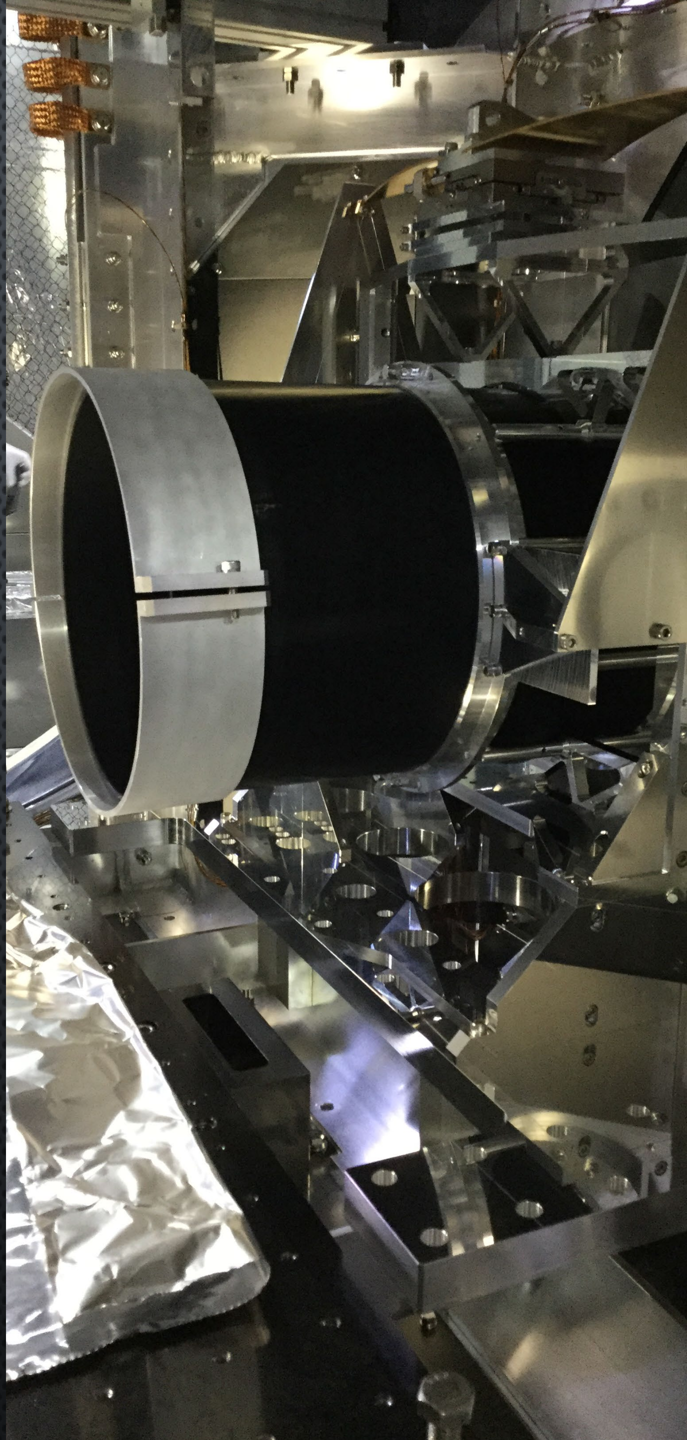

Type-A + Cryogenic Suspension

14m

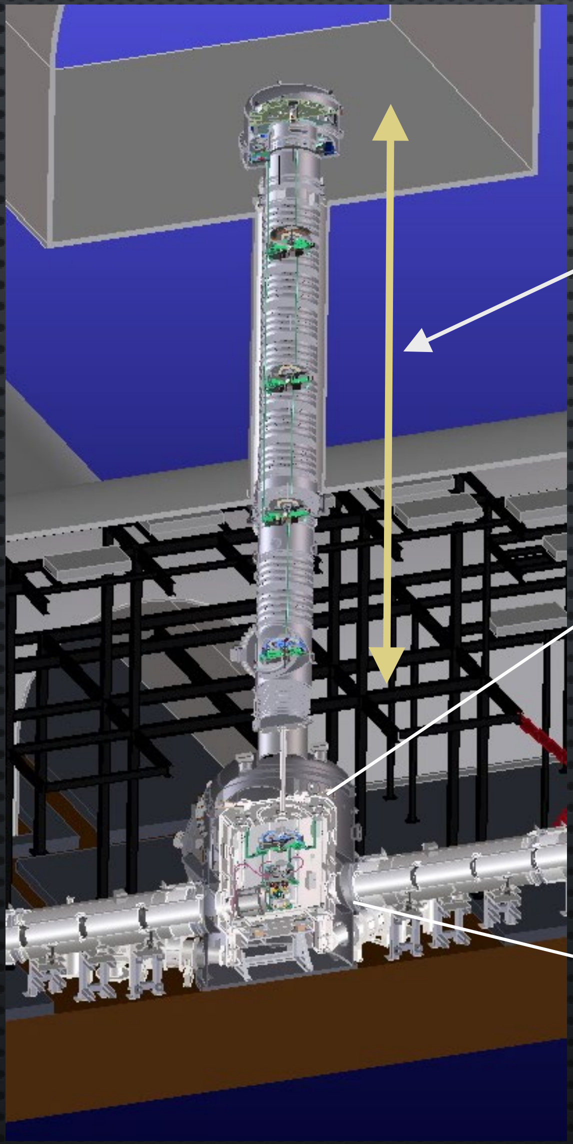

Type-A
(room temp.)

Cryo-Payload

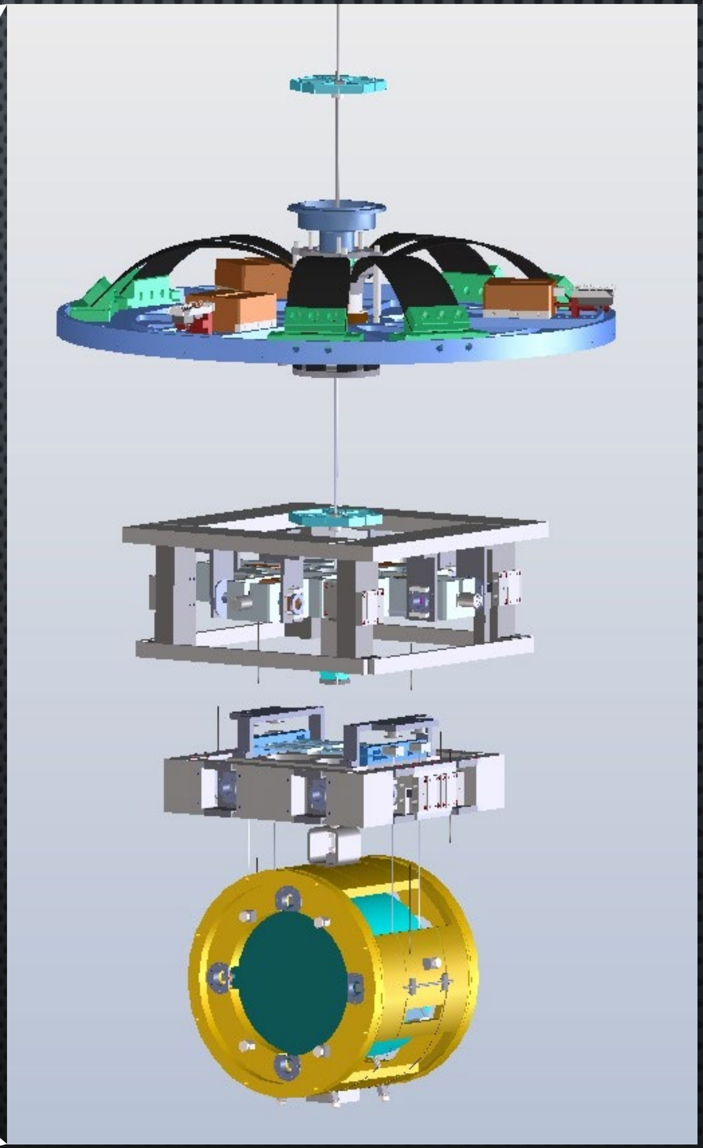

Type-A Suspension Installation

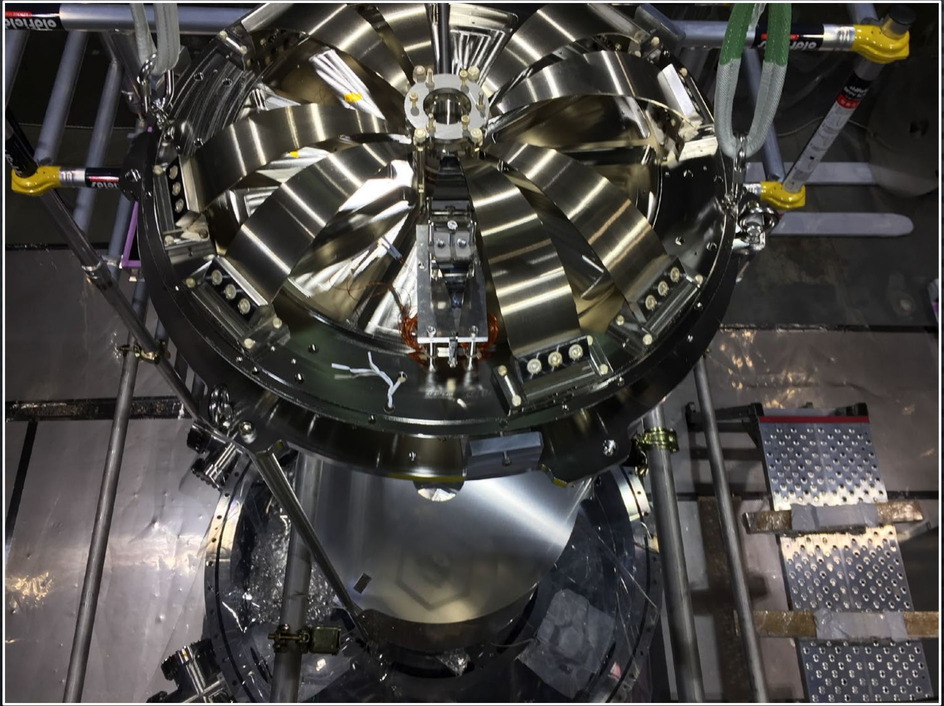

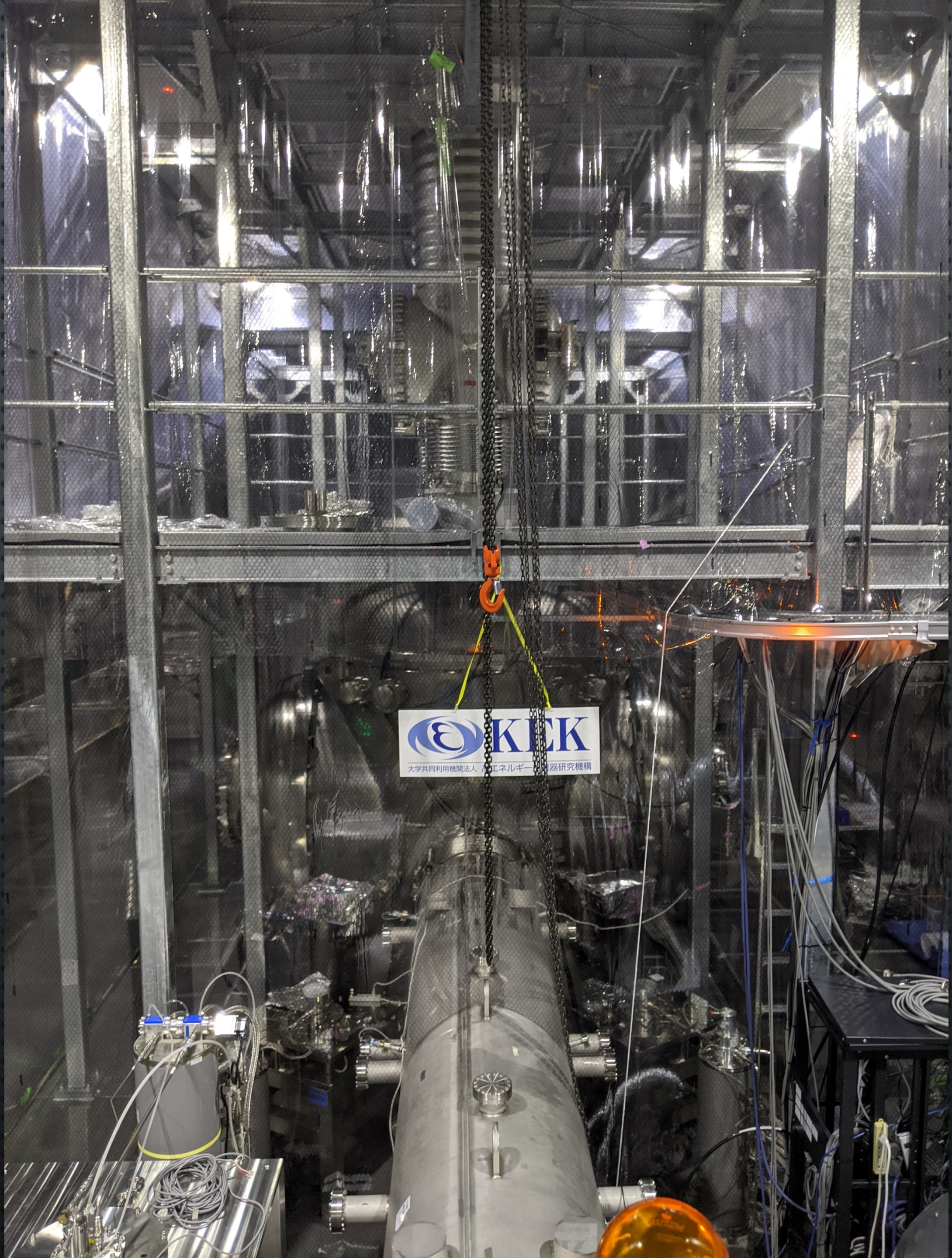
KEK

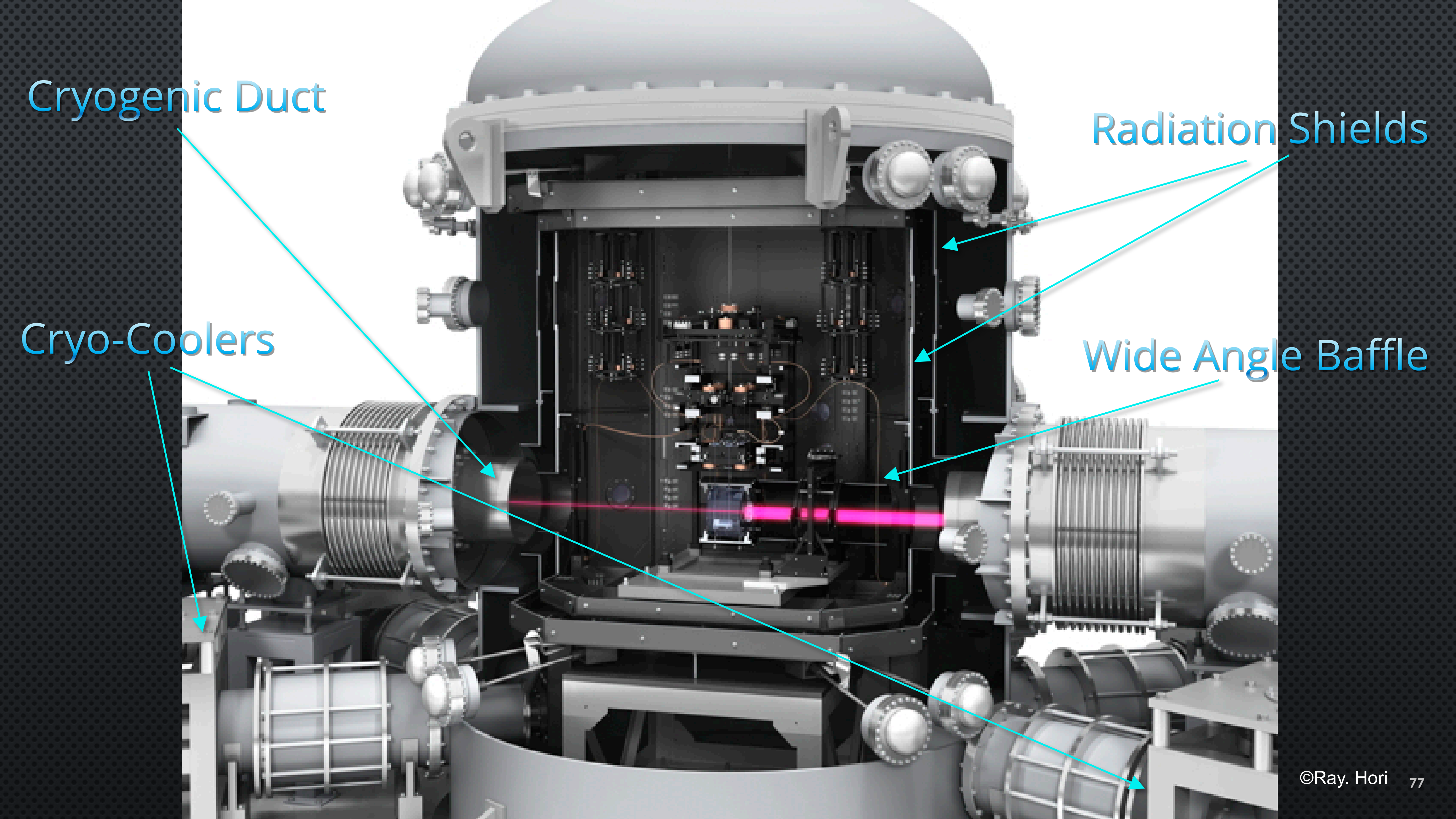

Cryogenic Duct
Radiation Shields
Cryo-Coolers
Wide Angle Baffle

©Ray. Hori

Dual-Recycled Fabry-Perot Michelson

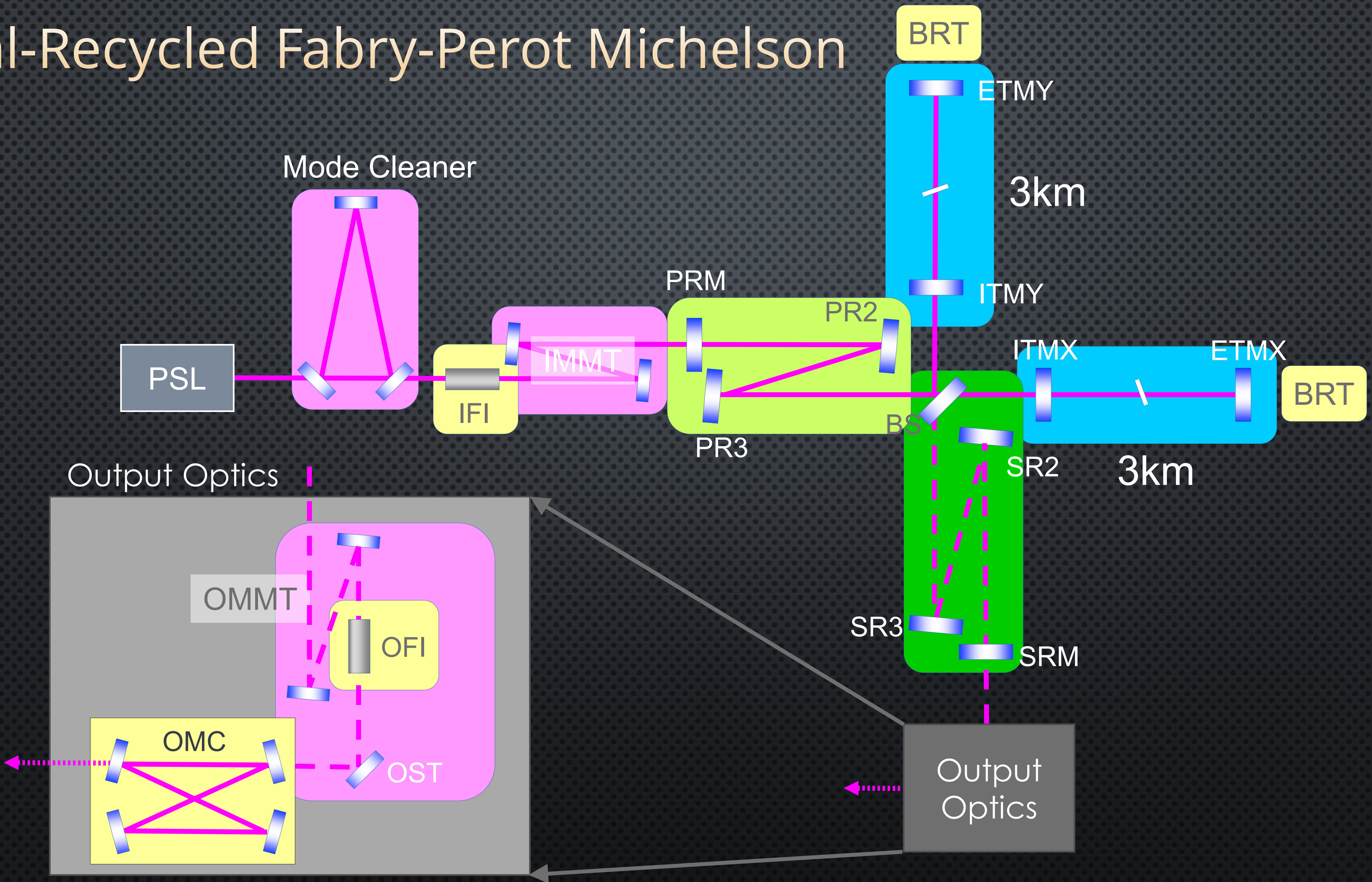

Fabry-Perot Michelson

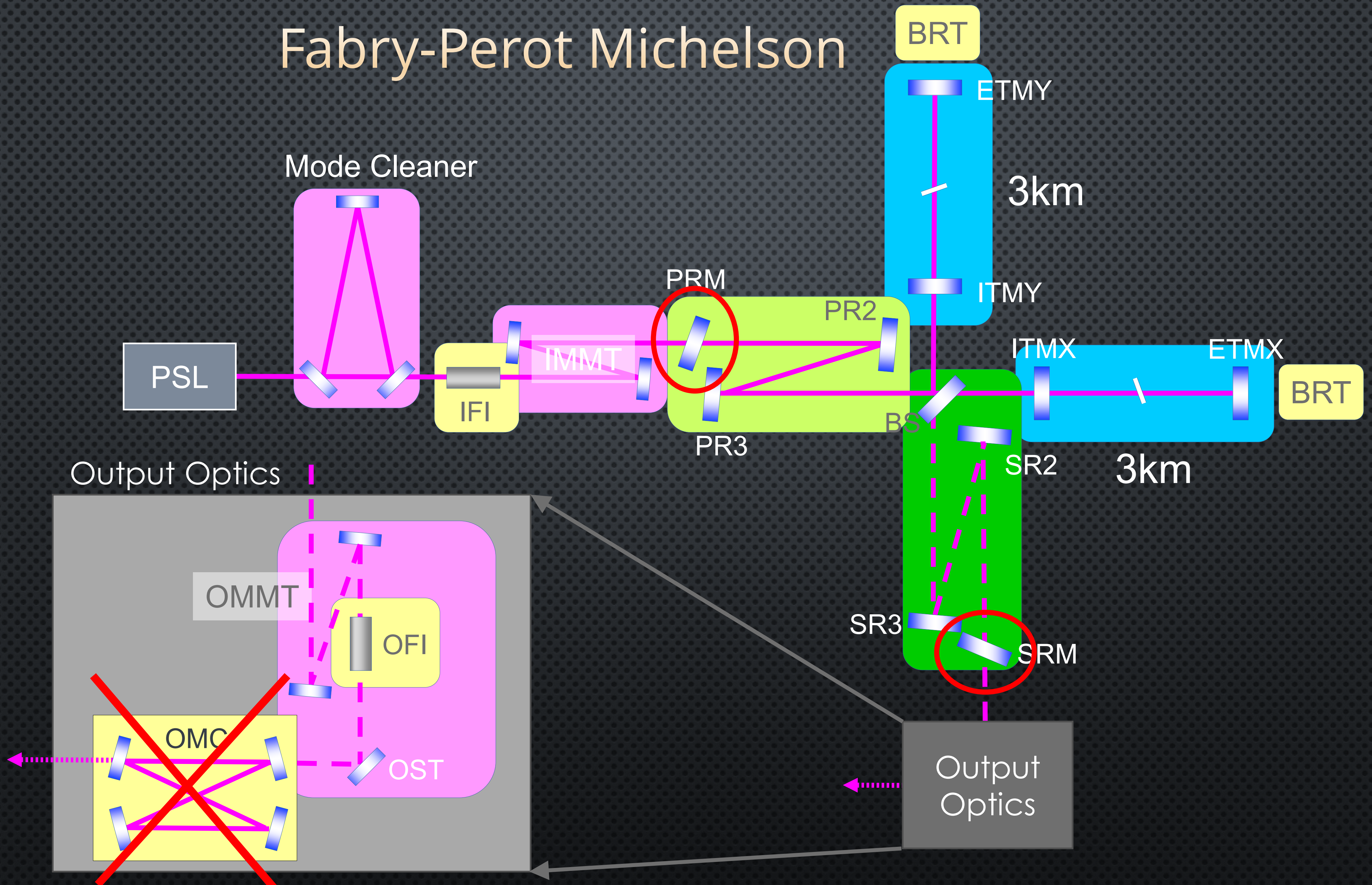

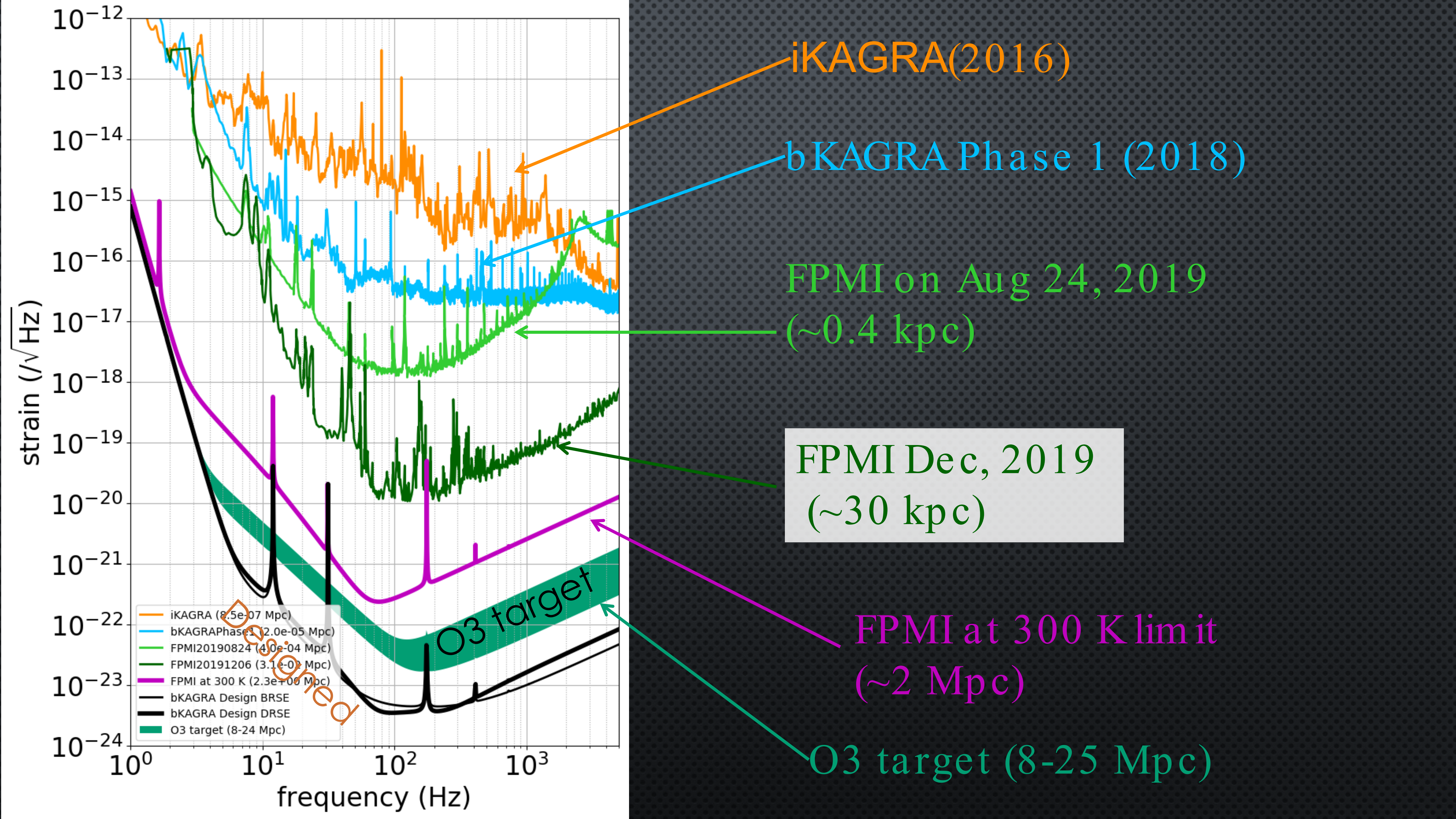

iKAGRA(2016)
bKAGRA Phase 1 (2018)
FPMI on Aug 24, 2019
(~0.4 kpc)
FPMI Dec, 2019
(~30 kpc)
FPMI at 300 K limit
(~2 Mpc)
O3 target (8-25 Mpc)
O3 target
Designed
iKAGRA (8.5e-07 Mpc)
bKAGRAPhase1 (2.0e-05 Mpc)
FPMI20190824 (4.0e-04 Mpc)
FPMI20191206 (3.1e-02 Mpc)
FPMI at 300 K (2.3e+00 Mpc)
bKAGRA Design BRSE
bKAGRA Design DRSE
O3 target (8-24 Mpc)
strain (/√Hz)
frequency (Hz)

GW source localization

Arrival time difference

→ Triangulation

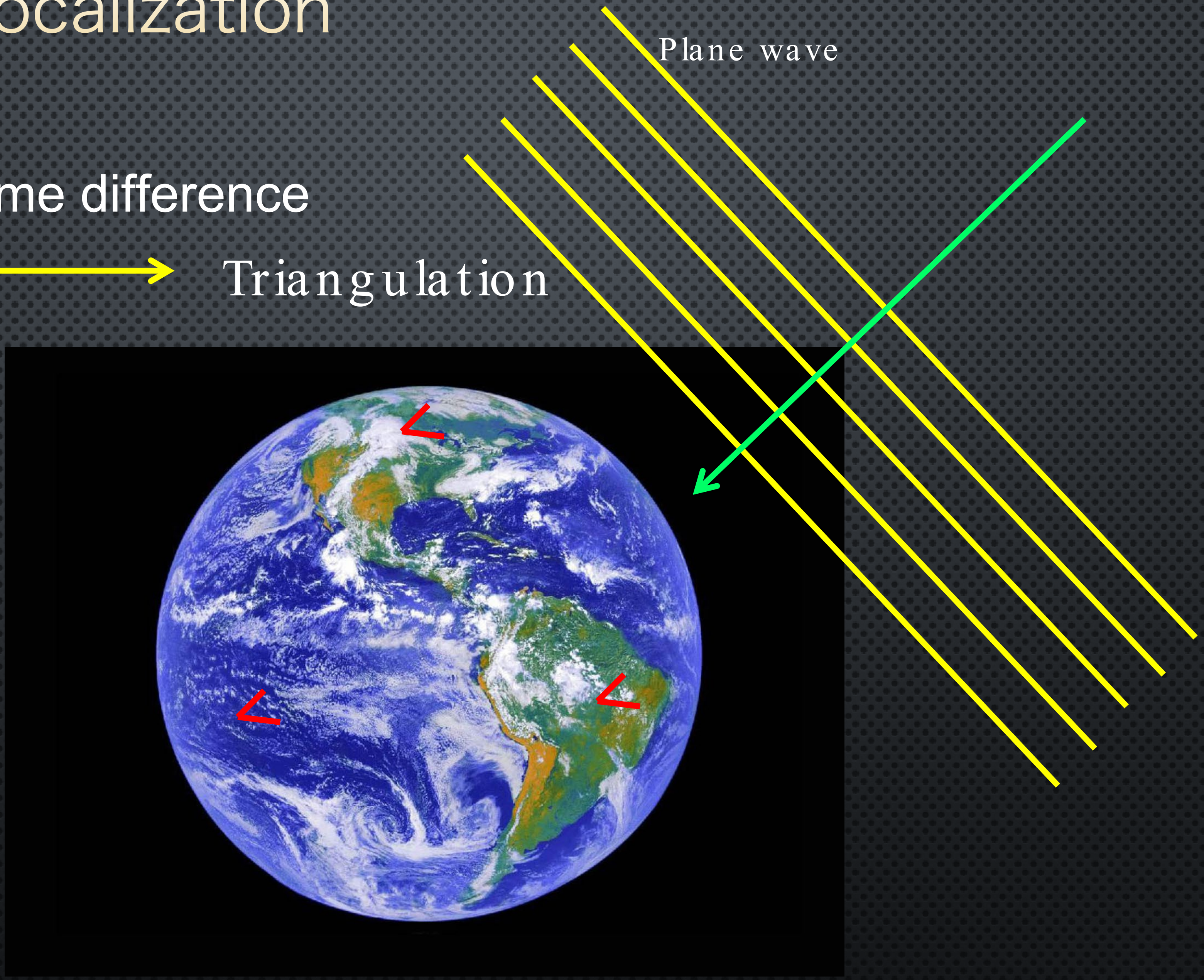

Improved event localization

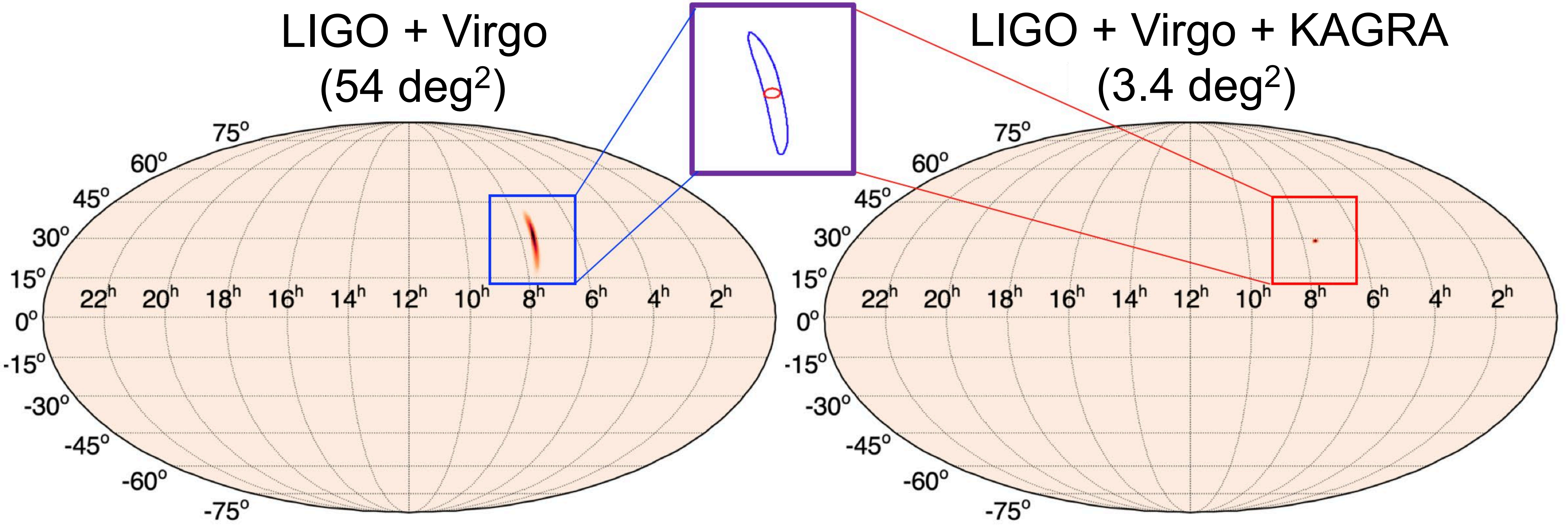

Worldwide network of GW detectors

What's next ?

Incremental upgrade: ~ 5 -year term

- Advanced LIGO +
- Advanced Virgo +
- KAGRA+ ?

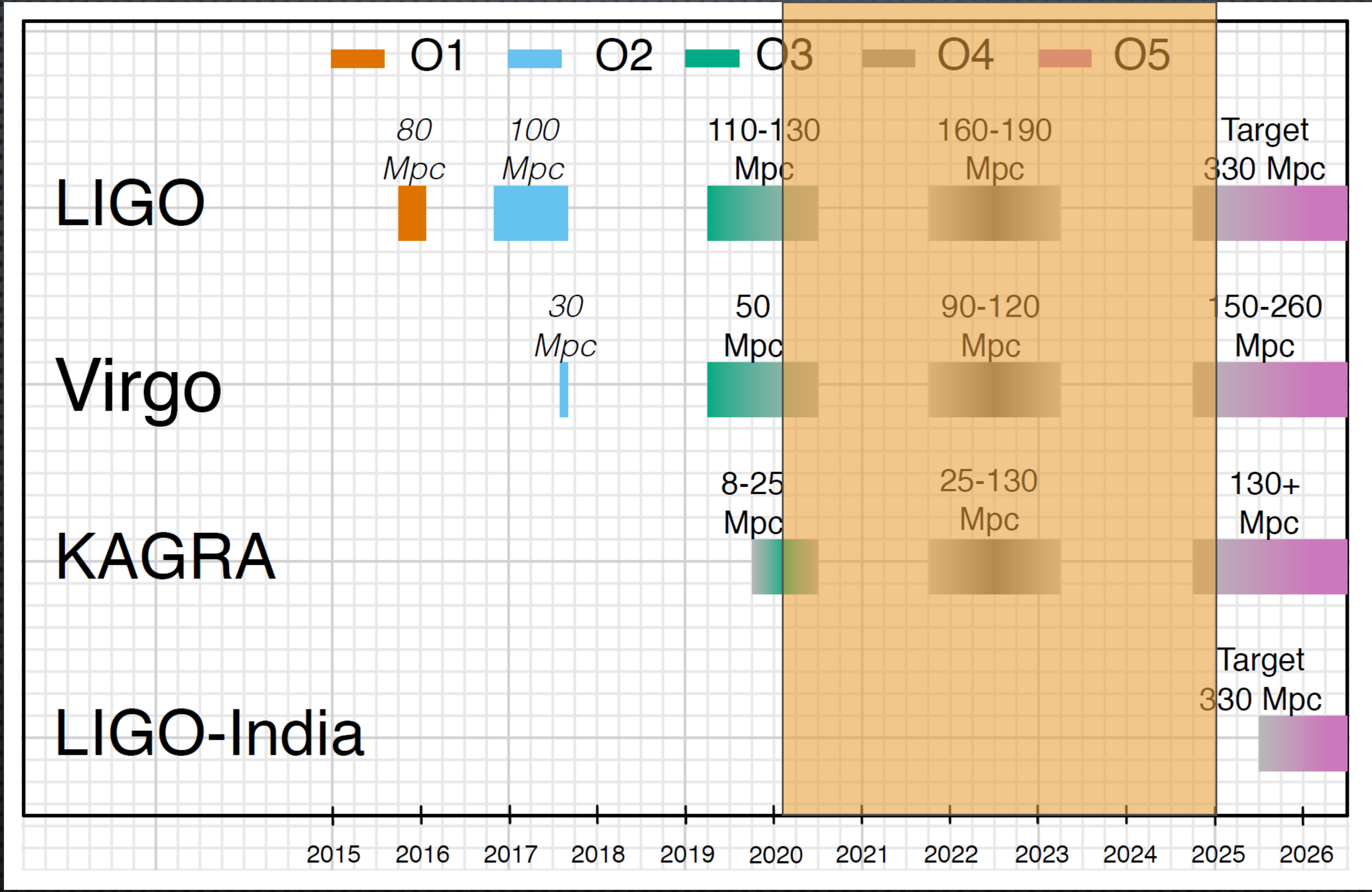
O1
O2
O3
O4
O5
LIGO
Virgo
KAGRA
LIGO-India
80 Mpc
100 Mpc
110-130 Mpc
160-190 Mpc
Target 330 Mpc
30 Mpc
50 Mpc
90-120 Mpc
150-260 Mpc
8-25 Mpc
25-130 Mpc
130+ Mpc
Target 330 Mpc
2015
2016
2017
2018
2019
2020
2021
2022
2023
2024
2025
2026

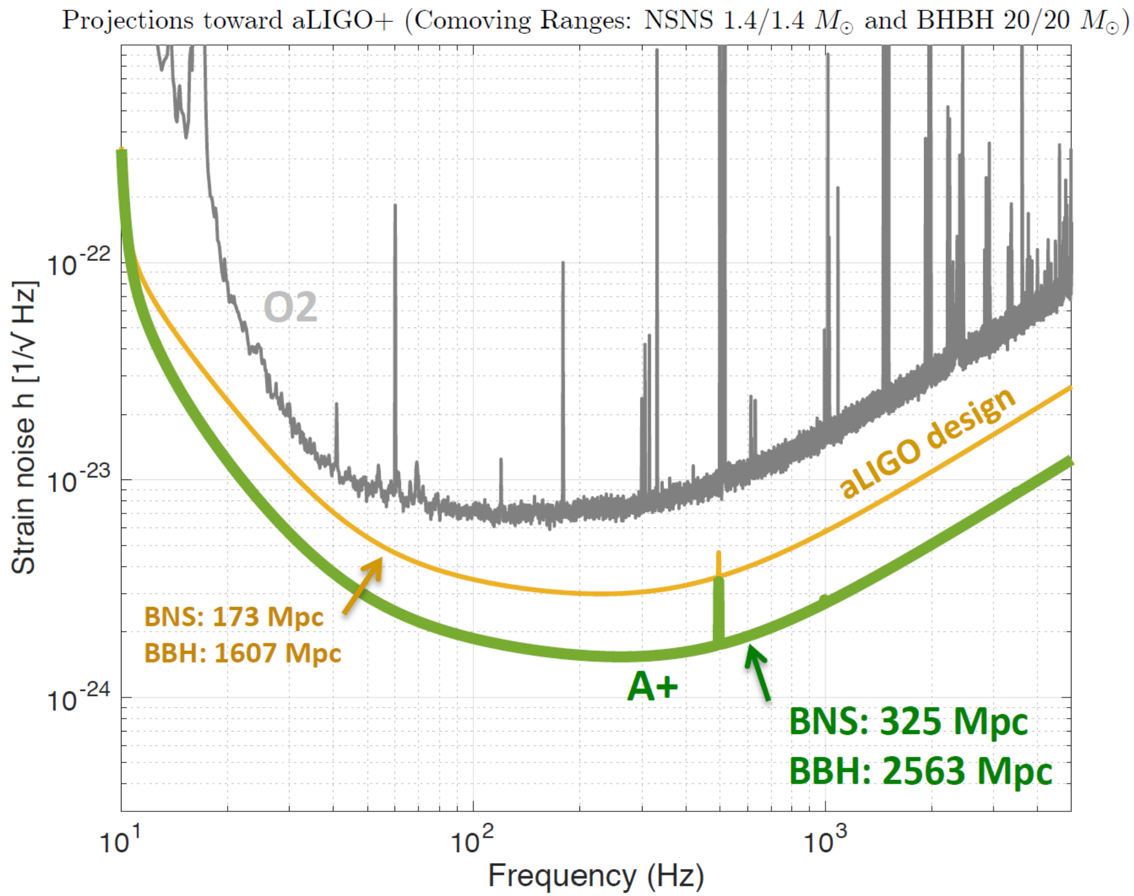

aLIGO+

aVirgo+

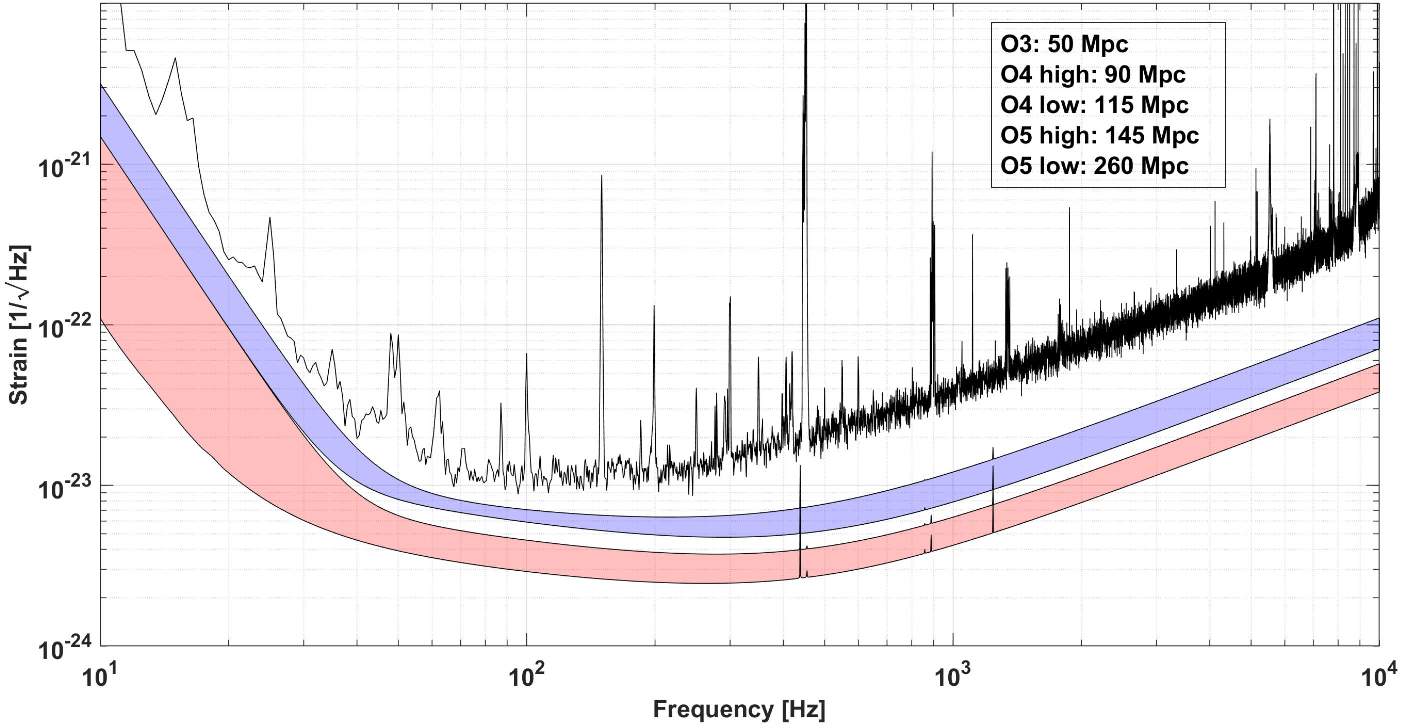

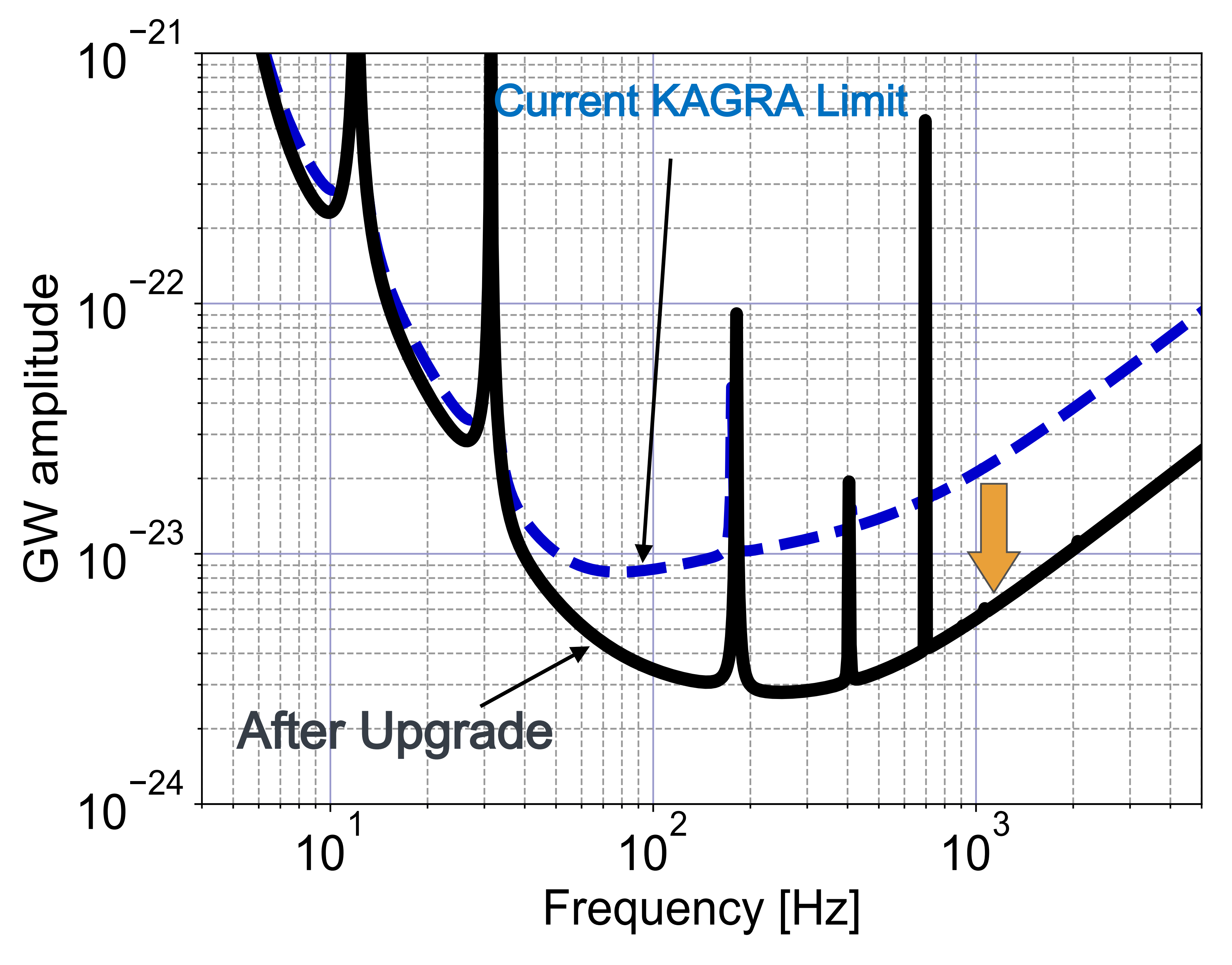

Current KAGRA Limit
After Upgrade
GW amplitude
Frequency [Hz]
10^{-21}
10^{-22}
10^{-23}
10^{-24}
10^{1}
10^{2}
10^{3}

Ingredients of incremental upgrades

- Higher Laser Power
- Lower thermal noise
  - Better coating
  - Larger mirror
- Birefringence free mirrors (KAGRA only)
- Frequency dependent squeezing
  - Filter Cavity

Ingredients of incremental upgrades

- Higher Laser Power
- Lower thermal noise
  - Better coating
  - Larger mirror
- Birefringence free mirrors (KAGRA only)
- Frequency dependent squeezing
  - Filter Cavity

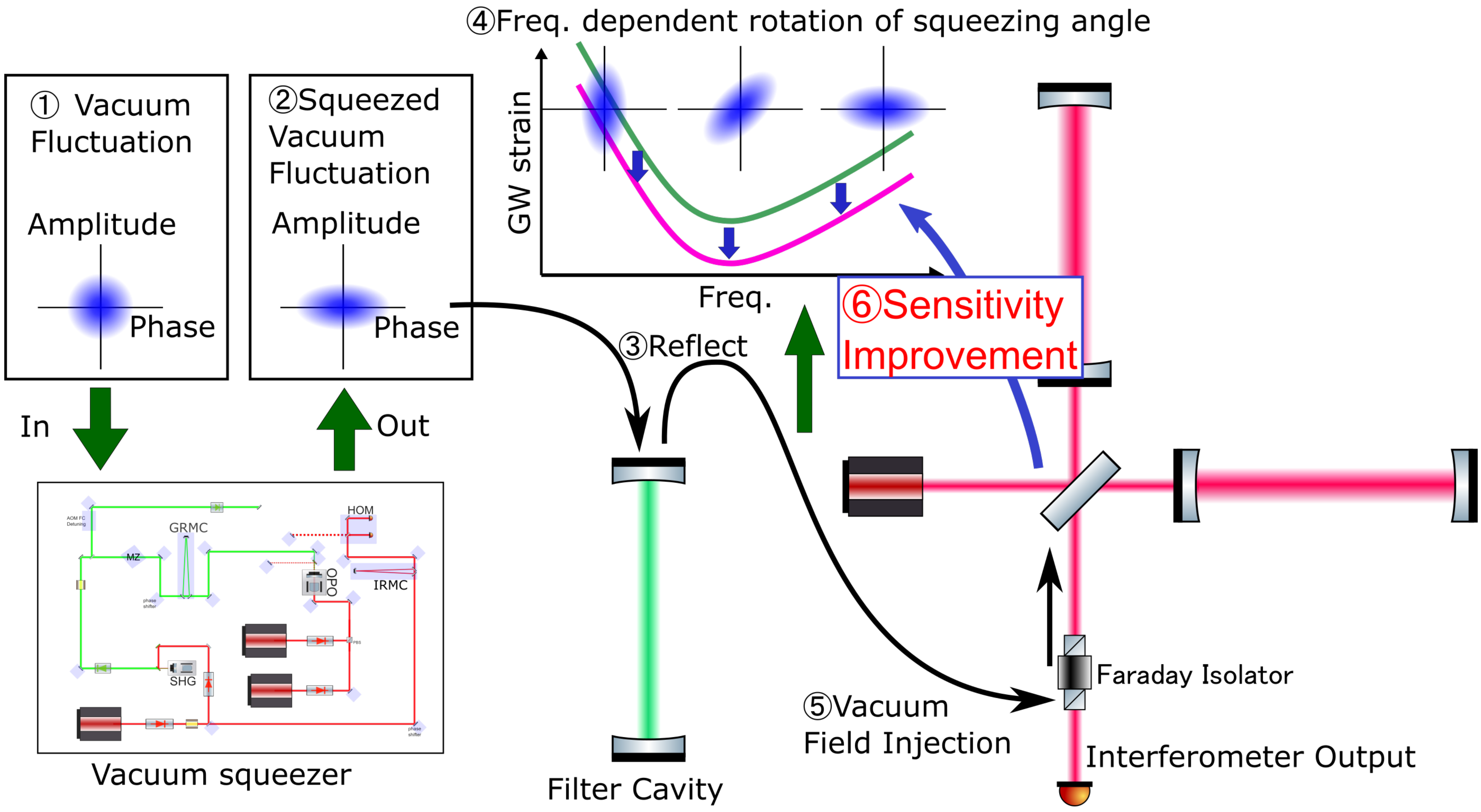

④Freq. dependent rotation of squeezing angle
① Vacuum Fluctuation
Amplitude
Phase
②Squeezed Vacuum Fluctuation
Amplitude
Phase
In
Out
GW strain
Freq.
③Reflect
⑥Sensitivity Improvement
AOM FC Detuning
GRMC
MZ
HOM
OPO
IRMC
SHG
Vacuum squeezer
Filter Cavity
⑤Vacuum Field Injection
Faraday Isolator
Interferometer Output

Observed rotation of squeezing angle

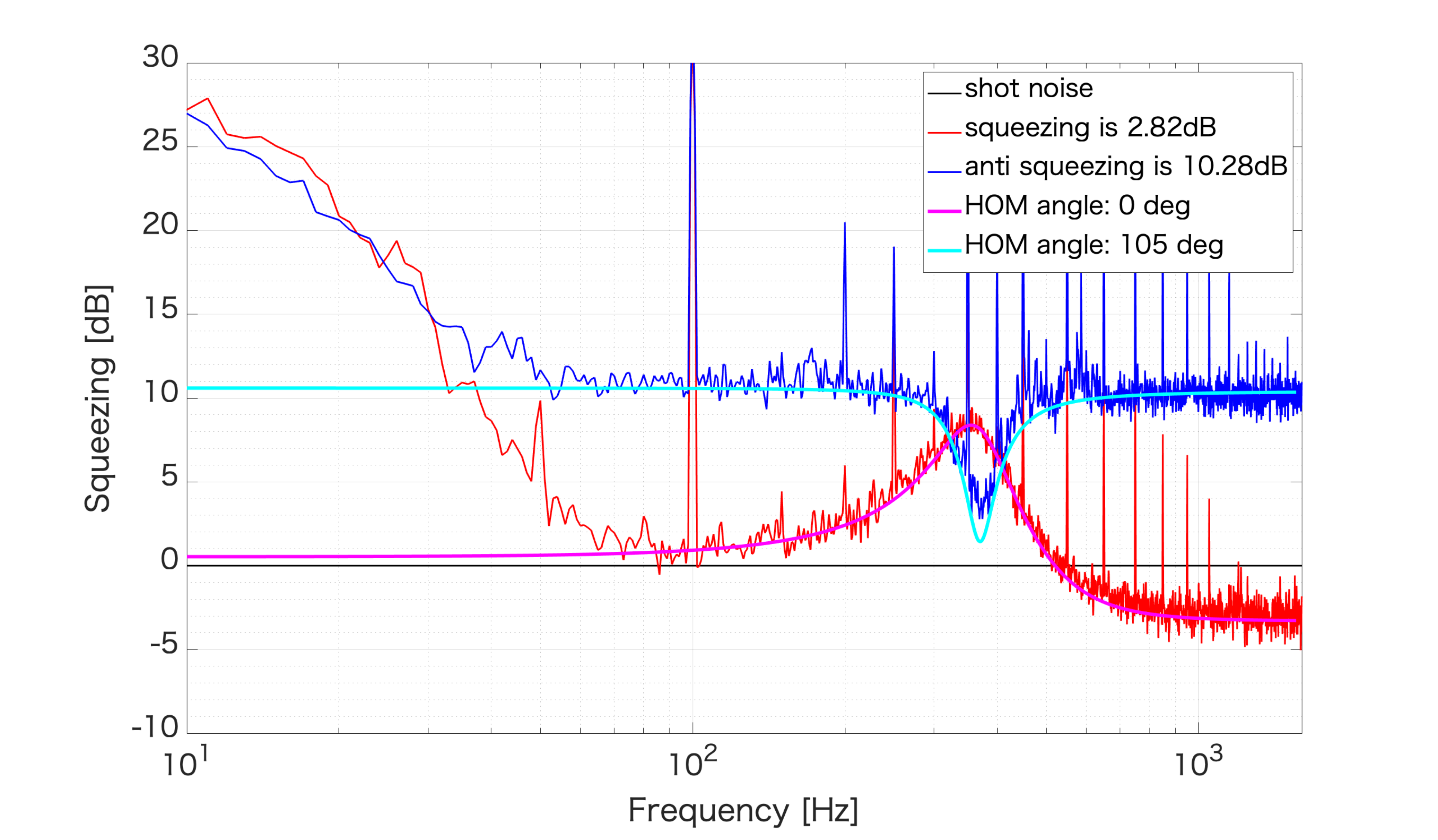

What's next ?

Incremental upgrade: ~ 5 -year term

- Advanced LIGO +
- Advanced Virgo +
- KAGRA+ ?

3G detectors: 10 – 20 years

- LIGO Voyager (USA)
- Cosmic Explorer (USA)
- Einstein Telescope (Europe)

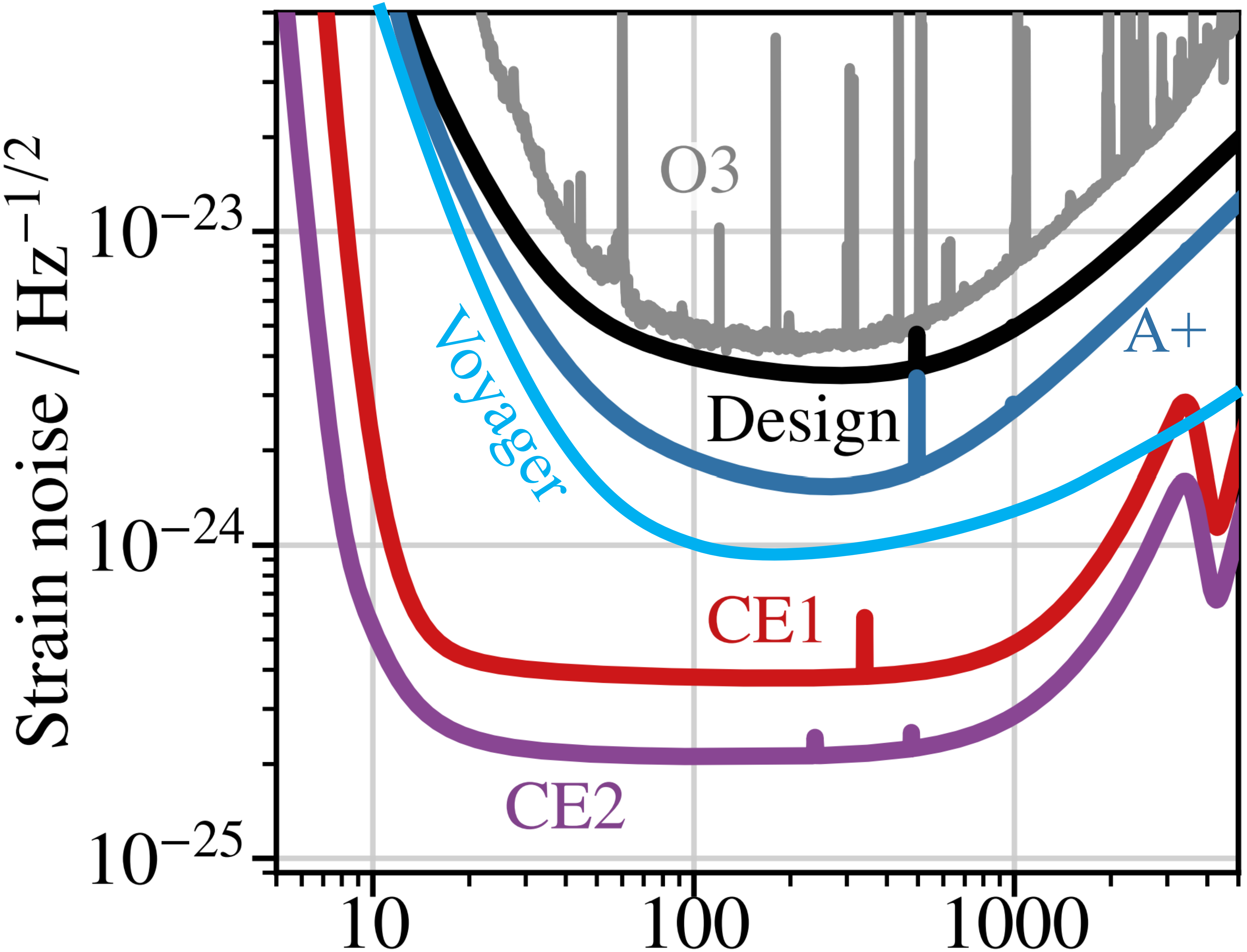
Strain noise / Hz^{−1/2}
10^{−23}
10^{−24}
10^{−25}
10
100
1000
O3
Design
A+
Voyager
CE1
CE2

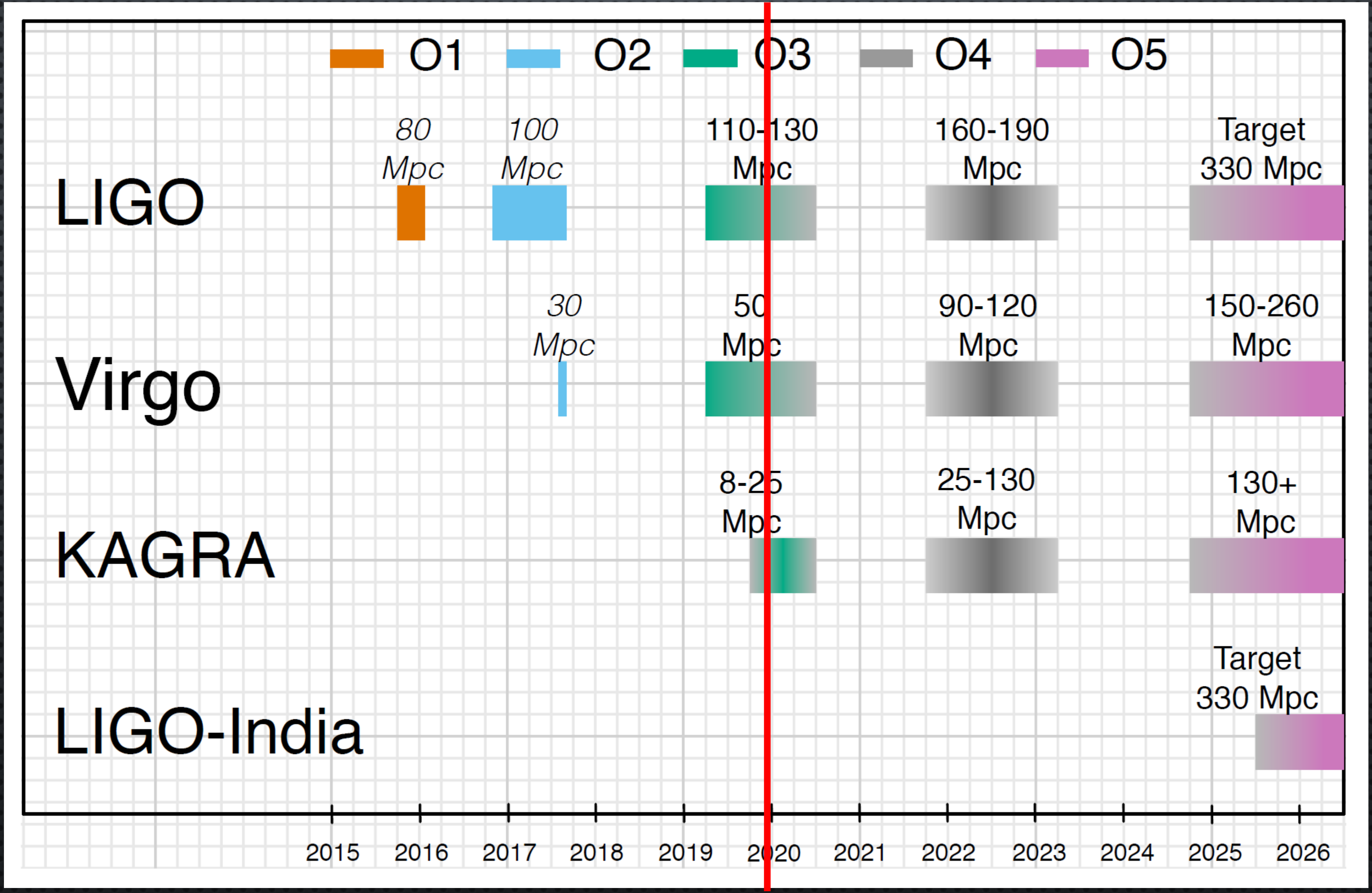
O1
O2
O3
O4
O5
LIGO
Virgo
KAGRA
LIGO-India
80 Mpc
100 Mpc
110-130 Mpc
160-190 Mpc
Target 330 Mpc
30 Mpc
50 Mpc
90-120 Mpc
150-260 Mpc
8-25 Mpc
25-130 Mpc
130+ Mpc
Target 330 Mpc
2015
2016
2017
2018
2019
2020
2021
2022
2023
2024
2025
2026

Now